Torsional Oscillations in the Earth's fluid core: theory, observation and geodynamic consequences

A thesis presented
by

Mathieu Dumberry

to

The Department of Earth and Planetary Sciences

in partial fulfillment of the requirements

for the degree of Doctor of Philosophy

in the subject of Geophysics

Harvard University

Cambridge, Massachusetts

May 2004

Advisor: Prof. Jeremy Bloxham Mathieu Dumberry

Torsional oscillations in the Earth's fluid core:
theory, observation and geodynamic consequences

Abstract

We present a study of a flow in the Earth's fluid core called torsional oscillations, which is described as azimuthal oscillations of rigid cylindrical surfaces aligned with the rotation axis. The latter are predicted by theory, are observed in the secular variation of the geomagnetic field, and consistently explain the decadal variations in the Earth's rotation rate. Consequently, they represent our most robust link between geophysical observations and our understanding of dynamic processes in the fluid core.

In the first part of our study, we focus on theoretical considerations. We present the details of a solution of a numerical model of the geodynamo which contains rigid flow motions akin to, but not exactly like, torsional oscillations. Based on results of the model, we propose an explanation for the excitation of torsional oscillations in the core.

In the second and third part, we focus on the geodynamic consequences of the presence of torsional oscillations in the core. First, from the deformation of the core-mantle boundary that they induce, we test whether they can be detected in the gravity field at the Earth's surface. We show that the predicted gravity field variations are an order of magnitude too small to be currently detected. Second, we investigate whether torsional oscillations are at the source of the Markowitz wobble, a decadal variation in the position of the Earth's rotation axis. We show that electromagnetic torques at the inner core boundary produced by torsional oscillations can tilt the geometric figure of the inner core, and lead to changes in the Earth's rotation that have similar characteristics than the observed Markowitz wobble.

In the final part, we attempt to extend the connection between geomagnetism and geodesy established by torsional oscillations to millennial timescales. We show that, in order to consistently explain the archaeomagnetic secular variation and a 1500-year oscillation in the length of day, azimuthal time-dependent flows in the core must have a shear in the direction along the rotation axis, in contrast to torsional oscillations at decade timescales.

Contents

List of Figures

List of Tables

Acknowledgments

Many people, for different reasons, have made my years at Harvard very enjoyable. The few lines below certainly do not do justice to the contribution that each of them made.

First, thanks to my many fellow students and friends for scientific discussions on the one hand and relief from science on the other. Special thanks, in no particular order, to Pippa Halverson, Pascale Poussart, Adam Maloof, Woody Fischer, Andy Bush, Sofy Low, Freddy Corredor, Jianfeng Pan, Susannah Porter, Bogdan Kustowski, Chris Guzofski, Meredith Nettles, Carlos Rivero, Miaki Ishii, Mathias Barth, Frederik Simons, Ellen Chang and Martha Kay Nelson. On the home front, I wish to thank my house mate during my final year, Will Phelan, and my former house mates, Jonathan Payne, Elizabeth Stuart and Fiona Barker, for three wonderful years at 335 Beacon.

I thank my office mates Jamie Kellogg, Thorsten Becker, Sabine Stanley, Kaushik Katari, Lada Dimitrova, Diana Valencia, Karin Louzada and Brandon Meade, for providing the perfect balance between work and fun. Special thanks to Jamie and Thorsten, true colleagues and good friends, who stimulated my scientific and non-scientific interests and made my days at the office so enjoyable. Special thanks as well to my academic twin sister Sabine Stanley, with whom I shared the ups and downs of the progression through graduate school.

To the administrative personnel, Maryorie Grande, Abigail Adams, Joan Donahue, Reyna Truscott and Chenoweth Moffatt, thank you for providing a safety net for my disorganized nature and for saving me on many occasions.

I have received considerable help on the academic front – thanks to Chris Cox for providing the J_2 data, to Monika Korte for the archaeomagnetic field model, and to Bruce Buffett for an initial version of the numerical code used in chapter 3. Constructive criticism on parts of this manuscript have been kindly provided by Steve Dickman, Richard Holme, Christopher Finley and Sabine Stanley. Discussions with many colleagues have improved the work presented in this thesis. I particularly acknowledge Weijia Kuang, Stephen Zatman and Bruce Buffett. Special thanks also to two professors in the department, Richard O'Connell and Paul Hoffman, for wide ranging discussions.

I wish I had better literary talent, only so I could properly acknowledge the role of my advisor Jeremy Bloxham to the level that he deserves. Isaac Newton once said: "If I have

seen farther than others, it is by standing on the shoulders of giants". I would not go so far as to say that I have seen much farther than others, but the second part of the quotation certainly applies. I have been extremely fortunate to benefit from his clarity of thought and unique ability to synthesize ideas. Jeremy, while providing sound advice, gave me complete freedom in my research projects and has also generously allowed me to whittle away his funding by attending numerous meetings.

Finally, to my best friend Fiona Barker, the ultimate thanks for the constant support, encouragement and guidance. It is difficult to imagine how the work in this thesis could have been achieved without the foundation that you provided. No words can truly acknowledge your contribution to my years in graduate school.

Partial funding for my Ph.D. program was provided by a postgraduate scholarships from *Natural Sciences and Engineering Research Council of Canada (NSERC)* and a *Bourse de doctorat en recherche* from *le Fonds pour la Formation de Chercheurs et l'Aide à la Recherche (FCAR) du Québec*. Additional support was provided by NSF Awards EAR-0073988, EAR-0112469, EAR-9725675 and EAR-0327843, and NASA grant NAG5-7616.

I wish to say a formal farewell to Stephen Zatman, a dearly missed colleague and friend. I got to know Stephen during our many interminable coffee breaks at the fall AGU meetings, and always greatly enjoyed his constant enthusiasm and excitement as well as his relentless questioning. This thesis is dedicated to him, as I am sure he would have equally loved, questioned, criticized and debated all aspects of this work.

The truth is rarely pure and never simple

Oscar Wilde

Chapter 1

Introduction

1.1 History of geomagnetism

The Earth's magnetic field has been, for centuries, one of the natural phenomena that kindled the curiosity of mankind. This is reflected by its long history of observation by various civilizations. The first known measurements of magnetic declination, the angle of misalignment between a compass needle and the geographic north, were made in China by the Buddhist astronomer Yi-Xing near the year 720 A.D. (Needham, 1962). Magnetic inclination, the angle between the compass needle and the horizontal plane, was discovered in 1544 by Georg Hartmann and rediscovered independently by Robert Norman in 1581 (Merrill *et al.*, 1996; Stern, 2002). In 1634, Henry Gellibran showed that the magnetic declination in London had undergone a systematic shift, and was the first to provide conclusive evidence that the Earth's magnetic field was changing with time (Malin and Bullard, 1981). Today, we have magnetic observatories distributed around the globe making continuous real time measurements, and satellite missions dedicated to the observation of the Earth's magnetic field.

Our scientific understanding of the Earth's magnetic field has had an equally rich history, dating back to the earliest scientific investigation. In his famous treatise on his experiments in magnetism entitled *De Magnete* published in 1600, William Gilbert concluded that the magnetic field observed at the surface was the consequence of the Earth itself being a great magnet (Gilbert, 1600). Magnetism became thereby the first property to be attributed to the entire body of Earth, preceding Newton's gravitation theory by 87 years. Obviously,

the findings of Henry Gellibran disputed this view. However, in an ingenious way of reconciling the idea of permanent magnetization while allowing for time-dependency of the magnetic field, Edmund Halley proposed in the early 1700's that the Earth was comprised of concentric spherical shells each with its own magnetization, and that a differential rotation between them was responsible for the observed variations of the field (Bullard, 1956).

As the physical process of magnetization became better understood and when it was realized that, apart from the upper 30 km at the Earth's surface, the temperature in the interior of the Earth is everywhere above the Curie point, the explanation of the origin of Earth's magnetic field in terms of permanent magnetization had to be abandoned. Today, we believe that the Earth's magnetic field to be generated and maintained against decay by convective motion in the electrically conducting fluid iron core, a process known as the geodynamo. Electrical currents resulting from these fluid motion are responsible for the field that we observe at the surface. The idea was first proposed by Sir Joseph Larmor (1919a; 1919b) and the first quantitative efforts in that direction were done by Walter Elsasser (1946a; 1946b; 1947; 1956) and Edward Bullard (1949a; 1949b). (More extensive reviews of the history of geomagnetism can be found, for example, in Malin (1987), Merrill *et al.* (1996), Stern (2002) and references therein)

Since these pioneering attempts, our theoretical understanding of the general properties of magnetohydrodynamics and of the geodynamo has improved considerably. The most recent advances have come from self-consistent three-dimensional numerical simulations of the geodynamo (Glatzmaier and Roberts, 1995; Glatzmaier, 2002; Kono and Roberts, 2002). In a sense, these simulations provide the ultimate proof that a planetary magnetic field can be maintained by convective motion in a conducting fluid shell.

1.2 Observations of the dynamics in the Earth's core

Despite the huge leap in the understanding of the geodynamo processes from its original proposition, many aspects of the dynamics involved remain poorly understood. The complexity of the dynamics still presents formidable challenges for theoretical and analytical models. The numerical simulations have helped tremendously in that regard. However the current limits in computation prevent the use of realistic Earth-like parameters and, as a result, the dynamics of the current state of the geodynamo cannot be revealed indisputably

by these simulations.

Perhaps the greatest impediment to unraveling the complications of the geodynamo is the lack of observations with which we can test the theoretical models and numerical simulations. In the end, as it is the case for all scientific studies, observation of a given mechanism remains the only true arbitrator of its existence.

The only direct observation of the dynamics that we have is the product of the geodynamo, the Earth's magnetic field itself. Our observations of the magnetic field originating from the core are however far from perfect. The mantle, the 2900 km thick spherical shell of silicate material external to the core, is finitely conducting and acts as a low-pass filter screening the higher frequency variations of the magnetic field (e.g. Gubbins and Roberts, 1987). Permanent magnetization in the crust at the surface also prevents the observation of the small scale features of the internally generated magnetic field (e.g. Harrison, 1987). In addition, the changes in the magnetic field at the surface that are from external origin, such as variations in ionospheric currents and other magnetospheric processes, must be properly eliminated in order to isolate the component originating from the core (e.g. Langel, 1987).

Despite these difficulties, a part of the field measured at the surface is clearly identifiable as being of core origin. While these observations of the magnetic field and its secular variation provide myriad information on the geodynamo processes, unfortunately, they only reveal the part of the magnetic field contained in the outermost layer of the fluid core. The details of the magnetic field deeper in the core are not directly observable at the surface. This is a complication because disparate models of the geodynamo with markedly different internal dynamics can all produce magnetic fields at the surface of the core that have similar Earth-like characteristics, making it difficult to discriminate between the models. In fact, the results of various numerical simulations illustrate this difficulty particularly well (e.g. Kuang and Bloxham, 1997a).

To observe other aspects of the dynamics involved in the geodynamo, we are forced to use indirect methods, making suitable dynamical assumptions along the way. The idea is to infer parts of the dynamics from its manifestations in the various geophysical observations at the surface. Of course these observations include the magnetic field as well. A good example of such indirect method is the use of "frozen flux hypothesis", with which one can build maps of time-dependent fluid motion at the surface of the core that are consistent with the observed secular variation. The obtained flows can then in turn be used as constraints on

the dynamics in the core. Another example, is to use the observed changes in the rotation rate of the mantle as a way to constrain flows in the core. If the angular accelerations of the mantle are caused by angular momentum exchange with the core, then the core flows that carry the changes in angular momentum in the core can be constrained.

This thesis is an effort in providing better constraints and understanding of the geodynamo. The central theme, linking all aspects of the work presented in this dissertation, is a component of the flow in the Earth's core called torsional oscillations. This flow is inferred in the core by the very indirect observations described above: it can explain both a part of the secular variation of the field and the changes in the Earth's rotation rate at decade timescales. The observation of torsional oscillations is a small triumph for geodynamo theory, which predicts the occurrence of this component of the flow. As a result, torsional oscillations are arguably the element of the dynamics in the core for which we have the most confidence.

Parts of the goals of this thesis are to extend our theoretical knowledge of torsional oscillations and to determine whether they manifest themselves in other geophysical observations at the surface. It is therefore apropos to present in a prelude the key concepts and historical development behind torsional oscillations.

1.3 Torsional oscillations

Torsional oscillations in the Earth's fluid core are the azimuthal oscillations of rigid cylindrical surfaces coaxial with the rotation axis (figure 1.1). Rigid azimuthal cylindrical flows of the sort are expected in the fluid core. In the absence of other forces, a fluid in rapid rotation must establish a balance between pressure gradients and the Coriolis force (e.g. Greenspan, 1968). The flows that can satisfy this force balance identically are called geostrophic and have the property that they are invariant along the rotation axis. This restriction on the fluid motion is known as the Proudman-Taylor constraint (Proudman, 1916; Taylor, 1917). In the fluid core, the spherical geometry of the solid boundaries imposes an even more severe restriction on the flow. Because radial flows must vanish at the boundaries, the only possible geostrophic flows are those in which cylindrical surfaces rotate rigidly in the azimuthal direction (Bullard and Gellman, 1954).

External forces do not vanish identically in the core and flows are not purely geostrophic.

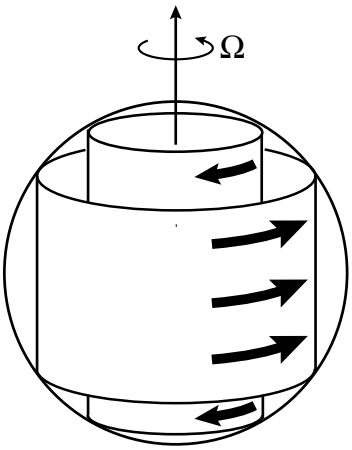

Figure 1.1: Torsional oscillations in the core. The direction of the azimuthal cylindrical flow indicated by the black arrows oscillates in time. The Earth's axis of rotation points in the direction of Ω.

When the Lorentz force is reintroduced, the cylindrical surfaces at different radii are no longer rotating freely relative to one another. The magnetic field that permeates the core tends to be "frozen" in the fluid and a differential rotation of the cylinders shears the radial component of the field in the azimuthal direction. By Lenz' law, this produces a force that opposes further relative motion between the cylindrical surfaces. Thus, the radial component of the magnetic field behaves as if it were elastic strings attached to the cylindrical surfaces, and provides a restoring force for the establishment of waves that propagate in the direction perpendicular to the rotation axis. These are torsional oscillations. Since the restoring force is purely magnetic, torsional oscillations are a type of Alfvén waves (Alfvén, 1942).

Strictly speaking, torsional oscillations are not a geostrophic flow, because they result from an azimuthal force balance between the fluid acceleration and Lorentz forces. However, since the force balance in the direction pointing away from the rotation axis remains geostrophic and the form of the flow is identical to that of geostrophic flows, it is convenient to think of torsional oscillations as time-dependent geostrophic flows.

The importance of these geostrophic flows in the core and their intimate connection to the dynamics governing the geodynamo was first established by Taylor (1963). He showed that if one integrates the azimuthal component of the momentum equation over the surface of cylinders coaxial with the rotation axis, the Lorentz force is the only term in the leading

order force balance that does not identically vanish. This imposes a morphological constraint on the magnetic field in the core, namely that the axial Lorentz torque must vanish at all times, i.e.

$$\int_{\Sigma} \left((\nabla \times \mathbf{B}) \times \mathbf{B} \right)_{\phi} d\Sigma = 0 , \tag{1.1}$$

where $d\Sigma = s\, d\phi\, dz$ and (s, ϕ, z) are cylindrical coordinates. This result is referred to as Taylor's constraint. The restriction on the magnetic field is severe: not only it must organize itself spatially to satisfy (1.1), its time changes from advection and shear by flow must also be such that (1.1) remains satisfied. In theory, when Ohmic diffusion is allowed, an equilibrium may be reached where the changes in the magnetic field due to flows are exactly compensated by diffusion. Starting from a state where Taylor's constraint is satisfied, it would then remained satisfied at all times and the geodynamo is said to be in a Taylor state.

In general though, one may expect that the core contain complex flows acting on a complicated magnetic field geometry and that the perfect equilibrium cannot be maintained. When the magnetic field changes so that (1.1) is no longer satisfied, one possibility to balance the Lorentz torque is by an azimuthal acceleration of the cylindrical surface,

$$\frac{\partial}{\partial t} \mathcal{V}_{\phi}(s) = \frac{1}{\rho \mu} \int_{\Sigma} \left((\nabla \times \mathbf{B}) \times \mathbf{B} \right)_{\phi} d\Sigma . \tag{1.2}$$

where $\mathcal{V}_{\phi}(s)$ is the geostrophic velocity, ρ is the density and μ is the permeability of free space. The class of motion described by the above equation is therefore not directly influenced by the Coriolis force, but only by the magnetic field. The above system allows oscillatory behavior of geostrophic motion (i.e. torsional oscillations) about an equilibrium position where the Lorentz torque vanish. The damping of these oscillations by diffusion of the magnetic field naturally brings back the system towards this equilibrium. The geostrophic flows are therefore an essential ingredient of the geodynamo as they always allow the system to relax towards a state where (1.1) is satisfied everywhere in the core. A dynamo that satisfies (1.2), and for which the part of the magnetic field that does not satisfy (1.1) is involved in torsional oscillations, is said to be in a quasi-Taylor state (e.g. Bloxham, 1998).

Braginsky (1970) was the first to exploit this theoretical concept in an effort to explain geophysical observations. He sought to explain the decade variations in the length of day

(LOD) as exchanges of angular momentum between the mantle and the core, where the angular momentum of the core would be carried by torsional oscillations. This type of fluid motion, he argued, would also be consistent with a part of the observed secular variation of the magnetic field. Braginsky established the wave equation for the torsional oscillations predicted by Taylor. For $\mathcal{V}_\phi(s)$ proportional to $\exp(-i\omega t)$, it is given by

$$-\omega^2 \rho s^2 h \mathcal{V}_\phi(s) = \frac{d}{ds}\left(\frac{s^3 h}{\mu} < (B_s)^2 > \frac{d}{ds}\frac{\mathcal{V}_\phi(s)}{s} \right) - i\omega f(s)\,, \tag{1.3}$$

where h is the height of the cylinder, $f(s)$ is the torque at the ends of the cylinders due to surface forces at the fluid-solid boundaries, B_s is the the s-component of the field which is assumed to remain steady on the timescale of the oscillations, and $<>$ denotes average over the cylinder surface. Note that the restoring force does not involve the steady azimuthal part of the magnetic field, as this component is not sheared by torsional oscillations. More complete treatment of equation (1.3) can be found in Braginsky (1970, 1984) and Jault (2003).

Solutions of the torsional oscillations equation depend on the knowledge of the radial magnetic field everywhere in the core and on the physical properties near the boundaries that enter $f(s)$. Exact solutions are then not obtainable without solving the dynamo problem as a whole. Nevertheless, estimates of the form and periodicity of the natural modes of oscillation can be obtained for simple magnetic field morphologies and no end-cylinder coupling. An order of magnitude estimate for the period of the fundamental mode is given by

$$\tau_{to} \approx c \left(\frac{\rho\mu}{< (B_s)^2 >} \right)^{1/2}, \tag{1.4}$$

where c is the radius of the core. As an example, using a typical value of $B_s = 0.5$ mT, we find $\tau_{to} \sim 25$ years, and corresponds to the timescale of the changes in LOD and of some of the secular variations.

Braginsky's original idea that torsional oscillations can both explain the LOD changes while being consistent with a part the observed changes of the magnetic field has since been confirmed. Jault *et al.* (1988) have reconstructed the changes in the rigid geostrophic velocities between 1969 and 1985 from maps of the flow at the top of the core which best explain the secular variations of the magnetic field. The changes in core angular momentum carried

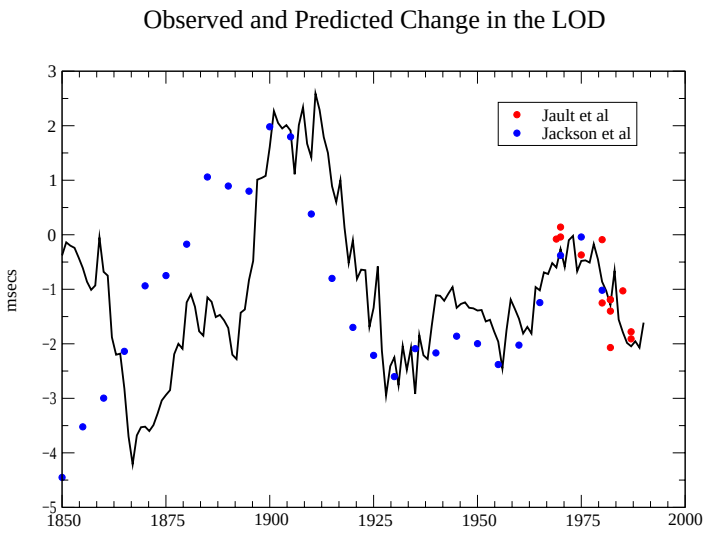

Figure 1.2: Variations in the length of day from geodetic measurements (solid line) and the prediction based on the assumption that the axially symmetric and equatorially symmetric azimuthal part of the geostrophic flow at the CMB is rigid within the core (red dots from Jault *et al.* (1988); blue dots from Jackson *et al.* (1993))

by these rigid flow motions correspond roughly to the changes in mantle angular momentum required to explain the LOD variations during that period (see figure 1.2). Jackson *et al.* (1993) subsequently showed that this correlation extends back to 1900. In addition, the time variations of the rigid cylindrical flows suggest large exchanges of angular momentum inside the core and relatively little exchange with the mantle, indicating that the motion is likely to be that of waves of the type consistent with torsional oscillations (Jackson *et al.*, 1993; Jault *et al.*, 1996), a fact that was later verified by Zatman and Bloxham (1997, 1998). The torsional oscillations in the Earth's core retrieved from the secular variation of the magnetic field between 1900 and 1990 are shown in figure 1.3, with velocity amplitudes on the order of 10 km/yr and typical periods of decades.

Recently, Bloxham *et al.* (2002) showed that torsional oscillations with shorter wavelength and shorter timescales provide a natural explanation for a puzzling part of the secular variation, the geomagnetic jerks. The latter are the sudden changes in the trend of the time-derivative of the magnetic field observed sporadically throughout the last century (Courtillot and Le Mouël, 1984). These sudden changes are global, yet specific events are

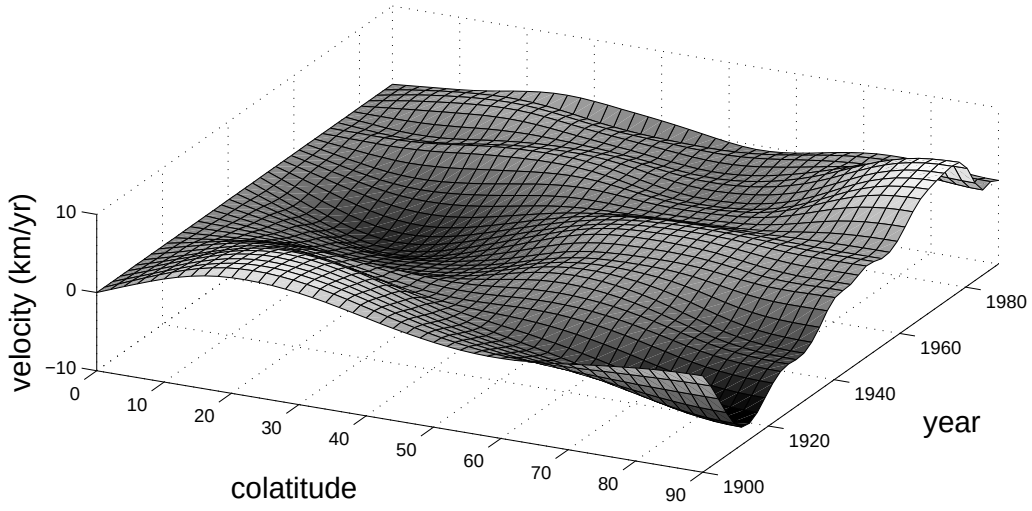

Figure 1.3: Rigid component of the azimuthal velocity in the core as a function of co-latitude between 1900 and 1990 obtained by Zatman and Bloxham (1997).

not recorded by all observatories. The study of Bloxham *et al.* (2002) showed that the geomagnetic jerks are well reproduced when the time-dependent part of the flow is restricted to rigid cylindrical motions, indicating that this part of the flow alone is sufficient to explain the jerks. The rigid motions were then shown to be comprised of waves consistent with torsional oscillations. This further confirms the presence of torsional oscillations in the core and indicates that higher modes than those shown in figure 1.3 are also excited.

Torsional oscillations are expected on theoretical grounds and their manifestation in the dynamics of the Earth's core is indeed observed. Therefore, they represent perhaps the most robust link between geophysical observations on historical timescales and the dynamics responsible for maintaining the field against Ohmic decay on geologic timescales. They are a window through which we can observe some aspects of core dynamics. Theoretical models of the dynamical processes involved in the geodynamo must then be consistent with torsional oscillations. Inversely, the observed torsional oscillations can be used to extract a wealth of physical quantities and dynamics in the core that are otherwise not directly observable. For instance, Zatman and Bloxham (1997, 1998) produced a model of the internal rms amplitude of B_s as a function of cylinder radius from the observed torsional oscillations. Similarly, Buffett (1998) and Mound and Buffett (2003) used equation (1.3)

in order to constrain physical parameters near the core-mantle boundary and the nature of the torque that transfers the angular momentum between the mantle and the core.

While a part of the secular variations of the magnetic field are explained by a combination of steady flow (Bloxham, 1992) and torsional oscillations, an important part of the signal remains unexplained (Jault, 2003). If the unexplained variations are due to fluid motion, time-dependent flows that contain a non-axisymmetric ingredient and also have meridional components are required in order to fully account for the secular variations. Thus, while torsional oscillations presents a simple theory of the dynamics, it is incomplete. Alternatively, if the remaining part of the secular variations are due to the propagation of a different type of waves (Hide, 1966; Jackson, 2003), the connection between these waves and torsional oscillations must be established. Probably the more developed body of work devoted to this issue is, once again, that of Braginsky. He investigated the possibility that a stably stratified layer at the top of the core may provide the connection between torsional oscillations and the remaining part of the secular variations. Convection in the Earth's core may be powered, at least in part, by the release of light fluid elements in the process of inner core crystallization (Braginsky, 1963, 1964). The lighter fluid may accumulate at the top of the core and form a stably stratified layer in which the dynamics would be markedly different than in the bulk of the core. Braginsky (1984, 1993, 1999) developed the theoretical foundation for these dynamics, with a focus on the types of waves that could develop in this layer and their interaction with the torsional oscillations. His main conclusion, that the unexplained part of the secular variations may indeed result from Magnetic-Archimedean-Coriolis (MAC) waves in this stratified layer, remains for the moment at the theoretical level.

Another important issue still unresolved is that of the excitation of torsional oscillations. Estimates of the coupling with the mantle suggest that torsional oscillations should be damped after a few periods (Zatman and Bloxham, 1997, 1998, 1999; Buffett, 1998; Mound and Buffett, 2003), which indicates that an efficient excitation mechanism must exist. The behavior described above, where torsional oscillations occur with respect to a steady equilibrium state, is correct only if the waves are excited by a mechanism which acts suddenly and then plays no further role in the dynamics. A perhaps more likely scenario is one where a forcing term needs to be added to equation (1.3) and plays an active role in the dynamics at all times. If this latter view is correct, the resulting geostrophic flows

would consist of a combination of forced and free "torsional oscillations". The nature of this forcing is at present unknown but perhaps it simply consists of the continual changes in the magnetic field, and hence of the Lorentz torque on any cylinder, produced by the convective dynamics in the core. This is the scenario envisaged by Taylor (1963). The changes in the Lorentz torque may occur on many different timescales but those that are close to the natural modes of torsional oscillations would provide efficient excitation.

The problem of the excitation of torsional oscillations is connected to the theoretical issues concerning Taylor state dynamos. Solutions of the magnetic field satisfying Taylor's constraint have been found for kinematic dynamos (e.g. Fearn and Proctor, 1987a; Jones, 1991; Hollerbach *et al.*, 1992; Jault, 1995), but a fully dynamic solution has yet to be achieved (e.g. Fearn and Proctor, 1987b). Because the magnetic field geometry most suitable for a Taylor state dynamo is not known, its time-dependent part that lead to torsional oscillations is not well known either. Therefore, the elucidation of the excitation mechanism will likely lead to an improved understanding of the equilibration mechanism involved in a Taylor state dynamo, and vice-versa.

1.4 Scope of this thesis

This thesis is concerned with some of the questions raised in the previous section. The work that it contains can be separated into three broad categories, all connected with torsional oscillations. The first category can be described as attempts to increase our theoretical understanding of torsional oscillations. The work in chapter 2 falls into this category. The second category, which corresponds to the work included in chapter 3 and 4, can be defined as attempts at observing the manifestation of torsional oscillations in other geophysical observations at the surface. The third category, in chapter 5, contains aspects of the first and second: it is an attempt at extending the bridge between theory and observations for flows in the core.

The results of the last three chapter of this thesis have implications that extend beyond geodynamo theory. Indeed, for all three, the purpose is to explain a specific geophysical observation with a mechanism involving dynamics in the fluid core. To be more specific, the variations in the Earth's rotation rate and its direction with respect to the mantle, and the variation in the Earth's gravitational field and geometric figure, are all geophysical ob-

servations that are touched by the work in this thesis. Other physical quantities, such as the elastic parameters of the inner core and lower mantle, also participate in these dynamical mechanisms and our results may help to constrain their values.

Below, a brief description of each of the next four chapters is presented. Each chapter is designed to be self-contained. An unfortunate consequence is that some of the ideas and concept are repeated. This is especially the case for the theoretical aspects of torsional oscillations.

1.4.1 Torsional oscillations in a numerical model of the geodynamo

A promising future avenue to further our understanding of torsional oscillations and of their excitation is through numerical models of the geodynamo. This is because the time span of the simulations can far exceed the historical record, and also because the simulations allow direct access to field variables at every location in the core and thus offer a means to examine the details of the dynamics. As for theoretical models of the geodynamo, realistic numerical models are constrained to include the dynamics of torsional oscillations.

In the second chapter of this thesis, we investigate whether torsional oscillations are produced in the Kuang-Bloxham numerical model of the geodynamo (Kuang and Bloxham, 1997a, 1999). We show that oscillations of geostrophic flows are indeed part of the dynamics resolved by the model and that their excitation is consistent with the above scenario of continual torques produced by the convective dynamics. However, these oscillations do not follow equation (1.3) because the current limits in computation prevent the use of realistic Earth parameters in the model, and the extrapolation of the results to the real Earth remains uncertain. Nevertheless, the ability of the numerical model to produce geostrophic flows is a step in the right direction. With numerical models becoming increasingly closer to Earth-like conditions, there is hope that they will soon comprise realistic torsional oscillations.

1.4.2 Torsional oscillations and the Earth's gravitational field

As we discussed above, torsional oscillations in the core are well established. One may wonder whether they may leave an imprint on other observable geophysical quantities as a result of their interaction with the mantle and the inner core. In chapter 3, we investi-

gate whether torsional oscillations may be detectable in the Earth's gravitational field and vertical ground motions at the Earth's surface.

The Coriolis force associated with rigid azimuthal cylindrical flows is balanced by pressure gradients, where surfaces of constant pressure coincide with the cylindrical surfaces of the rigid flow. Along the core-mantle boundary (CMB), the variation in geostrophic pressure with latitude results in gradients in surface force from the pole to the equator. Consequently, a latitude dependent radial deformation of the CMB is produced. Because of the density discontinuity between the fluid core and the mantle, radial deformations of the fluid-solid interface produce changes in the gravitational field. The same process also occurs at the inner core boundary (ICB). As the pressure variation caused by torsional oscillations is axisymmetric and vary on decade timescale, they may leave an imprint as decade variations in the zonal even harmonics of the gravitational field measured at the surface. The small radial deformations involved in the process may also be detectable at the surface.

We have built a model to calculate the changes in the gravity field and in radial deformations in the whole Earth that are produced by the geostrophic pressure associated with torsional oscillations. This model also includes the effects due to the changes in the rotation rate of the mantle and inner core that occur to balance the change in angular momentum carried by the torsional oscillations. One motivation behind the work in this chapter was to verify whether the recently observed episodic time-variations in the the elliptical part of the gravity field (J_2) about its secular trend (Cox and Chao, 2002) could be explained by this phenomenon. We show that the amplitude of the changes in the gravity field that are predicted from our model are 10 times smaller than the temporal changes in J_2 that are observed about the trend. The changes in the gravity field and the vertical ground motion produced are below the current level of precision in the measurement, but may be detectable in the near future.

1.4.3 Torques on the inner core and the Markowitz wobble

As for chapter 3, the objective of chapter 4 is to investigate the possibility that torsional oscillations may account for observed decade variations in a geophysical observation. In chapter 4, we are concerned about the variations in the orientation of the Earth's rotation

axis with respect to the mantle, commonly referred to as polar motions. Measurements seem to suggest the existence of a decadal polar molar motion that is somewhat irregular and polarized along a specific longitude. This polar motion is known as the Markowitz wobble, named after William Markowitz who first identified it in the data (Markowitz, 1960). The mechanism responsible for the Markowitz wobble is not known, but its main periodicities are similar to those of the variations in the Earth's rotation rate (Poma and Proverbio, 1980; Schuh *et al.*, 2001). Since torsional oscillations are at the source of the decadal variations in the Earth's rotation rate, they may also be at the source of the mechanism responsible for the Markowitz wobble.

The mechanism that we investigate in chapter 4 involves torques on the inner core. A tilted inner core permits exchange of angular momentum between the core and the mantle through gravitational and pressure torques and, as a result, changes in the direction of Earth's axis of rotation with respect to the mantle. We have developed a model to calculate the amplitude of the polar motion that results from an equatorial torque at the inner core boundary which tilts the inner core out of its alignment with the mantle. We show that a decade polar motion of the same amplitude as the observed Markowitz wobble requires a torque of 10^{20} N m which tilts the inner core by 0.07 degrees. This result critically depends on the viscosity of the inner core; for a viscosity less than 5×10^{17} Pa s, larger torques are required. We then investigate the possibility that a torque of 10^{20} N m with decadal periodicity can be produced by electromagnetic coupling between the inner core and torsional oscillations. We demonstrate that a radial magnetic field at the inner core boundary of 3 to 4 mT is required to obtain a torque of such amplitude. The resulting polar motion is eccentric and polarized, in agreement with the observations.

1.4.4 Azimuthal flows and changes in LOD at millennial timescales

A part of the time-dependent variations observed in archaeomagnetic field models consist of episodic eastward and westward drifts with a period of about a thousand years. Variations in the length of day reconstructed from ancient records of eclipses contain an oscillating component with a periodicity of roughly 1500 years. Time-dependent azimuthal flows in the core with variations at millennial timescales could reconcile these observations, just as torsional oscillations provide a consistent explanation for similar observations at decade

timescales.

In chapter 5, we attempt to extend the successful link between theory and observations obtained at decade timescales for torsional oscillations. Here, we are interested in flows that have millennial timescale variations. Using standard inversion techniques, we obtain time-dependent azimuthal flows at the surface of the core that can explain parts of the archaeomagnetic secular variation. We restrict the inversion to flows that carry angular momentum in the core. We show that the time-dependent azimuthal flows that can consistently explain both the magnetic field variations and the changes in angular momentum of the core are characterized by a shear in the axial direction, in contrast to the decade timescales variations. We interpret these as oscillations in the thermal and magnetic winds and discuss the implications for the geodynamo and core-mantle coupling at millennial timescales.

Chapter 2

Torque balance, Taylor's constraint and torsional oscillations in a numerical model of the geodynamo

2.1 Introduction

We believe that the magnetic field of the Earth is generated and maintained against decay by convective motions in the fluid outer core, a process known as the geodynamo. However, the exact details of the dynamics involved are unknown. This is partly because, although we have a several hundred-year long record of the global geomagnetic field at the core-mantle boundary (CMB) from which we can build flow maps, we have little information on the fluid velocity and magnetic field inside the core.

Indeed, the only part of the flow in the interior of the core that can be inferred from observation is a time-dependent zonal wind component which consists of azimuthal motions of rigid cylindrical surfaces aligned with the rotation axis. Because of its simple geometry, this rigid azimuthal flow is easily obtained from flow maps at the CMB: it represents the part of the axisymmetric azimuthal velocity that is symmetric about the equator. Since the angular momentum of the whole Earth must be conserved, changes in angular momentum of the core calculated from the time-dependent rigid azimuthal flows should correspond

[1] The work presented in this chapter has been published previously in modified form and is reprinted from *Physics of the Earth and Planetary Interiors* (Dumberry and Bloxham, 2003), with permission from Elsevier

with changes in the angular momentum of the mantle measured in terms of variations in length-of-day. The agreement between the two is particularly good for the last few decades (Jault *et al.*, 1988; Jackson *et al.*, 1993), indicating that the time-varying part of the recovered rigid azimuthal flow, which has the form of a wave with decade periods propagating in the direction perpendicular to the rotation axis (Zatman and Bloxham, 1997, 1998; Pais and Hulot, 2000; Hide *et al.*, 2000), is well determined.

These decadal oscillations of rigid cylindrical surfaces place a constraint on theoretical models of the geodynamo. One model that indeed predicts the occurrence of these time-dependent rigid azimuthal motions is that of a "Taylor state dynamo" (Taylor, 1963) in which the dynamics are controlled by a morphological constraint on the magnetic field: the azimuthal component of the Lorentz force must vanish when integrated on cylindrical surfaces co-axial with the rotation axis. When this constraint is not satisfied, rigid accelerations of cylindrical surfaces are produced in order to reestablish a Taylor state. In the process, rigid accelerations excite azimuthal oscillations of these rigid surfaces, which are referred to as torsional oscillations (Braginsky, 1970).

Observations thus suggest that the current dynamic state of the Earth's core is that of a "quasi-Taylor state", where the magnetic field is organized in such a way that the azimuthal Lorentz force integrated over cylindrical surfaces vanishes, except for the part involved in torsional oscillations. Important information about the dynamics in the core can then be extracted from the torsional oscillations. For instance, since the restoring force for the torsional oscillations is provided by the component of the magnetic field perpendicular to the rotation axis, we can then obtain information about the magnetic field strength inside the core for which we otherwise have no direct observation (Zatman and Bloxham, 1997, 1998). Similarly, the dissipation of the oscillating motion has revealed information about coupling between the core and the mantle at the CMB (Buffett, 1998; Zatman and Bloxham, 1999).

However, many questions remain unanswered. For instance, are the currently observed torsional oscillations being excited at their typical amplitudes, or are they at a maximum or minimum? A recent flow inversion suggests that the amplitude of higher wavenumber torsional oscillations has been growing for the last 50 years (Bloxham *et al.*, 2002). A more general question is whether torsional oscillations are a permanent feature of the dynamo or if they are simply a transient between two quasi-equilibrium Taylor states. For many

such questions, observations alone may be insufficient to provide answers. This is in part because our record of geomagnetic field data from which core flows can be built covers only the last 160 years, which corresponds to 2 or perhaps 3 full periods of the fundamental mode of torsional oscillations. Therefore it is difficult to assess whether the observed torsional oscillations are representative of the average state of the geodynamo.

Additionally, the excitation of torsional oscillations remains an open question. An efficient excitation mechanism would appear to be required since their damping time may be short (Zatman and Bloxham, 1997). Mechanisms that have been proposed include instabilities in MAC waves (Braginsky, 1970), mean torques generated by the nonlinear interaction of turbulent fluctuations in the flow (Braginsky, 1984), and coupling of the main flow in the core to a stratified surface layer at the CMB (Braginsky, 1993, 1999), in which instabilities could excite natural oscillations resembling Magnetic-Archimedean-Coriolis (MAC) waves, which could, in turn, excite torsional oscillations in the bulk of the core. An alternative mechanism is axial gravitational coupling between the inner core and the mantle (Buffett, 1996a,b): torsional oscillations couple the mantle, the inner core and the outer core, forming a coupled oscillating system. The natural frequencies of this system are excited by fluctuating axial electromagnetic torques on the inner core.

A different class of mechanisms is *in situ* excitation caused by the changes of the magnetic field in the core as originally envisaged by Taylor (1963). If the core is in a Taylor state, then the axial Lorentz torque is large everywhere on a cylindrical surface but cancels when averaged over the entire surface of the cylinder. Small local changes in the magnetic field due to the underlying evolution of the magnetostrophic balance could then produce a large Lorentz torque. The latter induces a rigid acceleration of the cylindrical surface which initiates torsional oscillations. Whether torsional oscillations are excited by this mechanism is a difficult question to address with observations since we do not have access to the convective flow and magnetic field morphology inside the core.

Perhaps a more promising avenue to study torsional oscillations is through three dimensional self-consistent numerical models of the geodynamo. Since the pioneering work of Glatzmaier and Roberts (1995), there exists now a large number of numerical models (recent reviews include Dormy *et al.* (2000), Glatzmaier (2002) and Kono and Roberts (2002)). These models provide direct access to all fields at any location and thus offer a means to examine the details of the dynamics. Moreover, simulations can extend in time

far longer than the time span of the historical record. Of course, the danger is that the numerical models might provide a correct solution to a mathematical problem which is not representative of the dynamics of the core. This is to some extent the current situation in geodynamo modeling as computational limitations force the use of a parameter regime that is different from the Earth's core (e.g. Glatzmaier and Roberts, 1995; Kuang and Bloxham, 1997a; Dormy *et al.*, 2000; Glatzmaier, 2002). However, as computing resources and numerical methods improve, our confidence in the results provided by these models will also improve.

In this chapter, we present a study of torsional oscillations in one such numerical model, the Kuang-Bloxham model (Kuang and Bloxham, 1997a, 1999). This model was built specifically in order to produce a dynamo which captures the dynamics of a Taylor state and is therefore well suited for our investigation. In a recent study, Kuang (1999) showed that the azimuthal force balance on cylindrical surfaces is such that the Lorentz force is mostly balanced by inertial forces, both of which are twice as large as viscous forces, hence suggesting the presence of strong torsional oscillations. Here, we investigate this question in more detail.

The primary goal of the present study is to demonstrate that the numerical model captures the essence of an inertial state, with rigid accelerations being produced in response to unbalanced axial torques on cylindrical surfaces. We will show that this is indeed the case. A second goal is then to investigate how the ensuing azimuthal oscillations of rigid surfaces may resemble or differ from torsional oscillations observed in the Earth's core. Additionally, we want to understand the way in which the torque balance is disrupted and, hence, how rigid accelerations are excited. Our hope is that the dynamics observed in the model may help to illuminate some aspects of a Taylor state dynamo and torsional oscillations. In the present study, we are only investigating one model calculation with a specific set of parameters. This is sufficient for a first study on torsional oscillations in numerical models since our primary concern is to demonstrate that they are indeed emerging as part of the solution. A more detailed analysis of the way that the torque balance is altered by the parameters of the calculation is left for future study. We also focus our investigation in this chapter on the region of the core outside the cylinder tangential to the inner core (the tangent cylinder). This is the region in which torsional oscillations are observed in the data and where it is most certain that the quasi-Taylor state applies.

One of the important results emerging from the model is that the nature of the equilibrium force balance on the cylinders is such that the contributing forces are continually fluctuating about their mean. One cause of these fluctuations is a large differential rotation between cylinders, which is continually shearing the non-axisymmetric velocity and magnetic field structures. This causes local changes in the Lorentz torque and Reynolds stresses and a chaotic evolution of the total torque on cylindrical surfaces. Continual chaotic rigid accelerations are then required to balance this torque. Results of the model therefore support the excitation of rigid azimuthal oscillations by *in situ* dynamics.

While we recognize the danger of relating the results of a numerical model operating with different parameters from the Earth's core, we argue that torsional oscillations in the core may result from a similar process. Under this scenario, the geometry of the magnetic field in the core is such that the time-averaged Lorentz torque vanishes (i.e. satisfies Taylor's constraint), but the instantaneous Lorentz torque is continually fluctuating in a chaotic way about this time-averaged Taylor state due to interactions between the non-axisymmetric part of the field and the mean differential rotation flow. The chaotic evolution of the Lorentz torque provides a continual excitation for free oscillations which propagate on top of this dynamic background. The observed torsional oscillations would then represent a mixture of free and forced oscillations.

This chapter is organized as follows. In the next section we revisit the dynamical constraints on cylindrical surfaces that lead to a quasi-Taylor state. This section provides the theoretical basis for the interpretation of the numerical results. Similar treatments can be found in the literature, for instance in reviews by Roberts and Soward (1992), Fearn (1994), Fearn (1998), and Bloxham (1998). In section 2.3, we discuss the limitations of the numerical model and how these limitations affect the prospect of capturing the dynamics of torsional oscillations. We then investigate the dynamics of the torque balance that emerges from the numerical model. In section 2.4, we focus on the rigid azimuthal oscillations, first by showing that the motion is quasi-rigid and then by testing if these rigid oscillations correspond to torsional oscillations. We also describe a mechanism responsible for the excitation of the rigid oscillations in the model. Finally, we discuss in section 2.5 how the results of the numerical model may be relevant for the Earth's core and consider future strategies to produce torsional oscillations in the numerical model.

2.2 Dynamical torque balance on cylindrical surfaces

2.2.1 Taylor's constraint

As first demonstrated by Taylor (1963), when one integrates the azimuthal component of the momentum equation over a cylindrical surface aligned with the rotation axis, some terms vanish from the force balance. The pressure gradient is identically zero, the Coriolis force vanishes if the fluid is assumed incompressible, and the buoyancy force is also zero because it has no azimuthal component. There remains a balance between inertial forces, Lorentz forces and viscous forces, given, in non-dimensional form, by

$$R_o \int_\Sigma \left(\frac{\partial \mathbf{u}}{\partial t} \right)_\phi d\Sigma + R_o \int_\Sigma (\mathbf{u} \cdot \nabla \mathbf{u})_\phi \, d\Sigma = \int_\Sigma ((\nabla \times \mathbf{B}) \times \mathbf{B})_\phi \, d\Sigma + E \int_\Sigma \left(\nabla^2 \mathbf{u} \right)_\phi d\Sigma \,. \quad (2.1)$$

Here, R_o is the Rossby number, E is the Ekman number, $\mathbf{u}$ is the velocity field, $\mathbf{B}$ is the magnetic field, t is time measured in units of magnetic diffusion timescale, and $d\Sigma = s\, d\phi\, dz$, where (s, ϕ, z) are the usual cylindrical coordinates. The azimuthal force on a cylindrical surface is proportional to the axial torque. For convenience, we will refer to (2.1) as the torque balance. The Rossby and Ekman numbers represent respectively the importance of inertial forces and viscous forces relative to the Coriolis force, and are defined by

$$R_o = \frac{\eta}{2\Omega r_o^2}, \qquad\qquad E = \frac{\nu}{2\Omega r_o^2}\,, \quad (2.2)$$

where r_o is the radius of the core, Ω is the frequency of Earth's rotation, η is the magnetic diffusivity and ν is the kinematic viscosity. The typical scales for length, time and magnetic field in the above non-dimensionalization are respectively, $L = r_o$, $\tau_\eta = r_o^2/\eta$ and $B = \sqrt{2\Omega\rho\mu\eta}$, where ρ is the mean density and μ is the magnetic permeability. Typical values for the Rossby and Ekman numbers are $R_o \approx 10^{-9}$ and $E \approx 10^{-15}$ (for molecular values of the viscosity). If the scale of the magnetic field inside the core is $O(1)$, which corresponds to a field of about 2 mT, then the inertial and viscous term in (2.1) are both vanishingly small with respect to the Lorentz term and,

$$\int_\Sigma ((\nabla \times \mathbf{B}) \times \mathbf{B})_\phi \, d\Sigma = 0\,. \quad (2.3)$$

The morphology of the magnetic field inside the core is such that the torque from the Lorentz force must vanish when integrated over a cylindrical surface co-axial with the rotation axis. This result is known as Taylor's constraint (Taylor, 1963) and solutions that satisfy (2.3) are said to represent a Taylor state.

2.2.2 Ekman state

Evidently, the Lorentz torque at any given time is not required to vanish identically but rather to have a magnitude on the order of the largest of the small terms in (2.1). One limiting case is obtained by balancing the Lorentz torque by viscosity. The viscous forces are most important in thin boundary layers at the CMB, and produce a secondary poloidal flow through the whole core as a result of Ekman pumping (e.g. Greenspan, 1968; Pedlosky, 1987). The viscous drag at the boundaries is thus communicated through the whole cylinder. The force balance in this case is given by

$$\frac{1}{4\pi s}\int_{\Sigma}\left((\nabla\times\mathbf{B})\times\mathbf{B}\right)_{\phi}\,d\Sigma = \frac{E^{\frac{1}{2}}}{(1-s^2)^{\frac{1}{4}}}\mathcal{V}_{\phi}(s)\,, \tag{2.4}$$

where $\mathcal{V}_{\phi}(s)$ is the rigid azimuthal velocity of the cylinder surface (Roberts and Soward, 1992; Fearn, 1994; Hollerbach, 1996). In the dynamo theory literature, $\mathcal{V}_{\phi}(s)$ is usually referred to as the geostrophic flow and we adopt this terminology throughout this paper. (We note that this should not be confused with the terminology used in core flow modeling, where "geostrophic flow" is employed in its more general sense to imply any velocity field which satisfies a balance between the Coriolis force and pressure gradients.) Equation (2.4) is no longer valid for $s \approx 1$. When (2.4) applies, the geodynamo is said to be in an Ekman state and changes in the magnetic field are balanced by a viscous readjustment of the geostrophic flow. Theoretical considerations of the Ekman state suggest that an equilibration of the Lorentz and viscous torque is only possible with a magnetic field amplitude of $O(E^{\frac{1}{4}})$ (Fearn, 1994). Even if turbulent values of the viscosity are adopted ($E \approx 10^{-9}$), this scaling implies a magnetic field amplitude of about 0.1 Gauss in dimensional units, two orders of magnitude smaller than the observed field at the CMB (e.g. Bloxham and Gubbins, 1985). The Ekman state is therefore not the appropriate balance for the Earth's core because the viscous torque alone cannot provide the balance for a non-zero Lorentz torque while maintaining a magnetic field of $O(1)$.

2.2.3 Model Z

Braginsky (1975, 1978, 1994) showed an alternative magnetic field configuration for which the Lorentz torque is balanced by dissipation at the CMB. In this model, called "Model Z", B_z and B_ϕ are both $O(1)$, while B_s is much smaller. The Lorentz torque in the bulk of the fluid is very small simply because B_s, on which the torque depends, is very small. The small Lorentz torque in the bulk of the core is balanced by viscous friction at the boundary, just as above, or by "magnetic friction" (Braginsky, 1970, 1988) if there is an electrically conducting layer at the base of the mantle. The advection of poloidal magnetic field lines by a geostrophic flow $\mathcal{V}_\phi$ is resisted by the finite time the field takes to diffuse through the layer. This produces a Lorentz force at the boundary which opposes $\mathcal{V}_\phi$, similar to a viscous friction effect.

It has been shown that if one keeps the acceleration term in the force balance, the scaling of Model Z breaks down when the spin-up timescale is longer than the timescale for inertial adjustment (Jault, 1995). For the Earth's core, the viscous spin-up timescale is on the order of 10^4 years (Gubbins and Roberts, 1987), while the magnetic spin-up timescale may be as short as 30 years if the conductance of the layer is as high as 10^8 S (Buffett, 1998). Hence, the decade timescale variations of the rigid azimuthal velocity observed in the flow may represent this adjustment through magnetic friction at the CMB in a Model Z dynamo. However, the amplitude of $\mathcal{V}_\phi$ that is required is an order of magnitude larger than the largest observed flow velocities (Braginsky, 1994). In addition, other observations also suggest that the Model Z is not the appropriate dynamic state of the core, as we argue in the next section.

2.2.4 Quasi-Taylor state and torsional oscillations

If the unbalanced part of the Lorentz torque in (2.3) is equilibrated by the acceleration term, then we have

$$R_o(1-s^2)^{\frac{1}{2}}\frac{\partial}{\partial t}\mathcal{V}_\phi(s,t) = \frac{1}{4\pi s}\int_\Sigma \left((\nabla\times\mathbf{B})\times\mathbf{B}\right)_\phi \, d\Sigma. \tag{2.5}$$

The evolution of the magnetic field that leads to changes in the Lorentz torque produces a rigid azimuthal acceleration of the cylindrical surface at a rate proportional to the unbalanced part of the Lorentz torque. The rigid acceleration has a feedback on the Lorentz

torque: it shears the s-component of the magnetic field, which induces azimuthal secondary magnetic fields and a Lorentz torque in the opposite direction. When the initial changes in the Lorentz torque are exactly balanced by this induced torque, the Taylor state is reestablished. However, the acceleration carries the cylindrical surface past the equilibrium position, which then builds an excess of Lorentz torque that opposes the motion. This balance between inertial acceleration and restoring magnetic force produces oscillations of rigid cylinder surfaces about a Taylor state. These oscillations in the geostrophic flow are torsional oscillations (Braginsky, 1970). The dynamo is then in a quasi-Taylor state, where (2.3) is satisfied except for the part providing the restoring force to the torsional oscillations. Damping of these oscillations will leave the system in a Taylor state.

The natural periods of torsional oscillations depend on the strength of the steady B_s field. When viscous effects and magnetic coupling at the boundaries are neglected, the normal modes of oscillations of $\mathcal{V}_\phi(s)$ satisfy the non-dimensional relation

$$\frac{d}{ds}\left(s^3(1-s^2)^{\frac{1}{2}} \left(\{\overline{B_s}^2\} + \{\overline{B_s'^2}\} \right) \frac{d}{ds}\frac{\mathcal{V}_\phi(s)}{s} \right) = -R_o\,\omega^2 s^2 (1-s^2)^{\frac{1}{2}}\,\mathcal{V}_\phi(s)\,, \qquad (2.6)$$

where ω is the non-dimensional frequency of oscillation such that $\mathcal{V}_\phi(s) = \mathcal{V}_\phi(s)\exp(-i\omega t)$, and $\overline{B_s}$ and B_s' are the steady axisymmetric and non-axisymmetric parts of the s-field ($\{\}$ denotes the average over z and the over-bar the average over ϕ of the cylindrical surface). We note that equation (2.6) is no longer valid for $s \approx 0$ or $s \approx 1$. Additionally, the general case includes a contribution from the magnetic coupling with the mantle at the CMB which produces "magnetic friction", as we described above in the context of Model Z. For the cylinders inside the tangent cylinder, there is also a similar contribution term from the magnetic coupling with the inner core which is non-negligible in the dynamics since the inner core conductivity is large. A simple order of magnitude estimate of the period of the fundamental mode is given by

$$\tau_{to} \approx \frac{{R_o}^{\frac{1}{2}}}{B_s}\,, \qquad (2.7)$$

where B_s is the "rms field". Using $R_o = 2\times 10^{-9}$, $B_s = 0.25$ ($\sim$ 5 Gauss), we find $\tau_{to} \sim 1.7\times 10^{-4}$, which is about 25 years, and corresponds to the timescale of the observed variations in the geostrophic flow.

Several lines of evidence suggest that the dynamical torque balance in the Earth's core is more likely to be that of torsional oscillations about a Taylor state as opposed to an Ekman state or Model Z. First, the observed amplitude of the time-dependent geostrophic velocity of different cylindrical surfaces is large compared with the changes of the total angular momentum of the core (Jackson *et al.*, 1993; Jault *et al.*, 1996), suggesting that large exchanges of angular momentum occur within the core and that the time variations of the geostrophic flow are likely to be torsional oscillations with relatively little exchange of angular momentum at the CMB. Indeed, the radial structure and time dependency of the geostrophic flow indicates a superposition of waves (Zatman and Bloxham, 1997, 1998; Pais and Hulot, 2000; Hide *et al.*, 2000). Second, the inferred s-component of the magnetic field strength which would give rise to torsional oscillations of the observed decade periods is similar to the value of the poloidal field at the CMB (Zatman and Bloxham, 1997, 1998), the only part of the magnetic field that we can directly observe. This suggests that, contrary to a Model Z type dynamo, $B_s \sim B_z$. Third, the recovered wave motion suggests that the inertial acceleration exceeds "friction" on decade timescales (Zatman and Bloxham, 1999), indicating that the dynamics follow oscillatory behavior as in (2.5), rather than a diffusive readjustment as in (2.4) or as in the Model Z. Dissipation, either through viscous or magnetic friction, certainly plays a role, but the first order dynamical state of the core is that of torsional oscillations about a Taylor state.

We note that the above description of torsional oscillations propagating about a Taylor state is convenient conceptually, but that it is most probably incorrect. The reason is that the changes in the Lorentz torque which lead to torsional oscillations in the first place would need to be driven by a mechanism which acts suddenly and then plays no further role in the dynamics. It is more likely that the changes in the Lorentz torque are gradual and, in order to excite efficiently torsional oscillations, that the timescale of the changes is similar to the periods of the natural modes of oscillations. Hence, the background Lorentz torque is itself being driven away from a Taylor state on the same timescale as the torsional oscillations. In other words, torsional oscillations do not propagate about a Taylor state, but about a dynamic underlying Lorentz torque which, on a time average, satisfies Taylor's constraint.

2.2.5 Reynolds stresses

In the above discussion, the role of the advective torque has been omitted. This torque is usually assumed to be smaller than the friction torque and the rigid accelerations because it is multiplied by the small quantity R_o and typical values of the velocity are also small. However, as we show in section 2.3, the advective torque, through the action of Reynolds stresses (e.g. Pedlosky, 1987), plays a leading role in providing a balance to the Lorentz torque in the numerical model. In the context of convection in a rapidly rotating spherical shell, large Reynolds stresses can be produced by a correlation between the non-axisymmetric components of the radial (in a cylindrical sens) and azimuthal flow (Busse and Hood, 1982; Zhang, 1992). This produces an axisymmetric axial torque on the cylindrical surfaces which can lead to a large amplitude zonal flow. In this chapter, we use the term "Reynolds stresses" to describe the "axisymmetric torque produced by the Reynolds stresses". While the large Reynolds stresses that are produced in the numerical model may be a consequence of the parameter regime of the calculation, as we explain in the next section, this finding warrants further consideration of the Reynolds stresses, at the very least for the purpose of providing a framework in which we can cast our results.

From (2.1), the amplitude of the Reynolds stresses averaged over a cylindrical surface ($\mathcal{T}_A$) scales as

$$\mathcal{T}_A \approx \frac{R_o U'^2}{L_u} \tag{2.8}$$

where U' is the rms non-axisymmetric velocity over a cylindrical surface and L_u is the length scale associated with the flow eddies. Using $R_o = 10^{-9}$, $U' = 400$ ($\sim$ 10 km yr^{-1}) and $L_u = 1$, the Reynolds stresses have an amplitude of $O(10^{-4})$, still very much smaller than the Lorentz torque of $O(1)$ if no cancellations were to occur; Taylor's constraint still applies.

However, it is not immediately clear that the Reynolds stresses play a secondary role to the viscous torque ($\mathcal{T}_V$) and/or the rigid inertial acceleration ($\mathcal{A}_\phi$) in the torque balance. The amplitude ratios between the Reynolds stresses and the viscous torque, and between the Reynolds stresses and the inertial acceleration are given by

$$\frac{\mathcal{T}_A}{\mathcal{T}_V} \approx \frac{R_o U'^2}{E^{\frac{1}{2}} \mathcal{V}_\phi L_u} \quad \text{and} \quad \frac{\mathcal{T}_A}{\mathcal{A}_\phi} \approx \frac{U'^2 \tau_{to}}{\mathcal{V}_\phi L_u} \tag{2.9}$$

Using $R_o = 10^{-9}$, $E = 10^{-15}$, $U' = 400$, $\mathcal{V}_\phi = 400$, $L_u \sim 1$ and $\tau_{to} = \sqrt{R_o}/B$ with $B = 0.25$, we obtain

$$\frac{\mathcal{T}_A}{\mathcal{T}_V} \approx 10 \quad \text{and} \quad \frac{\mathcal{T}_A}{\mathcal{A}_\phi} \approx 0.05\,. \tag{2.10}$$

This suggests that the Reynolds stresses are, at the very least, as important as the viscous torque, unless a turbulent value of the viscosity is used. On the other hand, the prevailing balance between the Lorentz torque and the rigid acceleration appears to be maintained. However, we note that the above scaling of the Reynolds stresses rests on quantities that we do not know well. The rms non-axisymmetric value of $U' = 400$ is based on typical values from flow maps at the CMB. The latter might represent attenuated values of the interior velocities, for instance due to the presence of an outer stably stratified layer (Takehiro and Lister, 2001). Similarly, we cannot infer flows at a length scale smaller than the resolved part of the geomagnetic field, which corresponds roughly to spherical harmonic degree 14 (Bloxham and Jackson, 1991). The actual length scale of some of the flow eddies may be smaller by an order of magnitude. Hence, it is not impossible that the Reynolds stresses may be of similar magnitude to the rigid accelerations in the core.

If this is the case, or if the Reynolds stresses are actually greater than the rigid accelerations, one direct consequence is that they may provide an effective way to balance part of the Lorentz torque, thus reducing the morphological constraint on the magnetic field. The system could then be in a state where it is the sum of the Lorentz and advective torque that nearly cancels over cylindrical surfaces. A second consequence is that the Reynolds stresses may then alter the dynamics of torsional oscillations. If departures from this modified Taylor state are balanced by rigid accelerations, the latter will induce changes in both the Lorentz torque and the Reynolds stresses. These changes will produce a feedback on the rigid accelerations in a way that may be more complicated than the restoring nature of the Lorentz force taken alone. In the numerical model, where we find that the Reynolds stresses are large, both of these effects are observed.

2.3 The torque balance in the geodynamo model

2.3.1 The parameter regime of the model

It is presently too computationally expensive to solve the geodynamo problem using Earth-like values of the Rossby and Ekman numbers. However, since the main force balance in the core is thought to be between the Coriolis force, the Lorentz force, pressure gradients, and buoyancy, the so-called magnetostrophic balance, then as long as R_o and E are sufficiently small, there is hope that the solution is in the asymptotic regime that corresponds to that of the Earth.

However, even if the leading order force balance is magnetostrophic, the larger values of R_o and E may alter the dynamical regime of the torque balance. As we discussed in section 2.2, observations suggest that the dynamical state of the core is one where departures from Taylor's constraint are balanced preferentially by rigid accelerations instead of viscous torques. The effect of a larger E is obviously to increase the viscous drag on the cylindrical surfaces and move the system towards an Ekman state. Similarly, one consequence of a larger R_o is to shift the spectrum of torsional oscillations to longer periods (see (2.7)). If the natural periods of torsional oscillations approach the viscous spin-up timescale, the system is again displaced towards an Ekman state. An additional effect of a larger R_o is that the advective torque may become more important than the rigid accelerations and the viscous torques. This has the effect of weakening Taylor's constraint and alters the dynamics of torsional oscillations, as we have described in the previous section. We note also that to derive the torsional oscillation equation (2.6), Braginsky (1970) neglected the effects of magnetic field diffusion in the induction equation. This is justified for the Earth since the decade period of oscillations are short compared to the magnetic diffusion timescale. However, this is probably no longer true in the model where the natural periods of oscillations are much longer.

The larger E and R_o used in the numerical simulations of the geodynamo therefore have important consequences for the dynamical regime of the solution, as it moves it away from a Taylor state with torsional oscillations. In order to alleviate some of these consequences, several strategies have been used in the Kuang-Bloxham geodynamo model, including the following two. First, in order to decrease the amplitude of the viscous torque, stress-free boundary conditions on tangential velocity are used at the spherical boundaries. The in-

tended effect is to produce a viscous torque which depends only on the shear between cylindrical shells in the core, of $O(\mathcal{V}_\phi E)$ (see equation (2.1)), as opposed to one dominated by the Ekman pumping at the spherical boundaries, of $O(\mathcal{V}_\phi E^{\frac{1}{2}})$ (see equation (2.4)). Second, only the axisymmetric part of the inertial term (including acceleration and advection) is retained in the force balance. This allows the system to capture the dynamics associated with rigid accelerations while maintaining a predominant magnetostrophic balance.

Despite these strategies, the viscous torque remains large, in part because of the use of hyperviscosity, but also simply because E remains too large. Similarly, the part of the advective force that is retained, the axisymmetric part, produces Reynolds stresses that are sufficiently large that they play a major role in the dynamics. As we will make clear in sections 2.3.2 and 2.3.3, the dynamical regime in the numerical model (for the set of parameters chosen) is not one where torsional oscillations propagate about a mean Taylor state.

All results presented in this chapter were obtained with the following set of parameters for the numerical model: $R_o = E = 2 \times 10^{-5}$; Rayleigh number $R_a = \alpha g_o h_T r_o^2 / 2\Omega\eta = 15000$; Prandtl number $P_r = \nu/\kappa = 1$; magnetic Prandtl number $P_m = \nu/\eta = 1$; and Roberts number $q = \kappa/\eta = 1$, where κ is the thermal diffusivity, α is the thermal expansion coefficient, g_o is the gravitational acceleration at the CMB and h_T is the heat flux at the inner core boundary.

2.3.2 Time-averaged torque equilibrium

In a Taylor state, the magnetic field is of $O(1)$ on cylindrical surfaces but it is organized in such a way that the Lorentz torque integrated over the whole surface vanishes. When the magnetic field changes, torsional oscillations are excited about the Taylor state. We therefore expect that the time variations of the Lorentz torque on a cylindrical surface will show large amplitude oscillations about a weak time-averaged value. We also expect that rigid accelerations of the cylindrical surface will counterbalance the fluctuations in the Lorentz torque. Hence by investigating the time-averaged torque balance and the fluctuations of this balance (in the next section) we can establish whether the numerical model is in a Taylor state.

In figure 2.1 we show the time-averaged torque balance as a function of cylinder radius.

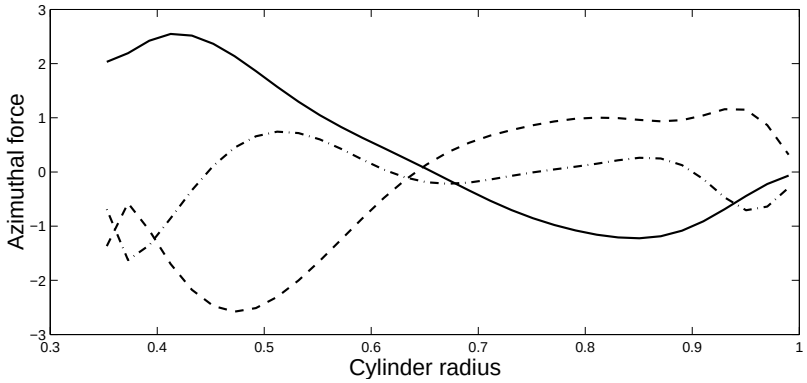

Figure 2.1: Time-averaged azimuthal force on cylindrical surfaces as a function of cylinder radius. The solid line is the Lorentz torque ($\mathcal{T}_L$); the dashed line is the advective torque ($\mathcal{T}_A$); and the dashed-dotted line is the viscous torque ($\mathcal{T}_V$). All quantities are dimensionless.

The Lorentz torque is $O(1)$. For this particular simulation, the non-dimensional amplitude of the magnetic field in the core is also $O(1)$, which indicates that little cancellation over the cylindrical surface occurs. This is because the advective and viscous torques are also $O(1)$, a result of the large R_o and E used in the model. It is immediately clear that the time-averaged state deviates from a true Taylor state. Instead, the balance involves all three torques,

$$\mathcal{T}_A + \mathcal{T}_L + \mathcal{T}_V = 0\,, \tag{2.11}$$

where

$$\mathcal{T}_A = \frac{-R_o}{4\pi s(1-s^2)^{\frac{1}{2}}} \int_\Sigma (\mathbf{u}\cdot\nabla\mathbf{u})_\phi \, d\Sigma, \tag{2.12}$$

$$\mathcal{T}_L = \frac{1}{4\pi s(1-s^2)^{\frac{1}{2}}} \int_\Sigma ((\nabla\times\mathbf{B})\times\mathbf{B})_\phi \, d\Sigma, \tag{2.13}$$

$$\mathcal{T}_V = \frac{E}{4\pi s(1-s^2)^{\frac{1}{2}}} \int_\Sigma \left(\nabla^2\mathbf{u}\right)_\phi \, d\Sigma. \tag{2.14}$$

A more comprehensive view of the dynamics that maintains this time-average balance is obtained by expanding $\mathcal{T}_A$, $\mathcal{T}_L$ and $\mathcal{T}_V$ in the following way,

$$\mathcal{T}_A = -R_o\left(\{\overline{\omega_z}\,\overline{u_s}\} - \{\overline{\omega_s}\,\overline{u_z}\} + \{\overline{\omega_z' u_s'}\} - \{\overline{\omega_s' u_z'}\}\right), \tag{2.15}$$

$$\mathcal{T}_L = \left\{\overline{J_z}\,\overline{B_s}\right\} - \left\{\overline{J_s}\,\overline{B_z}\right\} + \left\{\overline{J_z' B_s'}\right\} - \left\{\overline{J_s' B_z'}\right\}\,, \tag{2.16}$$

$$\mathcal{T}_V = E\left(\left\{\frac{\partial}{\partial s}\overline{\omega_z}\right\} - \left\{\frac{\partial}{\partial z}\overline{\omega_s}\right\}\right)\,, \tag{2.17}$$

where B_i, J_i, u_i and ω_i are respectively the i^{th} component of the magnetic field, electric current, velocity field and vorticity. The brackets $\{\}$ indicate an average in z whilst the overbar and prime denote respectively the axisymmetric (average in ϕ) and non-axisymmetric components.

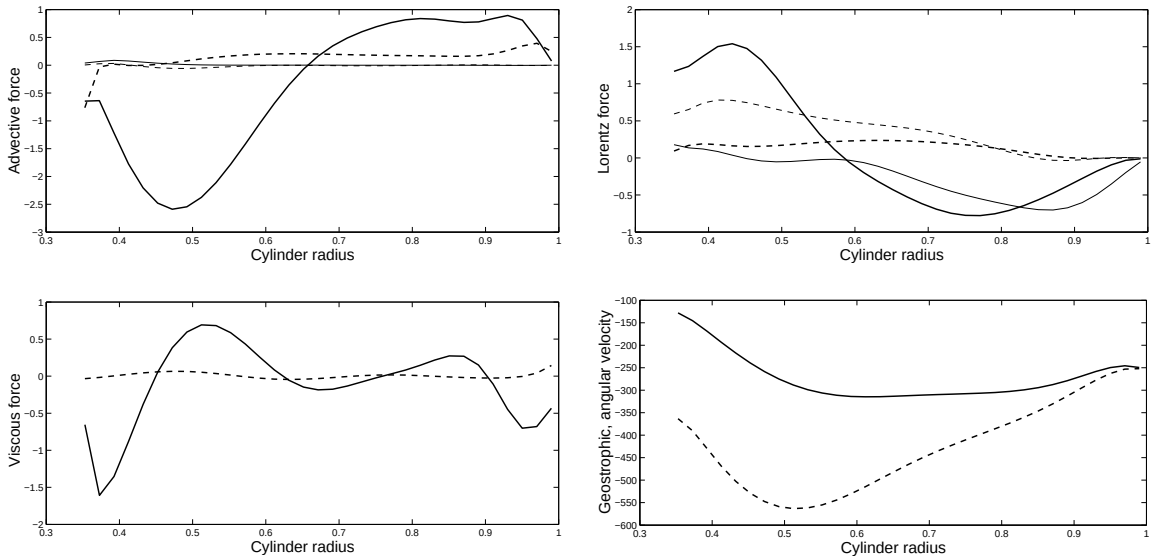

Figure 2.2: Upper left plot: Time-averaged azimuthal advective force on cylindrical surfaces of radius s. Thick solid line = $-R_o\{\overline{\omega_z' u_s'}\}$; thick dashed line = $R_o\{\overline{\omega_s' u_z'}\}$; thin solid line = $-R_o\{\overline{\omega_z}\,\overline{u_s}\}$; thin dashed line = $R_o\{\overline{\omega_s}\,\overline{u_z}\}$. Upper right plot: Time-averaged azimuthal Lorentz force. Thick solid line = $\{\overline{J_z' B_s'}\}$; thick dashed line = $-\{\overline{J_s' B_z'}\}$; thin solid line = $\{\overline{J_z}\,\overline{B_s}\}$; thin dashed line = $-\{\overline{J_s}\,\overline{B_z}\}$. Lower left: Time-averaged azimuthal viscous force. Solid line = $E\{\partial\overline{\omega_z}/\partial s\}$; dashed line = $-E\{\partial\overline{\omega_s}/\partial z\}$. Lower right: Time-averaged rigid velocity $\mathcal{V}_\phi$ (solid line) and rigid angular velocity $\mathcal{V}_\phi/s$ (dashed line).

In figure 2.2 we show the contribution of each of the terms in the expressions for $\mathcal{T}_A$, $\mathcal{T}_L$ and $\mathcal{T}_V$ in equations (2.15-2.17), as a function of cylindrical radius. All plots show time-averaged values. The term that dominates the advective torque is $\{\overline{\omega_z' u_s'}\}$, which represents the mean torque that arises from the interaction between the s- and ϕ-component of the non-axisymmetric part of the flow,

$$\{\overline{\omega_z' u_s'}\} = \left\{ \frac{1}{s^2} \frac{\partial}{\partial s} \left(s^2 \overline{u_s' u_\phi'} \right) \right\} . \tag{2.18}$$

This torque is what we refer to as the Reynolds stresses, and it dominates the other terms in (2.15) because the convection takes the form of columnar rolls aligned with the rotation axis (Busse, 1970b). When viewed in a plane perpendicular to the rotation axis, the convection cells are elongated in the prograde direction (Zhang, 1992), as in figure 2.3 where we show a snapshot of the non-axisymmetric part of the flow on the plane $z = 0.3$. The azimuthal tilting of the cells produces a correlation between u_s' and u_ϕ' and, as a result, a mean torque on the cylindrical surfaces.

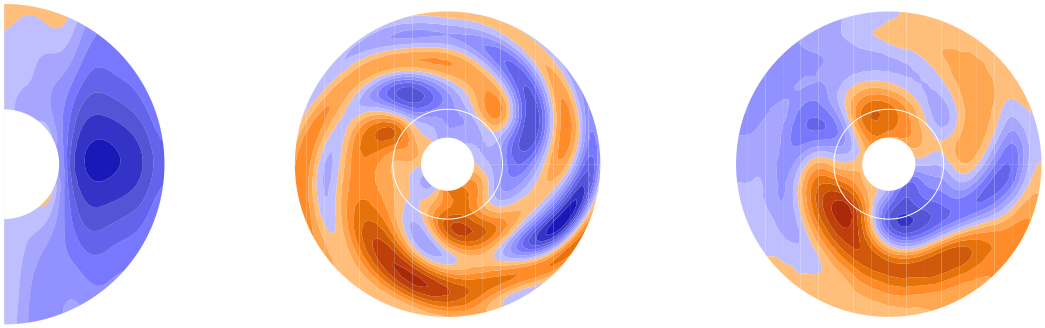

Figure 2.3: Left: Mean axisymmetric azimuthal flow in a meridional plane. Blue (red) correspond to westward (eastward) flow and the contour interval is 60 (dimensionless). Middle: stream function ψ_u of the horizontal (s and ϕ) component of the non-axisymmetric velocity field such that $\mathbf{u_h} = \nabla \times \psi_u \hat{\mathbf{z}}$. The contour interval is 4.6 (dimensionless). Right: stream function ψ_B of the horizontal component of the non-axisymmetric magnetic field such that $\mathbf{B_h} = \nabla \times \psi_B \hat{\mathbf{z}}$. The contour interval is 0.05 (dimensionless). For the middle and right figures, the z-plane is $z = 0.3$, the white solid circle is the inner core, the white circular line the tangent cylinder (located at $s = 0.35$, and blue (red) contours represent negative (positive) values of ψ and is associated with clockwise (counter-clockwise) circulation.

Similarly, the largest contribution to the Lorentz torque in figure 2.2 comes from the $\{\overline{J_z' B_s'}\}$ term, which represents the mean torque from the interaction of the s and ϕ component of the non-axisymmetric magnetic field,

$$\{\overline{J_z' B_s'}\} = \left\{ \frac{1}{s^2} \frac{\partial}{\partial s} \left(s^2 \overline{B_s' B_\phi'} \right) \right\} . \tag{2.19}$$

The magnetic field is advected by the columnar convection flow and magnetic field lines tend to wrap around the convection cells (Olson *et al.*, 1999). When viewed on a plane whose normal is parallel to the rotation axis, the morphology of the horizontal component (s- and ϕ-component) of the field is similar to that of the flow, with irregular cells tilted in the prograde direction. For illustration, we show in figure 2.3 a snapshot of the non-axisymmetric magnetic field on the z-level plane $z = 0.3$. The magnetic field pattern at other levels is similar to that shown in figure 2.3 but its magnitude varies with z (and reverses direction across the equator). Overall, a mean torque arises which is similar to the Reynolds stresses, but which involves the magnetic field. By analogy, we refer to this torque as the magnetic Reynolds stresses. The three other terms in (2.16) also participate in the Lorentz torque, but with smaller amplitude.

The viscous force shown in figure 2.2 is almost entirely a result of the $\{\partial \overline{\omega_z}/\partial s\}$ term which represents the part due to the shear of the time-averaged differential geostrophic flow $\mathcal{V}_\phi$,

$$\{\frac{\partial}{\partial s} \overline{\omega_z}\} = \left\{ \frac{\partial}{\partial s} \frac{1}{s} \frac{\partial}{\partial s} s \overline{u_\phi} \right\} \approx \frac{1}{h s^2} \frac{\partial}{\partial s} h s^3 \frac{\partial}{\partial s} \frac{\mathcal{V}_\phi}{s} , \tag{2.20}$$

where $h = (1 - s^2)^{\frac{1}{2}}$ is the semi-height of the cylinder and where we have used the stress-free boundary conditions on velocity. The time-averaged differential geostrophic flow is also shown in figure 2.2. It is the z-averaged part of the time-averaged azimuthal flow shown in figure 2.3. The differential geostrophic flow is maintained by the Reynolds stresses, as it is observed in thermal convection (Busse and Hood, 1982; Zhang, 1992), and also by the magnetic Reynolds stresses, which are as important as the Reynolds stresses in the Kuang-Bloxham model. For this particular calculation, the amplitude of the geostrophic flow is roughly equivalent to the largest non-axisymmetric velocities. We note that the use of hyperviscosity is responsible for a factor 5 to 10 increase in the viscous torque.

Hence, the mean torque balance in the simulation is one that is principally between the Reynolds stresses, the magnetic Reynolds stresses and the viscous shear associated with a mean differential geostrophic flow. A mean Taylor state is not achieved because the large viscous forces and the Reynolds stresses provide an efficient way to balance an $O(1)$ mean

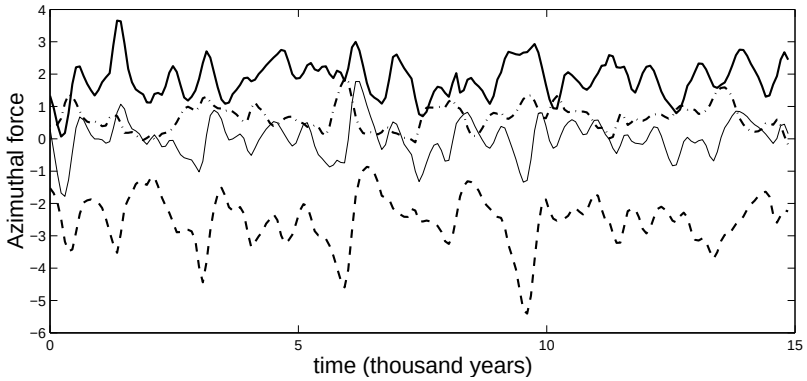

Figure 2.4: Variations in time of the azimuthal forces for cylinder radius $s = 0.5$. The thick solid line is the Lorentz torque; the dashed line is the advective torque; the dashed-dotted line is the viscous torque; and the thin solid line is the rigid acceleration.

Lorentz torque.

2.3.3 Time-dependent torque balance

If the model is in a viscous state, then we expect that

$$\mathcal{T}_A(t) + \mathcal{T}_L(t) + \mathcal{T}_V(t) = 0 \tag{2.21}$$

is respected at all times, i.e. the variations in the advective and Lorentz torque are balanced by a viscous readjustment of the geostrophic flow. On the other hand, in the case of an inertial adjustment, when the sum of the advective torque, Lorentz torque and viscous torque does not vanish on a cylindrical surface, we expect a rigid acceleration of the surface proportional to the unbalanced part,

$$\begin{aligned} \mathcal{T}_A(t) + \mathcal{T}_L(t) + \mathcal{T}_V(t) &= \frac{R_o}{4\pi s(1-s^2)^{\frac{1}{2}}} \int_\Sigma \frac{\partial}{\partial t} u_\phi(t)\, d\Sigma \\ &= R_o \frac{\partial}{\partial t} \mathcal{V}_\phi(t)\,. \end{aligned} \tag{2.22}$$

In figure 2.4 we show the evolution of $\mathcal{T}_A$, $\mathcal{T}_L$ and $\mathcal{T}_V$ for one particular cylindrical surface, $s = 0.5$. Each torque fluctuates about its time-averaged value. We also show in

figure 2.5 the time dependence of the Reynolds stresses, the magnetic Reynolds stresses and the viscous shear, in relation to the total advective torque, Lorentz torque and viscous torque. This shows that the terms that are the most important in the time-averaged balance are also the terms which carry most of the fluctuations about the mean. Results at different cylinder radii are not qualitatively different, except for s very close to 1.

We also show in figure 2.4 the rigid accelerations of the cylindrical surface $s = 0.5$, which fluctuate with amplitudes comparable to the fluctuations in the Reynolds stresses and the Lorentz torque. This indicates that at least part of the departures in the combined torque from the Reynolds stresses and Lorentz torque are balanced by rigid accelerations. The remaining part is balanced by the viscous torque. Given that the amplitude of the fluctuations in the viscous torque are similar to those of the rigid accelerations, the dynamical regime of the simulation presented is a combination of a viscous and inertial state.

In a related study of the dynamics of the Kuang-Bloxham geodynamo model, Kuang (1999) showed similar results to those reported here, for the same set of model parameters. In particular, it was shown that the Lorentz torque was mainly balanced by the inertial torque (including both acceleration and advective parts) and that the viscous torque was smaller than the latter two by a factor 2 or 3, in agreement with our present study. As a consequence, Kuang (1999) suggested that strong torsional oscillations would develop in the model, being slightly damped by viscous dissipation. By separating the inertial torque, we have been able to obtain a more precise picture of the dynamics: a large part of the total inertial torque is carried by the Reynolds stresses and while the rigid acceleration in general remains larger than the fluctuations in the viscous torque, the latter are often of comparable magnitude. Hence, our results suggest that while free oscillations of cylindrical surfaces may be produced, they would be damped somewhat rapidly. In the next section, we investigate explicitly whether the oscillations observed in figure 2.4 represent torsional oscillations.

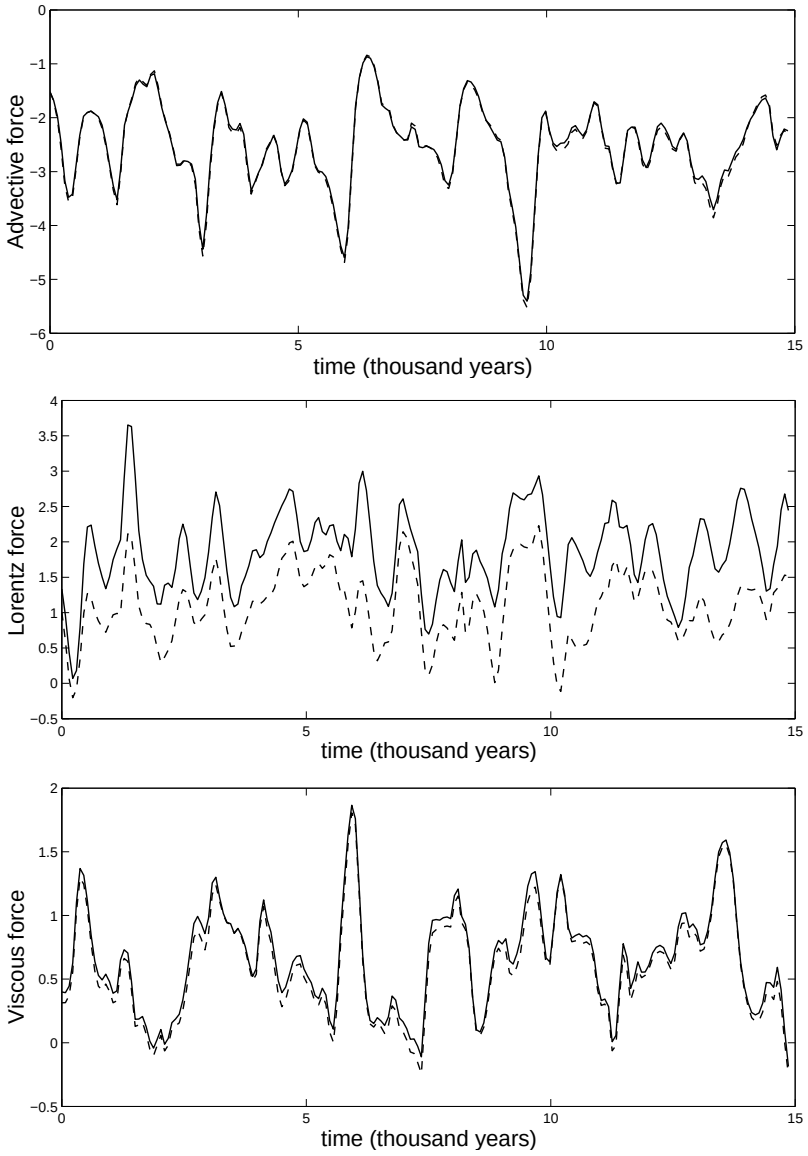

Figure 2.5: Top plot: variations in time of the total azimuthal advective force (solid line) and the the Reynolds stresses ($-R_o\{\overline{\omega_z' u_s'}\}$) (dashed line). Middle plot: variations in time of the total azimuthal Lorentz force (solid line) and the the magnetic Reynolds stresses ($\{\overline{J_z' B_s'}\}$) (dashed line). Bottom plot: variations in time of the total azimuthal viscous force (solid line) and the viscous shear due to the differential geostrophic flow ($E\{\partial\overline{\omega_z}/\partial s\}$) (dashed line).

2.4 Oscillations of rigid cylindrical surfaces

2.4.1 Rigid accelerations

From a purely mathematical point of view, equation (2.22) does not require that the azimuthal acceleration is rigid, but only that the axisymmetric acceleration averaged over z balances the total torque on the left-hand side. However, rapid rotation tends to prevent large variations in velocity parallel to the rotation axis, a constraint known as the Proudman-Taylor theorem (Proudman, 1916; Taylor, 1917). Indeed, the nearly two-dimensional columnar convection observed in the model is a consequence of this constraint. Even in the presence of a strong magnetic field, the latter organizes itself such that the Proudman-Taylor constraint is largely satisfied (Zhang, 1995; Olson *et al.*, 1999). Hence, we may expect that azimuthal velocities produced by a disequilibrium in the torques will also satisfy this constraint and be rigid. We now show explicitly that the rapid rotation dynamics are well captured by the numerical simulation and that azimuthal accelerations are almost rigid. In figure 2.6(A), we present the axisymmetric part of the azimuthal velocity $\overline{u_\phi}$ (vertical axis) as a function of height (depth axis) and time (horizontal axis), for the cylindrical surface at $s = 0.5$. At any given time, the structure of $\overline{u_\phi}$ along the z direction is almost symmetric about the equator and represents the combined effects of a thermal and magnetic wind. Over time, this structure remains more or less intact, while the whole length of the cylinder accelerates azimuthally as if it were rigid. In figure 2.6(B), the average azimuthal velocity at every height has been subtracted from $\overline{u_\phi}$, which shows that the motion is quasi-rigid. We have verified that these results hold for all cylinder radii outside the tangent cylinder.

The fact that unbalanced torques result in accelerations that are rigid can also be understood with the following considerations. The Proudman-Taylor constraint is obtained by taking the azimuthal component of the curl of the of the momentum balance in the absence of body forces. When the timescale considered is much longer than the rotation period, as is the case here, inertial accelerations can be neglected and we have $2\Omega\,\partial u_\phi/\partial z = 0$, i.e. a rigid azimuthal flow. This constraint can be broken by the effects of additional forces such as Lorentz forces, advective forces, viscosity or buoyancy, in which case we have, $2\Omega\,\partial u_\phi/\partial z = -(\nabla \times \mathbf{F})_\phi$. We are interested here in the changes in u_ϕ that result from torques on cylinders. However, the forces that are responsible for the changes in the torques are entirely in the azimuthal direction. Hence, the curl of these forces has no azimuthal

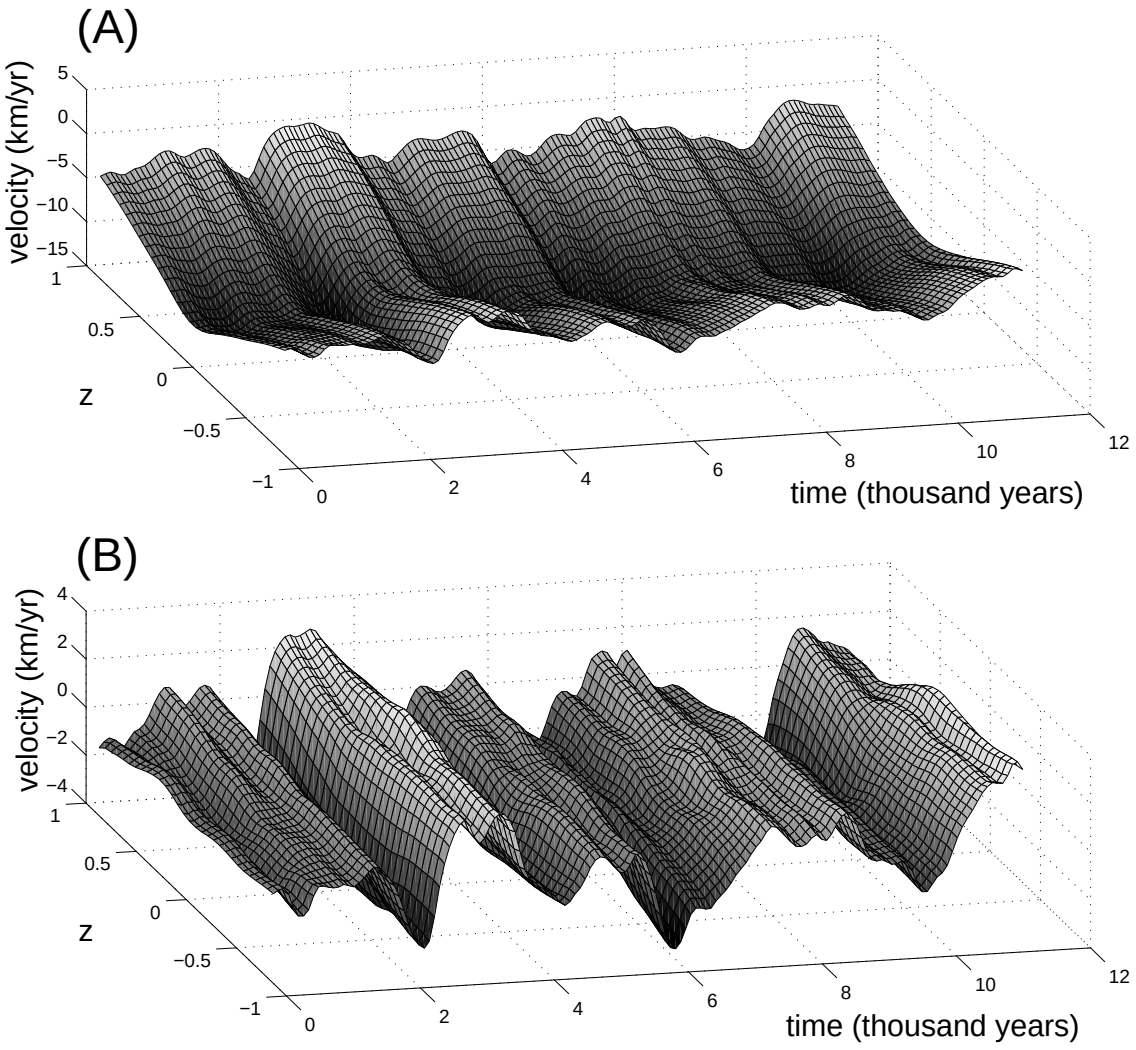

Figure 2.6: (A) Axisymmetric component of u_ϕ as a function of vertical position (z) and time for the cylindrical surface at $s = 0.5$. (B) Idem as (A), but minus the time-averaged value at each z.

component and they cannot maintain a vertical gradient in u_ϕ. Therefore, the azimuthal velocity that is produced in response to the torques must satisfy the Proudman-Taylor constraint. The small departures from a rigid velocity that are observed in figure 2.6(B), have to be attributed to non-azimuthal time-dependent forces. But as it is well illustrated by figure 2.6(A), the forces that can support an axial velocity gradient (i.e. those that produce the magnetic and thermal wind) must be in a nearly steady state balance, since the axial vertical gradient remains nearly constant. Hence the non-azimuthal forces do not change signifi-

cantly on the timescale of the azimuthal oscillations. The largest time-dependent forces are in the azimuthal direction, therefore indicating that the time-dependent dynamics in the model are largely controlled by the torque balance.

For cylindrical surfaces inside the tangent cylinder, we have observed a similar behavior with rigid accelerations propagating on a nearly steady thermal and magnetic wind background. However, we have also observed in this region occasional sudden episodes of large variations in the z-gradient of $\overline{u_\phi}$ that were of the same amplitude as the rigid oscillations of $\overline{u_\phi}$. Hence, even though the meridional force balance remains nearly steady for long periods of time, it does participate in the time-dependent dynamics during brief episodes.

2.4.2 Torsional oscillations in the geodynamo model?

We now investigate whether the fluctuations of the rigid accelerations shown in figure 2.4 are torsional oscillations. This particular calculation uses $R_o = 2 \times 10^{-5}$ and the rms magnetic field strength over the cylindrical surfaces is about 0.5 ($\sim$10 Gauss). According to (2.7) we expect the fundamental period of torsional oscillations to be on the order of a thousand years, in agreement with the periodicity of figure 2.4. However, the fluctuations in the rigid acceleration in figure 2.4 do not seem to be correlated strongly with those of the Lorentz torque, which is what we would expect for torsional oscillations. Instead, it appears that the rigid accelerations result from the combination of changes in the Lorentz torque and the Reynolds stresses. Moreover, the viscous torque is often almost as large as the rigid accelerations, which suggests that any free oscillations will be damped over one or two periods of oscillation and that the maintenance of the fluctuations has to be attributed to a forced oscillation component. We note in addition that because of the longer periods of free oscillations in the model, the effects of magnetic diffusion are certainly much stronger than they would be in the Earth's core.

Whether torsional oscillations are observed in the numerical model (with the current set of parameters) comes down to a matter of terminology. If one restricts "torsional oscillations" to refer only to the oscillations that arise as a balance between rigid accelerations and Lorentz forces, then the oscillations of figure 2.4 are not torsional oscillations because the Reynolds stresses participate in the dynamics. On the other hand, these fluctuations do represent inertial oscillations of rigid cylindrical surfaces and one may choose still to refer

to them as “torsional oscillations”, just ones that are also influenced by Reynolds stresses. In any case, a large part of the oscillations in the rigid accelerations are forced oscillations.

2.4.3 Radial and time dependency of the rigid azimuthal velocities

In order to get a sense of the spatial dependency of the fluctuations in the geostrophic flow produced in the model, in figure 2.7 we show $\mathcal{V}_\phi$ as a function of cylindrical radius and time. The mean differential geostrophic flow has been subtracted. The general pattern shows many oscillations with typical timescales of a thousand years that are propagating in the radial direction. The amplitude of the oscillations is on the same order as the amplitude of the mean geostrophic flow. The radial propagation of the waves further confirms the ability of the numerical model to capture the dynamics of inertial oscillations of rigid cylindrical surfaces.

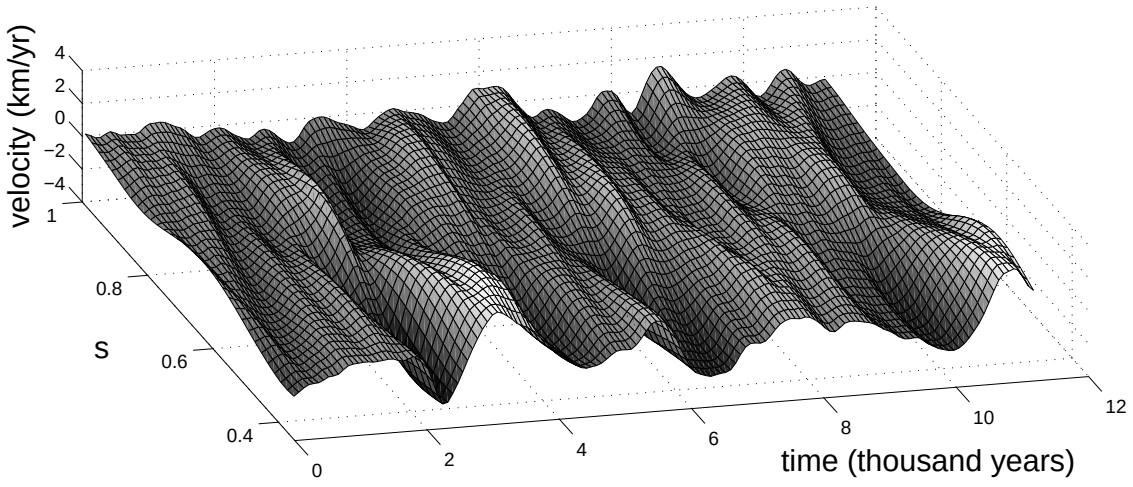

Figure 2.7: Rigid velocity $\mathcal{V}_\phi$ as a function of *s* and time outside the tangent cylinder. The mean differential velocity has been subtracted.

It is interesting to note that, in specific time intervals, the wave pattern observed in figure 2.7 is similar in many ways to the inverted flow which is inferred to represent torsional oscillations in the core (Zatman and Bloxham, 1997, 1998; Hide *et al.,* 2000). Hence, even if the dynamics of these waves is influenced by the Reynolds stresses and viscous forces, their radial and time dependency in small intervals reproduces a similar behavior to torsional oscillations. This issue will be reexamined in the discussion in section 2.5.

2.4.4 Generation of rigid accelerations in the model

In section 2.4.2, we argued that a large component of the oscillation in the rigid accelerations had to be attributed to a forced oscillation because of the large viscous dissipation. This allows for an investigation of the mechanisms that change the fields in such a way as to destroy the balance between the torques. In other words, it permits an investigation of the mechanism responsible for exciting the free oscillations in the model and by extension, torsional oscillations in the Earth's core.

One way in which the rigid accelerations are produced is through the chaotic nature of the convection. As we showed in section 2.3.2, the time-averaged torque equilibrium involves a mean differential geostrophic velocity maintained by the Reynolds stresses and the magnetic Reynolds stresses. Yet, the continual shearing of the non-axisymmetric structures of the velocity field and the magnetic field by this differential geostrophic flow produces continual changes in the Reynolds stresses and the magnetic Reynolds stresses. In order to maintain the torque balance at all times, rigid accelerations are continually produced and modify the differential geostrophic flow. Overall, a time-averaged equilibrium is established with continual chaotic fluctuations of the torques and of the differential geostrophic flow about their mean values. The equilibrium described above is a well established balance observed in numerical models of non-magnetic thermal convection in a chaotic regime (Sun *et al.*, 1993; Cardin and Olson, 1994; Christensen, 2002) and has also been observed in numerical models of the geodynamo (Grote and Busse, 2001).

A demonstration of the advective action of the differential rotation on the magnetic field is shown in figure 2.8. We present snapshots at 75 years intervals of the non-axisymmetric magnetic field on a z-level plane ($z = 0.3$). The contours are those of a stream function ψ_B of the in-plane magnetic field such that $\mathbf{B_h} = \nabla \times \psi_\mathbf{B}\hat{\mathbf{z}}$. The mean differential geostrophic flow profile is that of figure 2.2, with cylinders near $s \approx 0.5$ rotating at the fastest rate (in a retrograde direction). While these results are shown at a particular z-level, the average over z produces a similar picture because of the strong two-dimensionality of the convective structures. We identify three structures (labeled 1,2 and 3 on the figure) that we follow in time. Structure 1 is a filament that extends from the tangent cylinder to $s \approx 1$ in snapshot a. The differential rotation shears the filament, which disconnects into two distinct magnetic field vortices. The disconnection is completed by snapshot f. Structure 2 is similar to structure 1 in a, and is likewise sheared in two separate structures. The disconnection in this

case is accelerated by the intrusion from structure 3, which benefits from a faster retrograde rotation than the tail-end of structure 2. In snapshot *d* and *e*, structure 3 reconnects with the part that had previously disconnected from structure 1.

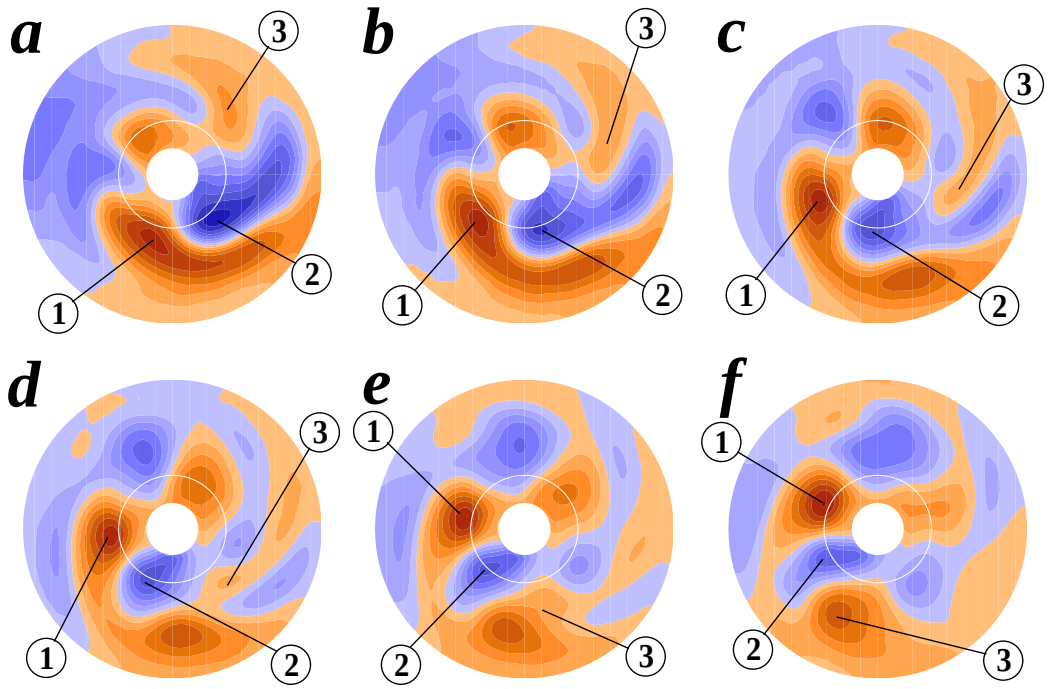

Figure 2.8: Snapshots at 75 years intervals of stream function ψ_B of the horizontal (s and ϕ) components of the non-axisymmetric magnetic field at $z = 0.3$, where $\mathbf{B_h} = \nabla \times \psi_B \hat{\mathbf{z}}$. The contour interval is 0.05 (dimensionless). The white solid circle is the inner core and the white circular line the tangent cylinder, located at $s = 0.35$. Blue (red) contours represent negative (positive) values of ψ_B and are associated with clockwise (counter-clockwise) magnetic field circulation.

The differential geostrophic flow creates changes in the s- and ϕ-component of the non-axisymmetric magnetic field (and hence in the magnetic Reynolds stresses) in two ways. First, it changes the tilt angle of the non-axisymmetric contours. Second, the constant advection of the non-axisymmetric structures by the differential rotation is physically displacing contours past one-another, which leads to disconnection and reconnection and local changes in the Lorentz torque. This is the crucial role played by the non-axisymmetric field in making the Lorentz torque fluctuate constantly in the presence of a mean differential geostrophic flow. If the field were purely axisymmetric, advection by a steady differential

geostrophic flow would shear a steady radial magnetic field until it is balanced exactly by diffusion, at which point a steady Lorentz torque would be established. The relative azimuthal displacements of non-axisymmetric structures at different radii prevents the establishment of such a steady state. In addition, as is also obvious from figure 2.8, instabilities which draw energy from the differential geostrophic flow also play a role in altering the local Lorentz torque. The Reynolds stresses are altered by the differential geostrophic flow in a similar way.

We note that the gradient in z of the mean zonal flow (shown in figure 2.3) produces a shear of the vertical non-axisymmetric structure of the velocity and magnetic field. However, as shown in figure 2.5, most of the the changes in time in the torques are carried by the shear of the z-plane structures as described above. The shear of the vertical structures represents then only a small contribution to the total time-dependent azimuthal torque. Hence, it is the differential geostrophic component of the total mean zonal flow that is mostly responsible for the chaotic evolution of the torque balance.

The dynamical regime of the geodynamo model is not one where free oscillations of rigid cylindrical surfaces are propagating with respect to a slowly varying background torque equilibrium. Instead, the nature of the torque equilibrium is such that rigid accelerations are continually produced in order to balance the chaotic evolution of the Reynolds stresses and the magnetic Reynolds stresses. In other words, the background torque equilibrium is varying on the same timescale as the periods of the free oscillations. The resulting rigid accelerations provide a continual and efficient excitation of the free oscillations.

2.5 Discussion and Conclusion

2.5.1 The dynamical state of the numerical geodynamo model

In this paper we have investigated the torque balance on cylindrical surfaces in the Kuang-Bloxham numerical geodynamo model. For the parameters of our investigation, we find that the time-averaged torque balance is not in a Taylor state, but one that consists in large part of a balance between the Reynolds stresses, the magnetic Reynolds stresses, and the viscous shear associated with a mean differential geostrophic flow. When a departure from this balance occurs, it is accommodated by a rigid azimuthal acceleration of the cylindrical

surface which excites free oscillations of these rigid surfaces that propagate in the direction perpendicular to the rotation axis. We have shown that the inertial acceleration of the cylindrical surfaces is indeed almost rigid, with little variations along the rotation axis. We have therefore confirmed that the model captures the dynamics of an inertial state dynamo, where rigid azimuthal accelerations of cylindrical surfaces are produced in response to a disequilibrium in the torque balance.

The rigid azimuthal oscillations that occur about the time-averaged state are not torsional oscillations in their conventional description because the Reynolds stresses play an important role in their dynamics. In addition, a large component of the observed fluctuations results from the changes in the underlying torque balance, which is continually fluctuating about its mean, a consequence of the advective action of the mean differential geostrophic flow which continually alters the Reynolds stresses and magnetic Reynolds stresses. Without this continual forcing, the free oscillating part of the fluctuations would be attenuated rapidly by viscous dissipation.

2.5.2 Reynolds stresses in the Earth's core

It is clear that one main reason why the numerical model fails to reproduce a dynamic state in which the unbalanced part of the Lorentz torque is counterbalanced by rigid accelerations of cylindrical surfaces is because of the large Reynolds stresses. Yet, the two conventional conceptual pictures of the torque balance in the core - a friction controlled state or torsional oscillations about a Taylor state - do not involve Reynolds stresses. The role of the Reynolds stresses in the torque balance of the Earth's core deserves closer examination.

In the model, the Reynolds stresses are of similar amplitude to the magnetic Reynolds stresses and provide a very efficient way of balancing a large Lorentz torque. This should not come as a surprise considering that they have an identical mathematical form but with opposite signs:

$$\mathcal{T}_A \approx -R_o \left\{ \frac{1}{s^2} \frac{\partial}{\partial s} \left(s^2 \overline{u_s' u_\phi'} \right) \right\}, \tag{2.23}$$

$$\mathcal{T}_L \approx \left\{ \frac{1}{s^2} \frac{\partial}{\partial s} \left(s^2 \overline{B_s' B_\phi'} \right) \right\}. \tag{2.24}$$

The convective motion in the form of spiraling rolls is directly responsible for each of these

torques and the amplitudes of u' and B' are dynamically adjusted in the model so that a mean torque balance is achieved. We have seen in figure 2.2 that these torques have indeed a similar magnitude and opposite signs. We can also verify the balance by considering an order of magnitude ratio of the two,

$$\frac{\mathcal{T}_L}{\mathcal{T}_A} \approx \frac{B'^2 L_u}{R_o U'^2 L_B}. \tag{2.25}$$

The typical values that emerge from the model are $B' \sim 0.5$, $U' \sim 100$ and $L_u/L_B \sim 1$, which gives $\mathcal{T}_L/\mathcal{T}_A \sim 1$. Preliminary results for calculations using smaller values of the Rossby and Ekman numbers ($E = R_o = 10^{-5}$ and $E = R_o = 5 \times 10^{-6}$) supports the above analysis: B' decreases while U' increases so that $\mathcal{T}_L/\mathcal{T}_A \sim 1$ is maintained. (We note that in these simulations, as a consequence of the decrease in the magnetic field strength, the system is more in a viscous state than an inertial state.)

However, it is uncertain whether the above balance can be extrapolated to the parameter regime of the Earth's core. As we have argued in section 2.2.5, in order for the Reynolds stresses to provide a balance to an $O(1)$ Lorentz torque, the combined increase in velocity and decrease in length scale of the flow eddies (both inferred from the flow inversions) has to be about 4 orders of magnitude. This is questionable and the above equilibrium between the Reynolds and the magnetic Reynolds stresses may no longer hold in the parameter regime of the Earth, otherwise the amplitude of B' would have to be much smaller than its observed value at the CMB.

Our main point here is not that the Reynolds stresses are necessarily important in the Earth's core, but that a proper assessment of their role in the torque balance and torsional oscillations may be desirable. We recall that we do not know the length scale and amplitude of the flow eddies in the core, and that an important contribution from the Reynolds stresses in the dynamics, such as we observe in the model, remains a possibility. One way to assess this question in a more quantitative way using the numerical model is to investigate how the torque balance is altered by changing the parameters that enter the calculation. Asymptotic laws can perhaps be derived and extrapolating these to core parameters may help provide a better understanding of the torque balance in the Earth. We leave such investigation to a future study.

2.5.3 Excitation of torsional oscillations in the Earth's core and the dynamic torque balance of the geodynamo

The dynamic torque balance observed in the numerical model may not be directly applicable to the Earth's core. This is for obvious reasons: the parameters used for the numerical calculation are different from those of the Earth's core and the results of the model may also be highly dependent on some of the approximations employed (such as retaining only the axisymmetric part in the momentum equation and using hyperdiffusivity). Nevertheless, some aspects of the dynamics of the torque balance observed in the model may apply to the Earth's core in a qualitative sense.

We propose here that a chaotic evolution of the torques on cylindrical surfaces, such as is observed in the model, may also occur in the Earth's core and would be responsible for exciting torsional oscillations. In the model, this chaotic evolution involves a large contribution from the Reynolds stresses, which may be much weaker in the Earth's core. However, even if the Reynolds stresses are unimportant, we expect that the torque balance will evolve in a similar chaotic fashion if the convective dynamics in the core involves a mean differential geostrophic flow. One can imagine a scenario in which, in concert with this mean differential geostrophic flow, the time-averaged torque balance involves only the Lorentz torque. In other words the time-averaged torque balance satisfies Taylor's constraint. Indeed, kinematic studies have shown that for a magnetic field configuration that satisfies Taylor's constraint, there exists a geostrophic flow that shears the field in the precise way so that it continues to satisfy Taylor's constraint (Taylor, 1963; Fearn and Proctor, 1987a; Jault, 1995). The inertial effects and their feedbacks on the magnetic field are neglected in the above studies, and hence this result remains appropriate for the time-averaged torque balance. In time, we expect that the advective action of the mean differential geostrophic flow on the non-axisymmetric part of the magnetic field would be dynamically similar to that which is observed in figure 2.8. Therefore, even in the absence of Reynolds stresses, the interaction between the differential geostrophic flow and the magnetic Reynolds stresses alone would require continual fluctuations in rigid accelerations in order to balance the continual fluctuations in the magnetic Reynolds stresses.

Such a chaotic evolution of the torque balance provides a mechanism to continually excite torsional oscillations. We expect the chaotic fluctuations in rigid accelerations to

cover a wide range of frequencies, but resonant amplification will occur at the natural frequencies of the free oscillations. If the observed torsional oscillations in the Earth's core are indeed the result of a chaotic interaction of the sort, then they would comprise both chaotically forced rigid accelerations and excited free oscillations.

If this dynamical picture is correct, an order of magnitude estimate of the differential geostrophic flow required to generate torsional oscillations to their observed level is easily obtained. The imposed differential rotation will shear the magnetic field in the exact same way that free oscillations would. Therefore, the amplitude of the differential geostrophic flow has to be similar to the amplitude of the observed torsional oscillations (about 5 km yr^{-1}). In reality, the required amplitude is probably less. The reason is that the differential geostrophic flow induces reconnections and disconnections which further change the local Lorentz torque. Other instabilities which draw their energy from the differential geostrophic flow may also create large local changes in the Lorentz torque.

Since the above scenario is largely dependent on the presence of a mean differential geostrophic flow with typical amplitudes on the order of 5 km yr^{-1}, one may wonder whether there is support for such a flow in the Earth's core. A mean differential geostrophic flow is a standard feature of thermal convection in spherical shells (Busse and Hood, 1982; Zhang, 1992; Sun *et al.*, 1993; Cardin and Olson, 1994), and is being driven by the Reynolds stresses. As we have shown in this study, it is also present in the Kuang-Bloxham geodynamo model, where it is also influenced by the magnetic Reynolds stresses. In general, the presence of a magnetic field tends to prevent a large scale geostrophic flow. The question is whether a sufficiently large mean differential geostrophic flow would be present if the Reynolds stresses were much weaker, as it is probably the case in the core. The answer to that question is unknown and re-emphasizes the need for a systematic parameter study of the torque balance. However, tentative support for a mean differential geostrophic flow comes from the kinetic considerations of a Taylor state as mentioned above (Taylor, 1963; Fearn and Proctor, 1987a; Jault, 1995), which suggest that a differential geostrophic flow of 5 km yr^{-1} is consistent with Earth-like magnetic field strengths (Jault, 1995). A second line of evidence supporting a mean differential geostrophic flow comes from inversions of the flow at the CMB. Over the last 160 years, most of the secular variations of the geomagnetic field can be explained with a steady flow which contains a rigid differential geostrophic component (Bloxham, 1992) with a typical amplitude of 5 km yr^{-1} (Zatman

and Bloxham, 1999). Although it is possible that this inverted steady differential rigid rotation flow is incorrect (Gubbins and Kelly, 1996), its typical amplitude is consistent with the amplitude of the observed torsional oscillations that would result from the scenario presented above.

The dynamical torque balance scenario that we have described here differs from the conventional picture of the quasi-Taylor state, where torsional oscillations are free oscillations propagating about a slowly evolving Taylor state. Rather, we suggest an alternative option in which the time-averaged torque satisfies Taylor's constraint and a mean geostrophic flow acting on the non-axisymmetric structures of the magnetic field leads to chaotic fluctuations of the Lorentz torque about this mean Taylor state. The background torque equilibrium on which the free oscillations propagate is then not quasi-static but dynamic and provides a continual and efficient excitation for the free oscillations. Thus, a quasi-Taylor state where the Lorentz torque vanishes except for the part involved in torsional oscillations remains a valid description, provided that the torsional oscillations consist of a mixture of free oscillations and chaotically forced accelerations.

We note that if the Reynolds stresses are important in the Earth's core, this dynamical description remains valid, except that the time-averaged torque balance would differ from a Tayor state, as we see in the model, and the Reynolds stresses would be involved in the chaotic fluctuations of the rigid accelerations and also participate in the dynamics of free oscillations.

Finally, as we pointed out in section 2.4.3, the rigid flow oscillations produced in the model shown in figure 2.7 resemble in many respects the recovered rigid velocities of the Earth's core. One may then suggest that this result argues in favor of a large influence of the viscous torque and the Reynolds stresses in the observed torsional oscillations in the core. However, this is not necessarily the case because the dynamical role of the viscous torque and Reynolds stresses can both be accomplished by the Lorentz torque alone. As explained above, we expect chaotic rigid accelerations even if Reynolds stresses are weak. Additionally, the attenuation of the free oscillations by the viscous torque can be substituted by a "magnetic friction" if there exists a conducting layer at the base of the mantle (Braginsky, 1970, 1988). Indeed, a layer with a conductance of 10^8 S, which is required to explain some of the discrepancies between the observed and predicted forced nutations of the Earth (Buffett, 1992), would be quite efficient at attenuating the torsional oscillations

in one or two periods (Buffett, 1998), as we observe in the model. The resulting rigid oscillations would then contain a large component of forced oscillations in order to compensate for the magnetic "friction", and would appear similar to that of figure 2.7.

2.5.4 Future numerical work

Finally, we wish to discuss future strategies for modeling the dynamical torque balance and torsional oscillations. Evidently, the chaotic torque balance observed in the model is obtained for one specific set of parameters. We have argued that this result may apply to the Earth in a qualitative way. However, it is certainly also possible that this chaotic torque balance is no-longer in effect for the parameter regime of the Earth's core. Therefore, additional numerical work is required to confirm our hypothesis. In order to better approximate the Earth's core, the influence of the viscous torque and Reynolds stresses have to be much weaker. Additionally, the timescale of the oscillations has to be shorter to limit the effects of magnetic diffusion. This can be achieved by reducing the Ekman and Rossby numbers. However, limits in computing resources do not permit drastic reductions of these parameters. Hence, as we have mentioned already, one strategy is to vary systematically the different parameters with the hope of extracting asymptotic laws for the torque balance. The calculations at smaller values of E and R_o, will be computationally expensive although we recall that to study the torque dynamics, it is only necessary to cover a time period that contains a few rigid oscillations, which is much shorter than the magnetic decay timescale. In reducing E and R_o, one has to be careful to maintain an inertial state. In other words, the inertial acceleration has to be at least of comparable magnitude and preferably larger than the viscous torque.

Under the assumption that Reynolds stresses are unimportant in the torque balance of the core, additional strategies in the numerical model might permit a better approximation of a Taylor state. One strategy is to neglect the Reynolds stresses altogether, even the axisymmetric part. This is certainly not consistent with the current parameter regime of the simulation because, as we have seen in the present study, the Reynolds stresses are indeed very large. However, subtracting their effect from the torque balance removes one possible way in which a Lorentz torque of $O(1)$ can be balanced. Hence, it can lead to a closer representation of a Taylor state and perhaps provide a more accurate view of the

dynamics in the core. Similarly, another strategy is to use a smaller Ekman number for the axisymmetric equation, or equivalently a lower degree of hyperviscosity. This will reduce the viscous torque of cylindrical shells without being prohibitively expensive numerically.

One last point we wish to discuss is whether the chaotic fluctuations and free oscillations of the cylindrical surfaces have an important effect on the long term evolution of the magnetic field. In other words, when one is interested in phenomena such as dipole field generation or reversals, whether it is appropriate to simply filter out the short timescale torsional oscillations, or, on the contrary, whether they are crucial for the long term equilibrium because they allow the instantaneous torque balance to relax towards its mean state? The above question may be addressed by comparing numerical solutions that have a common set of parameters, but different step sizes in time. We expect that solutions with different increments in time will have different time-histories of the torques. However, if the time-averaged torque balance remains unchanged, it suggests that the chaotic fluctuations and free oscillations have little influence on the long term torque equilibrium.

Chapter 3

Variations in the Earth's Gravity Field Caused by Torsional Oscillations in the Core

3.1 Introduction

Torsional oscillations are the azimuthal oscillations of rigid cylindrical surfaces aligned with the rotation axis (Taylor, 1963; Braginsky, 1970) (figure 1.1). This type of flow is predicted to occur in the core as a result of Taylor's constraint (Taylor, 1963), which specifies that, in steady state, the axial torque exerted by the magnetic force on any such cylindrical surface must vanish. If at any time this constraint is not satisfied on one cylindrical surface, a rigid azimuthal acceleration of the whole cylindrical surface is instigated in order to balance the torque. This process excites torsional oscillations, which have typical periods of a few decades and shorter (Braginsky, 1970, 1984).

Because of their rigid nature, it is possible to retrieve the torsional oscillations from flow maps at the core-mantle boundary (CMB): one can simply take the part of the axisymmetric azimuthal velocity that is symmetric about the equator (Jault *et al.*, 1988; Jackson *et al.*, 1993; Zatman and Bloxham, 1997; Hide *et al.*, 2000; Pais and Hulot, 2000). The torsional oscillations computed in this manner can be tested against an independent data set: since

[2]The work presented in this chapter has been submitted and accepted for publication in *Geophysical Journal International*

angular momentum of the whole Earth has to be conserved, the variations in time of the core angular momentum carried by torsional oscillations must be consistent with the changes in angular momentum of the mantle that are observed in terms of its variations in rotation rate (*i.e.* length of day variations). The agreement is especially good for the last few decades (Jault *et al.*, 1988; Jackson *et al.*, 1993), which places a high degree of confidence on the retrieved torsional oscillations.

Since it is the only component of the flow inside the core which we know with confidence, torsional oscillations are the window through which we can observe several aspects of the dynamics of the core. For instance, the restoring force that maintains the oscillations depends on the strength of the magnetic field perpendicular to the cylindrical surfaces, and therefore by investigating the periodicity and radial structure of the oscillations it is possible to extract information about the magnetic field inside the core (Zatman and Bloxham, 1997, 1998). Likewise, the attenuation of the waves contains information about the nature of the coupling between the core and the mantle at the CMB (Buffett, 1998; Zatman and Bloxham, 1999; Mound and Buffett, 2003). In addition, constraints about the dynamics involved in the convective motions in the Earth's core may be inferred from the requirement that these dynamics be able to excite and maintain torsional oscillations (see chapter 2).

Recently, it has been shown that, although there remains some unexplained signal, a large part of the secular variation of the geomagnetic field, including the "geomagnetic jerks", can be explained by a steady flow plus a more refined model of torsional oscillations (Bloxham *et al.*, 2002). More accurate models of torsional oscillations, in the spirit of this latter study, can then lead to a better characterization of some of the core processes. The current models are obtained by inverting the flow at the CMB capable of explaining the secular variation of the geomagnetic field. The torsional oscillations may also be constrained to be consistent with length of day variations. In this chapter, we propose a new way to attempt to observe torsional oscillations, and therefore provide additional constraints on the torsional oscillations flow models. We investigate whether it is possible to detect the torsional oscillations in the gravity field data at the surface of the Earth.

The large Coriolis force associated with rigid azimuthal flows of the sort involved in torsional oscillations is balanced by the establishment of a pressure gradient in the direction perpendicular to the rotation axis. This geostrophic force balance provides a simple way to visualize how torsional oscillations produce variations in the gravity field. Consider

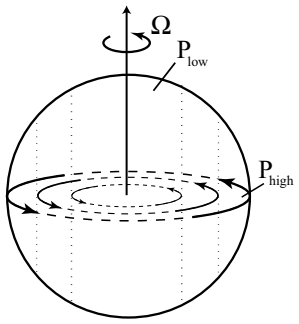

Figure 3.1: A prograde rigid rotation flow in the core (black arrows) gives rise to a geostrophic pressure that increases (quadratically) with distance from the rotation axis (Ω), from a low at the rotation axis to a high near the equator on the CMB. The flow and pressure are invariant in the direction parallel to the rotation axis.

for example a prograde rigid rotation of the whole core, where the rigid azimuthal velocity increases linearly with distance from the rotation axis (figure 3.1). This requires the establishment of a low pressure along the rotation axis and a high pressure at the equator of the CMB, with surfaces of constant pressure coinciding with the surface of coaxial cylinders. This geostrophic pressure gradient from the pole to the equator along the CMB produces latitudinal variations in surface forces on the CMB and deformations of this fluid-solid surface. The distortion of the CMB produces variations in the gravity field because there exists a large density discontinuity between the core and the mantle. The perturbation in gravity leads to adjustments in the mechanical equilibrium of the whole planet. It may then be observed at the surface, although with attenuated amplitude (figure 3.2). A similar effect is produced at the inner core boundary (ICB), with radial displacements of this boundary contributing to variations in the global gravity field. However, because the density discontinuity between the inner core and the fluid core is smaller, and because it is further away from the surface, we expect the contribution at the ICB to be less important than that at the CMB.

An additional effect that needs to be considered is the gravity field perturbation that results from the changes in the rotation rate of the mantle. As we have already mentioned, these are required in order to balance the changes in the axial angular momentum of the core carried by torsional oscillations. Changes in the rotation rate of the mantle modify the equilibrium balance between gravity and centrifugal forces. Consequently, this changes the

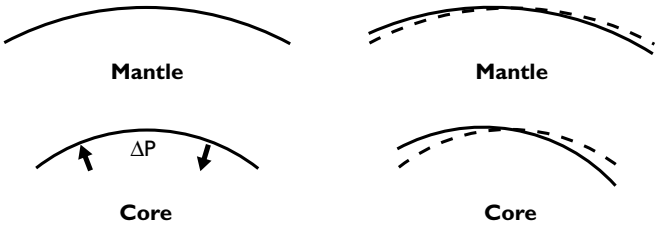

Figure 3.2: Horizontal gradients in pressure at the CMB (left), lead to a radial deformation of the CMB and the exterior surface (right).

elliptical component of the gravity field and the oblateness of the Earth. The change in the gravity field produced by the latter effect is opposite from the direct effect of the pressure force on the CMB by the torsional oscillations. So, for instance, if torsional oscillations produce a prograde net rotation of the core and tend to make the whole Earth more oblate, the associated retrograde rotation of the mantle tends to make the Earth less oblate.

A similar effect arises from changes in the rotation rate of the inner core. Because of strong electromagnetic coupling at the inner core boundary (ICB) (Gubbins, 1981), torsional oscillations will cause the inner core to undergo changes in its rotation rate. In addition, because of axial gravitational coupling between the mantle and the inner core (Buffett, 1996a) a change in the rotation rate of one also influences the other. As for the mantle, changes in the rotation rate of the inner core produce changes in oblateness and in the elliptical gravity field of the whole Earth.

Torsional oscillations are time-dependent flows and because of their geometry, we expect them to produce variations in the zonal harmonics of even degree in the gravity field. Hence, it may possible to detect time variations in the zonal components of the gravity field that are caused by the torsional oscillations. If so, the gravity data may then be used to provide better constraints on torsional oscillation flow models.

An additional motivation for this investigation comes from the gravity field data themselves. Large subdecadal timescale changes in the degree 2 zonal harmonic of the gravitational field have been recently reported (Cox and Chao, 2002) and these may perhaps be caused by the dynamical mechanism proposed above. As shown in figure 3.3, prior to 1998, the variations in the coefficient J_2 (which represents a measure of the degree 2 zonal

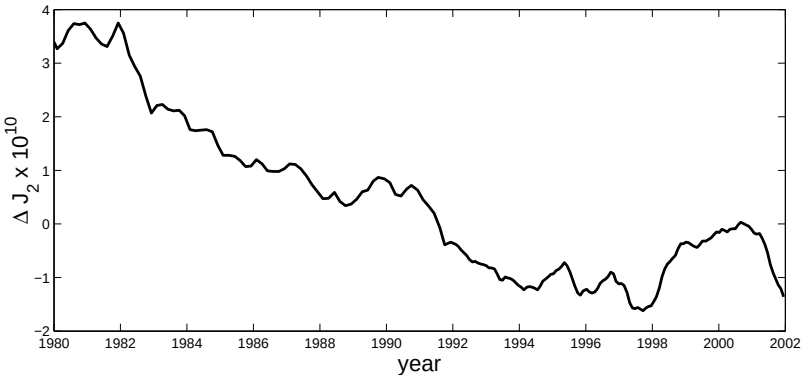

Figure 3.3: Variations in time of J_2, once the annual contribution is subtracted. The data presented are those obtained after a filtering by a 1-year moving window. (from Cox & Chao (2002))

harmonic (e.g. Jeffreys, 1970)), seem to consist essentially in a slow decreasing linear drift of $\sim -2.8 \times 10^{-11}$ year^{-1}. This linear secular trend is thought to represent the signature of post-glacial rebound: polar land masses are still uplifting from the removal of the glacier load that covered them during the last glaciation, resulting in a gradually less oblate Earth (Yoder *et al.*, 1983; Rubincam, 1984; Mitrovica and Peltier, 1993), and hence a decrease in J_2. However, a considerable departure from this linear trend has occurred between 1998 and 2002. This impulse in the signal is difficult to reconcile with the slow process of post-glacial rebound for which the timescale of variations is about a thousand years. Therefore this suggests the presence of at least one additional physical mechanism that participates in the temporal changes of J_2. Moreover, the fact that the temporal changes in J_2 is now on its way back to its pre-1998 trend suggests that this additional mechanism may be episodic and does not produce permanent changes.

The sudden increase in J_2 requires a mass transport from the polar regions to the equatorial regions, or an increase in the oblateness of the whole Earth, or a combination of both. In the original report of the impulse, Cox and Chao (2002) suggested possible mechanisms involving mass transport in the oceans and the atmosphere, and glacier-melting near the polar regions, although none of these possibilities were shown to be entirely satisfactory. More recently, Chao *et al.* (2003) have shown that variations in sea-surface height in the extratropic north and south Pacific ocean basins have a combined temporal variations that match remarkably well the time evolution of the recent sudden changes in J_2. However, the

amplitude of the variations predicted from this oceanagrophic event accounts for only one third of the observed anomaly. It has been proposed that the remaining part of the signal can be explained by glacier-melting at sub-polar latitudes (Dickey *et al.*, 2002). However, the sea-level rise that would accompany the ice-melt has not been observed (Chao *et al.*, 2003), which suggests that the melt water, if any, remained in the vicinity of its melting location, in which case there is no transport of mass towards the equator and no associated increase in J_2. Another problem with the latter scenario is that it should produce a sizable anomaly in J_3, which is not observed (Chao *et al.*, 2003). Additionally, it is difficult to explain the return of J_2 to its pre-1998 trend with a glacier-melting mechanism, because it would imply the reverse scenario: a sudden large accumulation of ice and snow at high latitude and a consistent sea-level drop, neither of which have been observed. Since it is more likely that the the departures in J_2 are caused by a single mechanism, this raises doubts on the validity of the mechanism proposed in that study.

Another possibility suggested by Cox and Chao involves the Earth's fluid core. As they pointed out, a geomagnetic jerk occurred in 1999 (Mandea *et al.*, 2000), in proximity to the time at which the departure in J_2 was recorded. Geomagnetic jerks, as we have mentioned above, can be explained by torsional oscillations in the core (Bloxham *et al.*, 2002). This indicates a possible correlation between the changes in J_2 and torsional oscillations. Moreover, geomagnetic jerks have also been observed in 1978 (Gavoret *et al.*, 1986; Gubbins and Tomlinson, 1986) and 1991 (Macmillan, 1996), and near both of these times we observe a somewhat larger departure of J_2 from the linear trend. These correlations suggest that jerks and changes in J_2 may have a common explanation and call for a proper investigation of the contribution of the torsional oscillations in the gravity field data.

In order to do so, we have built a model which predicts the variations in the gravitational potential caused by a given torsional oscillation flow model. This model computes the displacements, the changes in the gravity field and the changes in the stress field in the entire Earth that are produced by the radial forcing associated with torsional oscillations and changes in rotation rates of the mantle and inner core. We find that, by using a torsional oscillations flow model which is constrained to satisfy the length of day data and also provide a best fit to the geomagnetic jerks signal, the changes in J_2 that are predicted by our model are not well correlated with the observed changes, and have a magnitude 10 times too small. This suggests that the sudden observed changes in J_2 cannot be explained

directly with torsional oscillations and that the correlation between the geomagnetic jerks and the maxima in ΔJ_2 may be a coincidence. However, provided the origin of these large variations is identified and removed from the data, it may be possible in the future to detect the torsional oscillations in the gravity field data. We note that only the lowest harmonic degree of the torsional oscillation flow, t_1^0 and t_3^0, may produce observable changes in the gravity field. Our model also predicts vertical ground motions on the order of 0.2 millimeter to occur, which is presently too small to be observed, but may be observable in the near future. The results of our model also suggest that torsional oscillations have contributed to a secular change in J_2 of about -0.75×10^{-12} per year in the last 20 years.

Finally, we note that the two main concepts in the present chapter have been discussed in previous studies. First, the idea that changes in the gravity field at the surface could be caused by pressure changes due to flow in the core and producing deflections of the CMB has been investigated most recently in the work of Fang *et al.* (1996). In their work, the change in the geostrophic pressure at the CMB was deduced from the changes in the CMB flow between 1965 and 1975. This pressure field was then treated as a surface mass density perturbation at the CMB and the radial deflection and changes in the gravity field that resulted solely from this local perturbation were calculated. They reported changes J_2 on the order of 1.3×10^{-11} per year, similar in amplitudes to the observed changes reported by Cox and Chao (2002). Our current approach is different as we are only using the torsional oscillations component of the flow. Additionally, and most importantly, we specify the geostrophic pressure in terms of a surface force acting on the CMB instead of a surface mass density perturbation. This changes the results significantly. The earlier work of Lefftz and Legros (1992) is also noteworthy, where it was shown that variations in the topography at the CMB, for instance due to mantle convection, can produce significant changes in the gravity field. Secondly, the changes in the elliptical component of the gravity field resulting from variations in rotation rates of the mantle is also not a novel idea. Indeed, the discrepancy between the the observed and predicted values of the hydrostatic flattening was erroneously believed for a long time to be related to the deceleration of the Earth's rotation rate (e.g. Munk and MacDonald, 1960). More recently, Denis *et al.* (1998) have calculated the changes in elliptical gravity field that result from changes in rotation rate, and the method employed in the present chapter is inspired in many ways from this study.

3.2 Theory

We seek to determine the displacements and changes in the gravity field and stress field of the whole Earth that result from specified forcings: torsional oscillations in the fluid core and rotation rate changes in the mantle and inner core. The dynamics governing small perturbations in the mechanical equilibrium of a self-gravitating Earth is a well studied problem because it lies at the very base of the theoretical foundation on which normal modes seismology is built. In addition, the response of the Earth to external forcing, such as tidal forcing, and to surface loading, such as post-glacial rebound and sea-level change, are also based on the same theoretical framework. We take advantage of this extensive body of literature to construct our model.

The following assumptions and approximations are used. We assume that the undeformed Earth is spherically symmetric, self-gravitating and in hydrostatic equilibrium and consider the perturbations about that state. The spherically symmetric equilibrium implies that we are considering a reference state that is non-rotating. We also assume that the rotation does not influence the deformations in the sense that we neglect their associated Coriolis acceleration. The influence of rotation only enters our system through our prescription of the forcing in the fluid core, the inner core and the mantle that perturb the equilibrium state. We are considering the static response due to static forcings and we assume that a static equilibrium is maintained at all times during the deformations. In other words, we neglect all inertial accelerations in the momentum balance. We assume that the fluid core is inviscid and remains in hydrostatic equilibrium even in the deformed state, and that the mantle and inner core are perfectly elastic. We neglect the presence of oceans at the surface.

3.2.1 The Earth's external gravitational potential

The gravitational potential at a radius r outside an axisymmetric body of mean spherical radius a can be expressed as sum of Legendre Polynomials (e.g. Jeffreys, 1970)

$$\phi_g(a,\theta) = -\frac{GM}{r}\left(1 - \sum_{n=2}\left(\frac{a}{r}\right)^n J_n P_n^0(\cos\theta)\right). \tag{3.1}$$

where M is the mass of the Earth and the coefficients J_n are dimensionless numbers that

represent the contribution of each zonal harmonic. In particular, J_2 is the coefficient of oblateness and represents the equatorial bulging of the Earth as a result of its own rotation. We note that $J_2 > 0$ represents an increase in oblateness. At the surface ($r = a$), the time variations of the J_n are related to the time-dependent zonal harmonic coefficients of the gravitational potential $\Phi_n^0(a,t)$ by

$$\Delta J_n(t) = \frac{a}{GM}\Delta\Phi_n^0(a,t)\,. \tag{3.2}$$

Here, we are solely interested in the changes in the gravitational potential of the whole Earth that result from the variations in geostrophic pressure along the CMB caused by torsional oscillations in the core and from changes in the mantle and inner core rotation rates.

3.2.2 Deformations in the mantle and inner core

Small displacements in the mantle and inner core caused by a load or an external forcing lead to changes in the stress field and gravity field. In turn, these changes create forces which induce additional displacements and additional changes in the stress and gravity field. The resulting mechanical equilibrium in the deformed state is that for which the external force is balanced by the sum of the forces induced by the small displacements. In the present context, the forcing results from torsional oscillations in the fluid core or from changes in the rotation rate of the mantle and the inner core.

We follow the treatment of Dahlen (1972, 1974), except that we neglect the Coriolis force, assumed to be small in our problem, and we also eliminate the inertial terms because we are considering static perturbations. For a complete treatment of all the perturbation equations, we refer the reader to Dahlen and Trump (1998).

The mantle and inner core are assumed to be perfectly elastic and isotropic, though the elastic parameters and the density vary with depth. Their reference equilibrium configuration is defined in terms a zeroth order balance relating the hydrostatic pressure $p_o(r)$, the density $\rho_o(r)$ and the gravitational potential $\phi_o(r)$. The undeformed mantle is assumed to be in hydrostatic equilibrium

$$0 = -\frac{\partial}{\partial r}p_o(r) - \rho_o(r)g_o(r)\,, \tag{3.3}$$

and the gravitational potential satisfies Poisson's equation,

$$\left(\frac{\partial^2}{\partial r^2}+\frac{2}{r}\frac{\partial}{\partial r}\right)\phi_o(r)=4\pi G\rho_o(r)\,. \tag{3.4}$$

In the above equilibrium state, the gravitational acceleration $-g_o(r)\mathbf{e_r}$ is defined in terms of the gravitational potential by $g_o(r)=\frac{\partial}{\partial r}\phi_o(r)$, and G is the gravitational constant. We note that this definition of the gravitational acceleration implies that the gravitational potential is *negative* everywhere.

The deformed state of the mantle is expressed in terms of small perturbations about the above equilibrium. The perturbations are created by small displacements $\mathbf{u}(\mathbf{r})$, which represent displacements of material particle from their position in the reference Earth (*i.e.* Lagrangian displacements). The displacements cause perturbations in the stress field and the gravitational potential. The static equilibrium of the deformed Earth is governed by an ensemble of conditions that comprise the momentum equation which determines the mechanical equilibrium,

$$\mathbf{0}=\nabla\cdot\mathbf{T}-\nabla(\rho_o\mathbf{u}\cdot\nabla\phi_o)-\rho_o\nabla\phi_1-\rho_1 g_o\mathbf{e_r}+\mathbf{f_e}\,, \tag{3.5}$$

an elastic constitutive relation,

$$\mathbf{T}=\lambda_o\mathbf{I}(\nabla\cdot\mathbf{u})+\mu_o(\nabla\mathbf{u}+(\nabla\mathbf{u})^T)\,, \tag{3.6}$$

an equation for continuity,

$$\rho_1=-\rho_o\nabla\cdot\mathbf{u}-\mathbf{u}\cdot\mathbf{e_r}\frac{\partial\rho_o}{\partial r}\,, \tag{3.7}$$

and Poisson's equation, which determines the changes in the gravity field

$$\nabla^2\phi_1=4\pi G\rho_1\,. \tag{3.8}$$

The above set of four coupled equations are known as the linearized elastic-gravitational equations. The perturbations in the density $\rho_1=\rho_1(\mathbf{u})$ and the gravitation potential $\phi_1=\phi_1(\mathbf{u})$ are defined at fixed coordinate points $\mathbf{r}$, *i.e.* they are defined in a Eulerian reference frame. The incremental Lagrangian Cauchy stress tensor $\mathbf{T}=\mathbf{T}(\mathbf{u})$ involves the second rank identity tensor $\mathbf{I}$, the Lamé parameter $\lambda_o=\lambda_o(r)$ and the modulus of rigidity

$\mu_o = \mu_o(r)$. The latter two define the elastic state of the reference undeformed Earth. The externally applied body force $\mathbf{f_e} = \mathbf{f_e}(\mathbf{r})$ represents here the centrifugal force of the mantle rotation, which we write in terms of a centrifugal potential ϕ_c,

$$\mathbf{f_e} = -\rho_o \nabla \phi_c \,. \tag{3.9}$$

The forcing from the torsional oscillations will enter the perturbations in the mantle through the boundary conditions at the CMB.

Solutions of the above system are found by expanding $\mathbf{u}$, ϕ_1 and $\nabla \cdot \mathbf{u}$ in terms of surface spherical harmonics as (e.g. Alterman *et al.*, 1959)

$$\begin{aligned} \mathbf{u} &= \sum_{n=0}^{\infty} \sum_{m=-n}^{n} \left(U_n^m(r) Y_n^m \mathbf{e_r} + V_n^m(r) \nabla_1 Y_n^m \right) , \\ \phi_1 &= \sum_{n=0}^{\infty} \sum_{m=-n}^{n} \Phi_n^m(r) Y_n^m , \\ \nabla \cdot \mathbf{u} &= \sum_{n=0}^{\infty} \sum_{m=-n}^{n} \chi_n^m(r) Y_n^m , \end{aligned} \tag{3.10}$$

where ∇_1 represents the gradient operator on the unit sphere:

$$\nabla_1 = \mathbf{e}_\theta \frac{\partial}{\partial \theta} + \mathbf{e}_\varphi \frac{1}{\sin\theta} \frac{\partial}{\partial \varphi} \,. \tag{3.11}$$

The surface spherical harmonics Y_n^m are defined as

$$Y_n^m = Y_n^m(\theta, \varphi) = P_n^m(\cos\theta) e^{im\varphi} \tag{3.12}$$

where $P_n^m(\cos\theta)$ is the associated Legendre polynomial. We use the following normalization over the unit sphere,

$$\int_\Omega Y_n^{m*} Y_s^t \, d\Omega = \frac{4\pi}{2n+1} \delta_{ns} \delta_{mt} \,. \tag{3.13}$$

This choice is convenient because for $m = 0$ it is equivalent to the Gauss-Schmidt normalization used in geomagnetism. This will facilitate the calculation of the perturbations directly in terms of the conventional definition of the flow coefficients at the CMB.

It is possible to write the complete set of elastic-gravitational equations in the mantle as

a system of 6 coupled first order ODE's, for which a solution can be found with a numerical integration (e.g. Alterman *et al.*, 1959). The set of equations are presented in appendix A.1. In a compact notation, the system of ODE's can be written as

$$\frac{\partial}{\partial r}\mathbf{y} = \mathsf{A}\cdot\mathbf{y} + \mathbf{f} \tag{3.14}$$

with the vector $\mathbf{y} = [y_1, y_2, y_3, y_4, y_5, y_6]^T$, in which

$$\begin{aligned}
y_1 &= U_n^m \\
y_2 &= \lambda_o \chi_n^m + 2\mu_o \frac{\partial}{\partial r} U_n^m \\
y_3 &= V_n^m \\
y_4 &= \mu_o \left(\frac{\partial}{\partial r} V_n^m - \frac{V_n^m}{r} + \frac{U_n^m}{r} \right) \\
y_5 &= \Phi_n^m \\
y_6 &= \frac{\partial}{\partial r}\Phi_n^m + \frac{(n+1)}{r}\Phi_n^m + 4\pi G \rho_o U_n^m
\end{aligned} \tag{3.15}$$

The interpretation of each quantity is as follows: y_1 and y_3 are respectively the radial and tangential displacements; y_2 and y_4 are respectively the radial and tangential stresses; y_5 is the gravitational potential; and y_6 is a gravitational acceleration.

The vector $\mathbf{f} = [f_1, f_2, f_3, f_4, f_5, f_6]^T$ includes the externally applied body force. For our present case of a centrifugal force, the centrifugal potential ϕ_c is written in terms of a degree 2 zonal harmonic

$$\phi_c = Z_2 \frac{r^2}{a^2} Y_2^0 \,, \tag{3.16}$$

where a is the radius of the Earth, and where $Z_2 = \Omega_o^2 a^2/3$ in the case of a centrifugal force of a body rotating at angular velocity Ω_o, or alternatively, $Z_2 = 2\Omega_o \delta\Omega a^2/3$ in the case of a centrifugal force associated with an angular velocity change of $\delta\Omega$. Using the above decomposition of ϕ_c in (3.9) yields a forcing vector $\mathbf{f}$ for which the only non-zero contributions are

$$f_2 = \rho_o \frac{\partial}{\partial r}\left(Z_2 \frac{r^2}{a^2}\right) = 2\rho_o Z_2 \frac{r}{a^2} \,,$$

$$f_4 \;=\; \rho_o Z_2 \frac{r}{a^2}\,, \tag{3.17}$$

and restricted to harmonic degree 2.

The perturbations in the inner core are treated in an equivalent manner as those in the mantle. The set of elastic-gravitational equations in the inner core are

$$\frac{\partial}{\partial r}\mathbf{y^s} = \mathsf{A}\cdot\mathbf{y^s} + \mathbf{f^s}\,, \tag{3.18}$$

where $\mathbf{y^s}$ is the solution vector in the inner core and $\mathbf{f^s}$ is defined identically as $\mathbf{f}$ except that it represents the centrifugal force in the inner core. As for the mantle, the forcing from torsional oscillations enters the inner core equations through the boundary conditions at the ICB.

3.2.3 Deformations in the fluid core caused by torsional oscillations

The undeformed static reference state in the core is isotropic and spherically symmetric. As for the mantle and the inner core, the equilibrium between the hydrostatic pressure, the density and the gravitational potential is determined in terms of the hydrostatic balance (3.3) and Poisson's equation (3.4).

The perturbations in gravity field in the core that result from small displacements differ than those in the solid Earth because tangential stresses vanish everywhere. The appropriate way of calculating the perturbations in the static limit has been the subject of intense debate in the literature and is known as "Longman's paradox", or "static core paradox" (Longman, 1963; Jeffreys and Vicente, 1966; Smylie and Mansinha, 1971; Pekeris and Accad, 1972; Israel *et al.*, 1973; Dahlen, 1974; Chinnery, 1975; Crossley and Gubbins, 1975; Dahlen and Fels, 1978). The controversy arises as a result of the absence of rigidity in the core, which forces the adoption of a neutrally stratified core or one for which the deformations are divergence-free, neither cases being completely physically realistic. Recent discussions on the static core paradox can be found in the work of Fang (1998) and Denis *et al.* (1998). Here, we choose to adopt the divergence-free approximation and follow the approach of Dahlen (1974), Chinnery (1975), and Crossley and Gubbins (1975), which showed that some of the controversy could be eliminated by requiring that the hydrostatic equilibrium in the fluid core is maintained at all times. In this case, displacements in the core can still

be represented using a Lagrangian description but only provided that they be interpreted as the displacements of equipotential surfaces.

If hydrostatic equilibrium is maintained even in the deformed state, the surfaces of constant density, constant fluid pressure and constant gravitational potential always coincide. The fluid displacements parallel to the equipotential surfaces are undetermined. The static equilibrium in the core under small (Lagrangian) displacements $\mathbf{u}(\mathbf{r})$ of the equipotential surfaces is governed by the linearized first order perturbations in the hydrostatic balance,

$$\mathbf{0} = -\nabla p_1 - \rho_o \nabla \phi_1 - \rho_1 g_o \mathbf{e_r} + \mathbf{f_e}\,, \tag{3.19}$$

the linearized first order Poisson's equation,

$$\nabla^2 \phi_1 = 4\pi G \rho_1\,, \tag{3.20}$$

an equation for continuity

$$\rho_1 = -u_r \frac{\partial \rho_o}{\partial r}. \tag{3.21}$$

in which we have used the divergence-free condition, $\nabla \cdot \mathbf{u} = 0$. As for the solid Earth, $\rho_1 = \rho_1(\mathbf{u})$, $\phi_1 = \phi_1(\mathbf{u})$, and $p_1 = p_1(\mathbf{u})$ are all Eulerian variables. Here, $\mathbf{f_e} = \mathbf{f_e}(\mathbf{r})$ is the radial force from torsional oscillations acting on the equipotential surfaces. This force is equivalent to the Coriolis force associated with the torsional oscillations velocity $\mathbf{v} = v_\varphi \mathbf{e}_\varphi$, and is given by $\mathbf{f_e} = -2\rho_o \Omega \times \mathbf{v}$, where $\Omega = \Omega_o \mathbf{e_z}$ is the Earth's rotation.

Torsional oscillations are azimuthal flows for which the quantity $\rho_o v_\varphi \mathbf{e}_\varphi$ is independent of z, the coordinate parallel to the rotation axis. The Coriolis force associated with this type of flow is conservative, because

$$\nabla \times (\Omega \times \rho_o \mathbf{v}) = \Omega(\nabla \cdot \rho_o \mathbf{v}) - \Omega \cdot \nabla \rho_o \mathbf{v} = -\Omega_o \frac{\partial}{\partial z} \rho_o \mathbf{v} = 0\,. \tag{3.22}$$

We can therefore express it as a gradient of a potential, $2\Omega \times \rho_o \mathbf{v} = -\nabla p_g$, where we call p_g the geostrophic pressure. The perturbation in the hydrostatic balance (3.19) can then be written as

$$\mathbf{0} = -\nabla(p_1 - p_g) - \rho_o \nabla \phi_1 - \rho_1 g_o \mathbf{e_r}\,. \tag{3.23}$$

By decomposing (3.23) into its radial and transverse components and using (3.21), it follows that

$$p_1 = -\rho_o \phi_1 + p_g \,, \tag{3.24}$$

$$u_r = -\frac{\phi_1}{g_o} \,. \tag{3.25}$$

Equations (3.21), (3.24) and (3.25) represent the coherent displacements of surfaces of constant density, gravitational potential, and the combination of the pressure and geostrophic pressure.

By inserting (3.21) and (3.25) in (3.20), we get a second order linear differential equation for ϕ_1,

$$\nabla^2 \phi_1 = \frac{4\pi G}{g_o} \frac{\partial \rho_o}{\partial r} \phi_1 \,. \tag{3.26}$$

This version of Poisson's equation implies that the perturbations in the gravitational potential within the core are independent of the local geostrophic forcing. The geostrophic forcing creates the disturbances in ϕ_1 by displacing the solid-fluid boundaries, and enters the system through the boundary conditions that will be specified in section 3.2.5. The changes in ϕ_1 within the core are entirely a consequence of the disturbances at the boundaries. Once a solution for ϕ_1 is obtained, the displacement of equipotential surfaces u_r and the perturbations in pressure p_1 may be subsequently determined from the known p_g.

The solutions of this equations can be found by expanding ϕ_1 in spherical harmonics

$$\phi_1 = \sum_{n=0}^{\infty} \sum_{m=-n}^{n} \Phi_n^m(r) Y_n^m \,. \tag{3.27}$$

Upon substitution of (3.27), (3.26) separates into a set of equations in $\Phi_n^m(r)$ for each n and m,

$$\frac{\partial^2 \Phi_n^m}{\partial r^2} + \frac{2}{r} \frac{\partial \Phi_n^m}{\partial r} - \left(\frac{n(n+1)}{r^2} + \frac{4\pi G}{g_o} \frac{\partial \rho_o}{\partial r} \right) \Phi_n^m = 0. \tag{3.28}$$

It is convenient to rewrite (3.28) in a form similar to the set of equations that determine the perturbations in the solid Earth. This will later facilitate the implementation of the boundary conditions and the solution of the entire problem. We therefore use the same

change of variable,

$$\begin{aligned} y_5^c &= \Phi_n^m \\ y_6^c &= \frac{\partial y_5^c}{\partial r} - \frac{4\pi G\rho_o}{g_o} y_5^c + \frac{n+1}{r} y_5^c \,, \end{aligned} \tag{3.29}$$

where the superscript c is used to identify fluid core variables, and where we have used (3.25) for the radial displacement y_1^c.

Equation (3.28) can be written as a coupled ODE system in terms of y_5^c and y_6^c. In matrix form, with $\mathbf{y^c} = [y_5^c, y_6^c]^T$, we get

$$\frac{\partial}{\partial r}\mathbf{y^c} = \mathsf{B} \cdot \mathbf{y^c} \,, \tag{3.30}$$

where

$$\mathsf{B} = \begin{pmatrix} \frac{4\pi G\rho_o}{g_o} - \frac{n+1}{r} & 1 \\ \frac{8\pi G\rho_o}{g_o}\frac{(n-1)}{r} & \frac{(n-1)}{r} - \frac{4\pi G\rho_o}{g_o} \end{pmatrix} . \tag{3.31}$$

The above development is equivalent to that presented by Wu and Peltier (1982). The changes in $\mathbf{y^c}$ that result from both the torsional oscillations and the variations in the rotation rate of the mantle and inner core will enter the above equations through the boundary conditions at the CMB and ICB.

3.2.4 Geostrophic pressure

The geostrophic pressure that produces the distortion of the CMB is completely determined by the torsional oscillations. We now wish to express the spherical harmonic coefficients of the geostrophic pressure in terms of this flow. As we defined above,

$$2\Omega \times (\rho_o \mathbf{v}) = -\nabla p_g \,. \tag{3.32}$$

Torsional oscillations are purely azimuthal flows, $\mathbf{v} = v_\varphi \mathbf{e}_\varphi$, and therefore

$$2\Omega_o \rho_o v_\varphi \mathbf{e_s} = \nabla p_g \,, \tag{3.33}$$

where $\mathbf{e_s}$ is the direction perpendicular to the rotation axis. The geostrophic pressure is only a function of s, the distance away from the rotation axis. In other words, p_g is constant along lines parallel to the rotation axis. The value of p_g at any point in the core may then be determined by an axial projection of its value at the CMB. This allows a determination of p_g in terms of a torsional oscillation flow represented at the CMB. Such a relationship is easily obtained by taking $\mathbf{e_r}\times$ (3.33), which gives

$$2\Omega_o b\rho_o \cos\theta v_\varphi \mathbf{e}_\varphi = \mathbf{e_r} \times \nabla_1 p_g \,, \tag{3.34}$$

where b is the radius of the CMB, and ∇_1 is defined on a unit sphere.

We first require a representation of the core surface flow v_φ in a spherical harmonic decomposition. The general representation of the tangential velocity at the CMB obtained from the geomagnetic field secular variation is usually written in terms of a toroidal and poloidal decomposition (e.g. Bloxham and Jackson, 1991)

$$\mathbf{v_h} = \mathbf{v}_T + \mathbf{v}_P = \nabla_1 \times (\mathcal{T}\mathbf{e_r}) + \nabla_1 \mathcal{S} \,, \tag{3.35}$$

where $\mathcal{S}$ and $\mathcal{T}$ are respectively the poloidal and toroidal scalars which are expanded in spherical harmonics. For torsional oscillations, the only non-zero contributions are from the zonal toroidal components that are symmetric about the equator. Hence the spherical harmonic decomposition is limited to the coefficients t_n^0 for *n odd*,

$$\begin{aligned} \mathbf{v_h} &= v_\varphi \mathbf{e}_\varphi = \nabla_1 \times (\mathcal{T}\mathbf{e_r}) = -\mathbf{e_r} \times \nabla_1 \mathcal{T} \,, \\ \mathcal{T} &= \sum_{n\,odd} t_n^0 Y_n^0 \,. \end{aligned} \tag{3.36}$$

We note that, in geomagnetism, the expansion of $\mathcal{T}$ and $\mathcal{P}$ is usually done in terms of real spherical harmonics instead of our choice defined in (3.12). However, the two expansions are identical for the zonal harmonics. The coefficients t_n^0 in (3.36) are therefore equivalent to those given by CMB flow inversion studies. We also note that the coefficients t_n^0 are defined in this study with respect to a reference frame rotating at angular velocity $\mathbf{\Omega}_o$.

With (3.34), we can relate spherical harmonic coefficients of the geostrophic pressure at the CMB $\Psi_n^m(b)$, defined as

$$p_g(b) = \sum_{n=0}^{\infty} \sum_{m=-n}^{n} \Psi_n^m(r) Y_n^m \,, \tag{3.37}$$

to the coefficients of torsional oscillations defined above in (3.36). The details of the derivation of this relationship are presented in appendix A.2. The only non-zero coefficients of the geostrophic pressure are those with both $m = 0$ and *n even*. This is consistent with our expectation that torsional oscillations produce perturbations that are axisymmetric and symmetric about the equator. In Appendix A.2, we demonstrate the more general result that torsional oscillations are in fact the only component of the flow that produce changes in the even zonal harmonics of the geostrophic pressure at the CMB. Here, we simply present the result: for an *even* degree n, the coefficients $\Psi_n^0(b)$ are given by

$$\Psi_n^0(b) = -\Omega_o b \rho_o \left(\frac{2(n-1)}{(2n-1)} t_{n-1}^0 + \frac{2(n+2)}{(2n+3)} t_{n+1}^0 \right) . \tag{3.38}$$

Hence, the geostrophic pressure coefficient at a given n depends only on 2 coefficients of the flow, t_{n-1}^0 and t_{n+1}^0.

To complete the problem, we also need to compute the coefficients $\Psi_n^0(c)$ that represent the geostrophic pressure at the ICB ($r = c$). Because the only non-zero coefficients are those with $m = 0$, we can expand the geostrophic pressure in terms of Legendre polynomials as

$$p_g(c, \theta) = \sum_{n\,even} \Psi_n^0(c) P_n^0(\cos\theta) \,, \tag{3.39}$$

and relate the coefficients $\Psi_n^0(c)$ to the coefficients $\Psi_n^0(b)$ defined at the CMB in (3.38). Because the geostrophic pressure is constant on *cylindrical* surfaces aligned with the rotation axis, this is done by taking the axial projection of the Legendre polynomial expansion at the CMB onto the interior radius c,

$$p_g(c, \theta) = \sum_{n'\,even} \Psi_{n'}^0(b) P_{n'}^0(\cos(\arcsin(\frac{c}{b}\sin\theta))) \,, \tag{3.40}$$

and expanding this later expression in terms of Legendre polynomials defined on the interior radius c. Equating (3.39) and (3.40) gives the contribution of the CMB coefficient at degree n' to the ICB coefficient at degree n. We note that as a result of the axial projection, we expect that the coefficients $\Psi_n^0(c)$ also contain contributions from coefficients of *higher* harmonic degrees n' of the forcing defined at the CMB.

The determination of the $\Psi_n^0(c)$'s according to the above scheme is relatively straightforward. However, compared to the CMB deformations, the effect on the gravity field at the surface caused by the distortion of the ICB are much smaller. This is because the density jump is smaller at the ICB, and most importantly, because the perturbation created at the ICB are more attenuated when they reach the surface than those at the CMB. We have verified that including the ICB deformation has a negligible effect on the results of this study. Therefore, for the sake of simplicity, we have decided to neglect the effects of the geostrophic pressure at the ICB, and from now on we assume that $\Psi_n^0(c) = 0$.

3.2.5 Boundary conditions

The solution of the coupled ODE's for the perturbations in the core in (3.30) depends upon 2 constants of integration. Likewise, the solution for the perturbations in the mantle in (3.14) and in the inner core (3.18) each require 6 constants of integration. These 14 degrees of freedom are specified in terms of boundary conditions at the origin, the ICB, the CMB and the Earth's surface.

The conditions that the variables of our system have to obey at these interfaces are as follows. At each discontinuity in density or elastic parameters, including at the Earth's surface, the gravitational potential ϕ_1 and the gravitational flux $\mathbf{e_r} \cdot (\nabla\phi_1 + 4\pi G\rho_o \mathbf{u})$ must be continuous. At internal boundaries between two solid regions, all displacements and traction forces must be continuous. At a boundary between a solid and inviscid fluid, tangential displacements may be allowed. The traction force must still be continuous at a fluid-solid boundary, but since an inviscid fluid cannot support shear, the tangential traction vanishes at the boundary. At the Earth's surface, in the absence of surface load, the traction forces must vanish.

The above requirements impose that, at radial surfaces in the mantle and the inner core where there exists a discontinuity in ρ_o, λ_o or μ_o, all 6 y_i's are continuous. At the CMB, the appropriate way of incorporating the above conditions has been discussed by a number of authors and is related to the static core paradox mentioned above (see earlier references). For the case of static deformations which maintain the hydrostatic equilibrium in the core, the difficulty stems from the fact that deformations in the core coincide with displacements of equipotential surfaces, whilst this is generally not the case in the mantle. Hence, the

CMB may penetrate the equipotentials in the core. Allowance for this is incorporated by introducing arbitrary constants in the fluid-solid boundary conditions. At the CMB, we have

$$\begin{aligned} y_1(b) &= -\frac{y_5^c(b)}{g_o(b)} + C_5\,, \\ y_2(b) &= C_5 g_o(b)\rho_o(b^-) - \Psi_n^0(b)\,, \\ y_3(b) &= C_4\,, \\ y_4(b) &= 0\,, \\ y_5(b) &= y_5^c(b), \\ y_6(b) &= y_6^c(b) + 4\pi G\rho_o(b^-)C_5\,. \end{aligned} \tag{3.41}$$

where (b^-) indicates a quantity evaluated in the fluid side of the boundary. The constant C_5 represents the apparent jump in radial displacement, and C_4 is the arbitrary tangential displacement at the base of the mantle. The boundary condition on the normal stress (y_2) introduces the forcing from the geostrophic pressure in the system. The normal stress on the fluid side includes the geostrophic pressure (it is given by (3.24)), which leads to the above condition.

By analogy, a similar set of boundary conditions applies at the ICB. However, because the method of solution involves an integration of the perturbation equations from $r \to 0$ towards the external radius, the boundary conditions at the ICB are manipulated into a more convenient way. In the fluid core, we are only concerned about y_5^c and y_6^c, and the propagation of these two variables across the ICB is given by

$$\begin{aligned} y_5^c(c) &= y_5^s(c)\,, \\ y_6^c(c) &= y_6^s(c) - \frac{4\pi G}{g_o(c)}\left(y_2^s(c) + \Psi_n^0(c)\right)\,, \end{aligned} \tag{3.42}$$

where we have used the condition on y_2 across the ICB. Two additional conditions must be obeyed by the solution in the inner core at the ICB:

$$y_4^s(c) = 0\,, \tag{3.43}$$

$$g_o(c)\rho_o(c^+)y_1^s(c) - y_2^s(c) + \rho_o(c^+)y_5^s(c) - \Psi_n^0(c) = 0\,, \tag{3.44}$$

where (c^+) indicate a quantity evaluated on the fluid side of the ICB, and where the second of these condition is obtained from combining the conditions on y_1 and y_2. According to our approximation in the previous section, we set $\Psi_n^0(c) = 0$ in the last two sets of equations.

The conditions that ensure the solution in the inner core to remain finite as $r \sim 0$ can be determined by an analytical solution near the origin. Following Crossley (1975), if we assume that near the origin $\partial\rho/\partial r \to 0$, then $g_o \to 4\pi G\rho_o r/3$, and an analytical solution can be obtained by a power-series expansion of the variables. The solution of the 6 variables at a small radius ε depends on three independent coefficients and the solution can be written as,

$$\mathbf{y^s}(\varepsilon) = C_1\mathbf{y^{\varepsilon 1}} + C_2\mathbf{y^{\varepsilon 2}} + C_3\mathbf{y^{\varepsilon 3}}\,. \tag{3.45}$$

The coefficients C_1, C_2 and C_3 are three additional constants of integration and the vectors $\mathbf{y^{\varepsilon 1}}$, $\mathbf{y^{\varepsilon 2}}$ and $\mathbf{y^{\varepsilon 3}}$ are given in appendix A.3.

At the top of the mantle, in the absence of any external load, the radial stresses, the tangential stresses and the gravitational flux all vanish, which specifies 3 additional conditions:

$$y_2(a) = y_4(a) = y_6(a) = 0\,. \tag{3.46}$$

We therefore have a total of 19 boundary conditions which are specified in terms of 5 constants. The value of these constants are those for which all 19 boundary conditions can be simultaneously satisfied. The determination of the constants removes 5 degrees of freedom in the system and allows a unique solution for the whole problem. The solution can be found by integrating (3.18) from a small r, using (3.45) as a starting solution. The boundary conditions (3.42) at the ICB are applied and the solution is propagated in the core with (3.30). The set of boundary conditions at the CMB are applied and the solution is propagated to the surface with (3.14). The integration is iterated by varying the 5 constants until the conditions (3.43) and (3.44) at the ICB and the 3 boundary conditions at the surface (3.46) are all satisfied.

3.2.6 Love numbers

The contribution of the torsional oscillations to the perturbations from the reference state is determined by setting $Z_2 = 0$ in (3.16). From a known torsional oscillation flow decomposition, the coefficients $\Psi_n^0(b)$ for the forcing at degree n on the CMB are determined by (3.38). It is useful to represent the perturbation in the gravitational potential at the surface $\Phi_n^0(a)$ in terms of the $\Psi_n^0(b)$'s by casting the whole problem under the formalism of Love numbers (Love, 1909). Let us define

$$\Phi_n^0(a) = -k_n \frac{\Psi_n^0(b)}{\bar{\rho}}, \tag{3.47}$$

where the Love number k_n represents the gravitational potential perturbation at harmonic degree n at the surface of the Earth that results from a geostrophic pressure of the same degree at the CMB. For a normalization of our system of equations with typical scales for r, g_o and ρ_o given respectively by a, $\bar{g}$ and $\bar{\rho}$, where $\bar{g}$ is the acceleration at the surface and $\bar{\rho}$ is the mean density of the Earth, the Love numbers k_n are then simply the solution for variable y_5 at $r = a$ for $\Psi_n^0(b) = 1$ and neatly summarize the effects of elastic deformation of the whole planet.

The perturbation in gravitational potential that results from the change in rotation rate of the mantle can similarly be expressed in terms of a Love number representations. For the centrifugal potential given by (3.16), we define

$$\Phi_2^0(a) = k_m Z_2^{(m)}, \tag{3.48}$$

so that k_m represents the amplitude of the gravity field perturbation at degree 2 at the surface that results from a centrifugal potential in the mantle which has a unity amplitude at the surface, *i.e.* $Z_2^{(m)} = 1$. Likewise, we define

$$\Phi_2^0(a) = k_{ic} Z_2^{(ic)}. \tag{3.49}$$

Hence, k_{ic} represents the amplitude of the gravity field perturbation at degree 2 at the surface that results from a centrifugal potential in the inner core with $Z_2^{(ic)} = 1$. We note that $Z_2^{(ic)}$ is set to zero to calculate k_m (and vice-versa) and that in both cases the torsional oscillations forcing is set to zero.

Table 3.1: Parameters used in calculations

Parameters	value
Gravitational constant	$G = 6.67 \times 10^{-11}$ m^3 kg^{-1} s^{-2}
Mass of the Earth	$M = 5.97 \times 10^{24}$ kg
Earth's rotation rate	$\Omega_o = 7.29 \times 10^{-5}$ s^{-1}
mantle axial moment of inertia	$I_m = 7.12 \times 10^{37}$ kg m^2
core axial moment of inertia	$I_c = 0.92 \times 10^{37}$ kg m^2
radius of Earth	$a = 6.371 \times 10^6$ m
radius of the core	$b = 3.480 \times 10^6$ m
radius of the inner core	$c = 1.2215 \times 10^6$ m
acceleration at the surface	$\bar{g} = GM/a^2 = 9.82$ m s^{-2}
mean density	$\bar{\rho} = 5515$ kg m^{-3}

We define similar Love numbers to characterize the radial displacements at the surface $D_n^0(a)$:

$$\begin{aligned} D_n^0(a) &= h_n \frac{\Psi_n^0(b)}{\bar{\rho}\,\bar{g}}, \\ D_2^0(a) &= -h_m \frac{Z_2^{(m)}}{\bar{g}}, \\ D_2^0(a) &= -h_{ic} \frac{Z_2^{(ic)}}{\bar{g}}. \end{aligned} \tag{3.50}$$

3.3 Results

The solutions depend on the reference Earth model upon which the perturbations are imposed. We use here the Earth model PREM (Dziewonski and Anderson, 1981) which specifies a radially symmetric Earth with a reference density $\rho_o(r)$ (from which a gravitational acceleration $g_o(r)$ and gravitational potential $\phi_o(r)$ are determined), and elastic parameters $\lambda_o(r)$ and $\mu_o(r)$ for every radial surface. The outermost region in PREM represents an overriding ocean. For now, we simply neglect the additional dynamical effects of oceans and extend the parameters of the previous region (crust) to this outermost radius. In Table 3.1 we list the values of all other relevant parameters used in our calculations.

3.3.1 Solutions of the perturbation problem

The perturbations in the degree 2 zonal harmonic of y_1 and y_5 as a function of radius that result from a centrifugal potential with $Z_2^{(m)} = 1$ in the mantle and zero forcing in the fluid core and inner core is presented in figure 3.4 (thick line). For a comparison, we have also plotted the solutions obtained above for a centrifugal force acting everywhere in the Earth (thin line). We note that each variable has been normalized so that the solution at the surface equals the Love numbers k_m and h_m and we find $k_m = 0.2345$ and $h_m = 0.4769$. To get the dimensional value of y_5, one needs to multiply the values on figure 3.4 by the dimensional amplitude of the forcing potential. The dimensional value of y_1 is obtained by multiplying the result by the forcing potential divided by the gravitational acceleration at the surface.

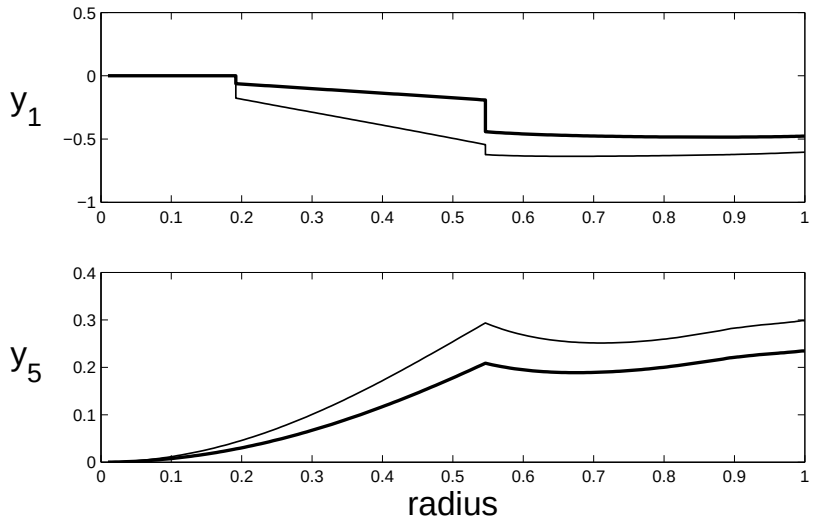

Figure 3.4: Solutions of the zonal spherical harmonic coefficient of degree 2 of the radial displacement y_1, and of the perturbation in gravitational potential y_5 as a function of radius for a centrifugal force acting on the mantle only (thick line), and for a centrifugal force acting on the whole Earth (thin line). Solutions are dimensionless. We recall that y_1 represents the displacements of material surfaces in the inner core ($0 \leq r \leq 0.1917$) and the mantle ($0.5462 \leq r \leq 1$) but is defined as the displacements of equipotential surfaces in the fluid core ($0.1917 < r < 0.5462$).

The solution in y_1 and y_5 as a function of radius that result from a centrifugal potential with $Z_2^{(ic)} = 1$ in the inner core and zero forcing in the fluid core and mantle is presented in figure 3.5. The solutions at the surface determine k_{ic} and h_{ic} and we find $k_{ic} = 1.47 \times 10^{-6}$

and $h_{ic} = 1.29 \times 10^{-6}$. Compared with the previous solution, the amplitudes of y_1 and y_5 are much smaller. The change in the elliptical gravity field and radial displacement at the surface is 5 orders of magnitude larger for a change in mantle rotation rate than for an equivalent change in inner core rotation rate. This difference is in part because for an equivalent change in rotation rate, the forcing at the surface is roughly 25 times larger than at the ICB. The remaining part of the discrepancy is mostly a consequence of the smaller density jump at the ICB and the attenuation of the perturbation as it propagates to the surface.

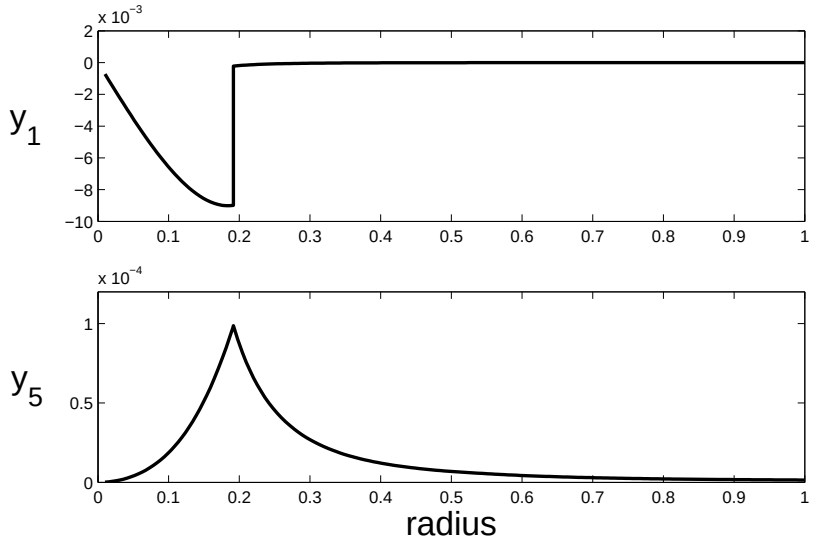

Figure 3.5: Same as figure 3.4, but for a centrifugal force that acts only on the inner core.

We now solve for the perturbations that result from the forcing of the torsional oscillations in the core. We set $Z_2^{(m)} = Z_2^{(ic)} = 0$, and compute the perturbations at degree n in the whole Earth that results from a torsional oscillation flow which produces a unit amplitude geostrophic potential of the same degree at the CMB, *i.e.* $\Psi_n^0(b) = 1$. In figure 3.6, we present the solutions of the perturbation in radial displacement and gravitational potential for $n = 2$. The solutions at the surface give respectively the Love numbers k_2 and h_2. We find $k_2 = 0.1116$ and $h_2 = 0.2302$.

An estimate of the amplitude of the radial displacements of the surfaces of constant geopotential can be obtained from figure 3.6. The geostrophic pressure scales as $\Psi \sim \rho_o \Omega_o b v_{to}$, and a typical amplitude of the change in torsional oscillation velocity is about a kilometer per year ($v_{to} \sim 3 \times 10^{-5}$ m s^{-1}). The normalized radial displacements in the core

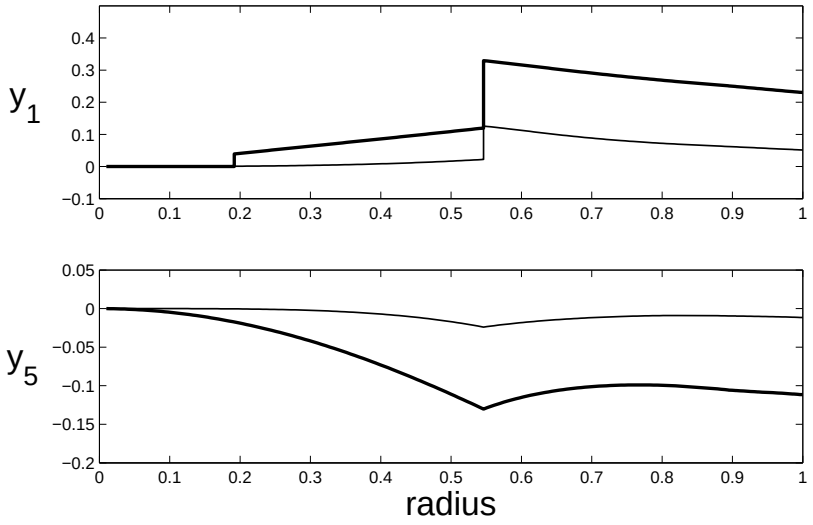

Figure 3.6: Solution of y_1 and y_5 (dimensionless) as a function of radius for a geostrophic potential at the CMB of $\Psi_2^0(b) = 1$ (thick line) and $\Psi_4^0(b) = 1$ (thin line).

Table 3.2: Love numbers

k_m	$= 2.345 \times 10^{-1}$	h_m	$= 4.769 \times 10^{-1}$
k_{ic}	$= 1.47 \times 10^{-6}$	h_{ic}	$= 1.29 \times 10^{-6}$
k_2	$= 1.116 \times 10^{-1}$	h_2	$= 2.302 \times 10^{-1}$
k_4	$= 1.156 \times 10^{-2}$	h_4	$= 5.135 \times 10^{-2}$
k_6	$= 1.957 \times 10^{-3}$	h_6	$= 1.366 \times 10^{-2}$
k_8	$= 4.171 \times 10^{-4}$	h_8	$= 4.013 \times 10^{-3}$

shown in figure 3.6, $y_1 \sim 1$, corresponds to a dimensional displacement of $\rho_o \Omega_o b v_{to} / \bar{\rho}\,\bar{g}$, which gives ~ 1.5 millimeter.

The solution obtained at degree $n = 4$ is also shown in figure 3.6. The results are similar to those obtained with $n = 2$ but with smaller amplitudes. The values of the Love numbers for $n = 4$ are $k_4 = 0.01156$ and $h_4 = 0.05135$. The Love numbers for a few of the larger harmonics are presented in Table 3.2.

3.3.2 Time variations in the zonal harmonics of the gravity field

With the Love numbers calculated above, the perturbations in even degree n of the gravitational potential at the surface can be readily obtained for a given torsional oscillation flow. Since the flow is time-dependent, the variations in time at the surface are then obtained from the instantaneous torsional oscillation flow at each time step. Using (3.2), (3.47),(3.48) and (3.49), the variations in the coefficients J_n, for $n > 2$, are then given by

$$\Delta J_n(t) = -k_n \frac{a}{GM} \frac{\Psi_n^0(b,t)}{\bar{\rho}}, \tag{3.51}$$

and the variations in J_2 are given by

$$\Delta J_2(t) = \frac{a}{GM} \left(-k_2 \frac{\Psi_n^0(b,t)}{\bar{\rho}} + k_m Z_2^{(m)}(t) + k_{ic} Z_2^{(ic)}(t) \right). \tag{3.52}$$

Let us first consider the role of a change in inner core rotation rate in the variations in J_2. We found k_{ic} to be 5 orders of magnitude smaller than k_m. In other words, the changes in rotation rate of the inner core have to be 5 orders of magnitude larger than the changes in rotation rate of the mantle for the former to play a role as important as the latter in the variations in J_2. We can estimate directly the variations in J_2 caused by changes in inner core rotation rate $\delta\Omega_{ic}$ by using $Z_2^{(ic)} = 2\Omega_o \delta\Omega_{ic} a^2/3$ in (3.52),

$$\Delta J_2 = \frac{2}{3} \frac{a^3 \Omega_o}{GM} k_{ic}\, \delta\Omega_{ic}\,. \tag{3.53}$$

Using the values in Table 3.1, and $k_{ic} = 1.47 \times 10^{-6}$, this implies $\Delta J_2 \approx \delta\Omega_{ic} \cdot 10^{-5}$ s. Hence, in order to produce changes in J_2 of the scale of the "1998 anomaly" (10^{-10}), we need a change in rotation rate of the inner core on the order of 10^{-5} s^{-1}, or $\approx 1/7$ of the actual rotation rate of the Earth. So for instance, considering a 10^{-10} per year change in J_2 for 3 years, the required rotation rate change of the inner core would have rotated it by 180 degrees with respect to the mantle!

Such a high rotation rate of the inner core is unrealistic because it is 2 orders of magnitude large than the largest estimates inferred from seismology (Song and Richards, 1996; Su *et al.*, 1996) (see also Laske and Masters (1999); Souriau and Poupinet (2000)). Physically, it is also very unlikely because the inner core is tightly coupled electromagnetically to the fluid core (Gubbins, 1981) and gravitationally to the mantle (Buffett, 1996a). Zatman

(2003) estimated the change in rotation rate of the inner core by assuming perfect coupling at the ICB with the rigid cylindrical flows inside the tangent cylinder. He obtained changes on the order of 0.3 degrees per year, or $\delta\Omega_{ic} \approx 1.6 \times 10^{-10}$ s^{-1}. While it is questionable whether the assumption of perfect coupling at the ICB is valid and whether the flow inside the tangent cylinder can be well recovered in the data, this value is nevertheless a good approximation of the amplitude of $\delta\Omega_{ic}$. Indeed, this is also the predicted amplitude of $\delta\Omega_{ic}$ if a large part of the length of day variations result from free oscillations between the mantle, inner core and torsional oscillations (Mound and Buffett, 2003). Such a change in rotation rate of the inner core would produce changes in J_2 on the order of 10^{-15}, clearly too small to be observable.

Since the above considerations suggest that the inner core has a negligible role in the changes in J_2, and since we do not have reliable observations of the variations of inner core rotation rate at decade periods, for convenience, we neglect its contribution in (3.52). This latter equation can be further reorganized. As we pointed out in the introduction, our confidence in the torsional oscillations stems from the good agreement between the changes in angular momentum in the core that they carry and the changes in the mantle angular momentum, observed in terms of changes in length of day. We can take advantage of this fact and express the changes in J_2 explicitly in terms of the variations in the length of day.

In what follows, we make the assumption that changes in the axial angular momentum in the core $L_c(t)$ and the mantle $L_m(t)$ are solely due to variations in their respective rotation rates. In other words, the axial moment of inertia of the core I_c and the mantle I_m remain constant. (We note that the variations in axial angular momentum produced by the secondary effect of changes in the moments of inertia due to changes in the rotation rate are on the order of a factor 1000 smaller.)

Measured in a reference frame fixed to the mantle, the change in angular momentum in the core is carried by only two of the torsional oscillation flow components (Jault and Le Mouël, 1991; Jackson *et al.*, 1993),

$$L_c^{(m)}(t) = \frac{I_c}{b}\left(t^{(m)}{}_1^0 + \frac{12}{7}t^{(m)}{}_3^0\right). \tag{3.54}$$

The coefficients $t^{(m)}{}_1^0$ and $t^{(m)}{}_3^0$ are also measured with respect to the mantle fixed frame and

are the coefficients obtained from the inversion of the geomagnetic data. Their relationship to the flow coefficients t_j^0 defined here with respect to a frame rotating at angular velocity Ω_o is given by

$$\begin{aligned} t_1^0 &= {t^{(m)}}_1^0 + b\,\delta\Omega_m(t)\,, \\ t_j^0 &= {t^{(m)}}_j^0, \qquad \text{for } j>1\,, \end{aligned} \tag{3.55}$$

where $\delta\Omega_m(t)$ is the change in mantle rotation rate with respect to Ω_o. In the reference frame rotating with angular velocity Ω_o, the total core angular momentum is then

$$\begin{aligned} L_c(t) &= L_c^{(m)}(t) + I_c\delta\Omega_m(t)\,, \\ &= \frac{I_c}{b}\left({t^{(m)}}_1^0 + b\,\delta\Omega_m(t) + \frac{12}{7}{t^{(m)}}_3^0\right), \\ &= \frac{I_c}{b}\left(t_1^0 + \frac{12}{7}t_3^0\right), \end{aligned} \tag{3.56}$$

Conservation of angular momentum between the core and mantle implies that $L_c(t) = -L_m(t) = -I_m\delta\Omega_m(t)$, and from (3.56) we get a relationship between the torsional oscillation flow component and the changes in rotation rate of the mantle,

$$\left(t_1^0 + \frac{12}{7}t_3^0\right) = -\frac{I_m}{I_c}b\,\delta\Omega_m(t)\,. \tag{3.57}$$

The harmonic degree 2 of the geostrophic forcing at the CMB in (3.38) contains the same ratio of t_1^0 to t_3^0,

$$\Psi_2^0(b) = -\frac{2}{3}\rho_o(b)\Omega_o b\left(t_1^0 + \frac{12}{7}t_3^0\right). \tag{3.58}$$

Using $Z_2^{(m)} = 2\Omega_o\delta\Omega_m a^2/3$ and $\delta\Omega_m = -\Delta T\,\Omega_o^2/2\pi$, we can write the changes in J_2 in (3.52) as

$$\Delta J_2(t) = \frac{a^3\Omega_o^3}{3\pi GM}\Delta T\left(\frac{b^2}{a^2}\frac{\rho_o(b)}{\bar{\rho}}\frac{I_m}{I_c}k_2 - k_m\right), \tag{3.59}$$

where ΔT represents the changes in the length of day (ΔLOD).

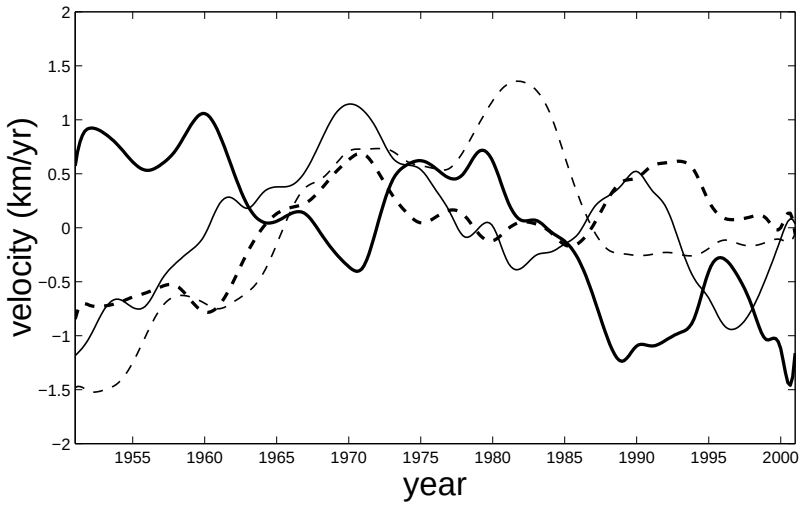

Figure 3.7: Coefficients of the torsional oscillations model as a function of time: t_1^0 (thick solid line); t_3^0 (thick dashed line); t_5^0 (thin solid line); t_7^0 (thin dashed line).

We use a torsional oscillation flow model which is constrained to give the best fit to the geomagnetic jerks (Bloxham *et al.*, 2002), and also constrained to be consistent with the changes in the length of the day. We show in figure 3.7 the first few coefficients of the torsional oscillation flow. We note that we have subtracted the mean steady component of each coefficient since we are interested in the changes with respect to a steady background. We show in figure 3.8 the data for length of day variations from the International Earth Rotation Service (IERS) and from which we have subtracted a secular change of 1.4 ms per century. We also show in the same figure the predicted changes from the torsional oscillation flow model, with the latter constrained to minimize the misfit with the ΔLOD data. In all subsequent calculations, the solid curve is used for ΔT.

In figure 3.9 we show the changes in J_2 predicted by (3.59). The model predicts extrema in ΔJ_2 near when geomagnetic jerks are observed. This is because these are the times when the differential cylindrical velocities are the largest (Bloxham *et al.*, 2002). Consequently, this is also when the geostrophic potential is at its maximum in amplitude. As expected, the contribution from the change in rotation rate of the mantle is opposite to the contribution of the torsional oscillations. The largest amplitude of the total variations in J_2 are roughly 2×10^{-11} for the last two decades. The total variations in J_2 from our model is compared to the observed variations in J_2 about the secular linear trend for the last 20 years in figure 3.10.

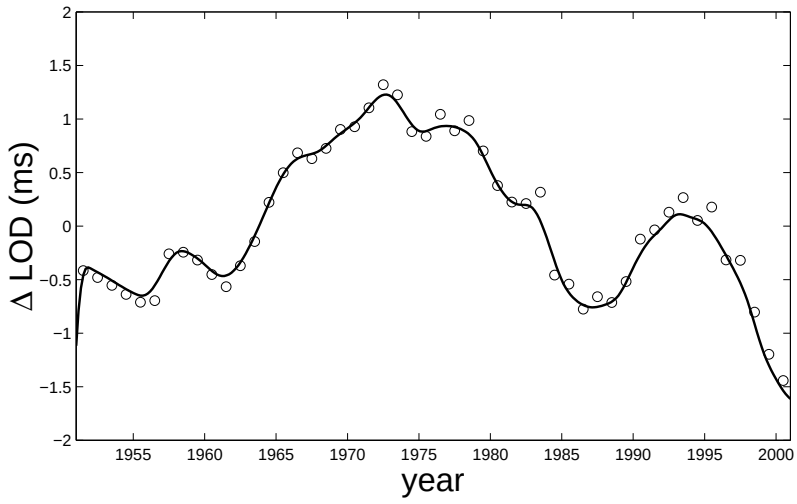

Figure 3.8: Variations in the length of day in milliseconds about an average value for the time period considered. The open circles are the data from the IERS, from which we have subtracted a trend of 1.4 milliseconds per century. The solid line is the prediction from the torsional oscillation flow model from equation (3.57) and $\delta\Omega_m = -\Delta T\,\Omega_o^2/2\pi$.

Our model produces amplitudes that are too small by a factor of about 10 to explain the observed variations and by a factor 30 to explain the larger variations that started near 1998. Moreover, the predicted changes in J_2 are not well correlated with the observations. This suggests that torsional oscillations in the core do not account for the subdecadal changes in J_2. Similarly, although we do not show it here, the changes in J_4 predicted by (3.51) are also a factor 10 too small and not well correlated with the observed changes in J_4 reported in Cox and Chao (2002).

As we see in figure 3.9, torsional oscillations also cause changes on longer timescales of about 30 years. Since 1980, the overall variation in J_2 predicted from our torsional oscillation model is about -1.5×10^{-11}. This gives a contribution to the secular linear decrease in J_2 of -0.75×10^{-12} yr^{-1}. This is about 40 times smaller than the observed linear trend of -2.8×10^{-11} yr^{-1} , which is believed to represent the signature of post-glacial rebound (Yoder *et al.*, 1983; Rubincam, 1984; Mitrovica and Peltier, 1993). However, this contribution from the torsional oscillations to the secular trend is on the same order as the effect produced by artificial reservoir water impoundment (Chao, 1995), and more important than the effects produced by mass redistribution from earthquakes (Chao *et al.*, 1995), subduct-

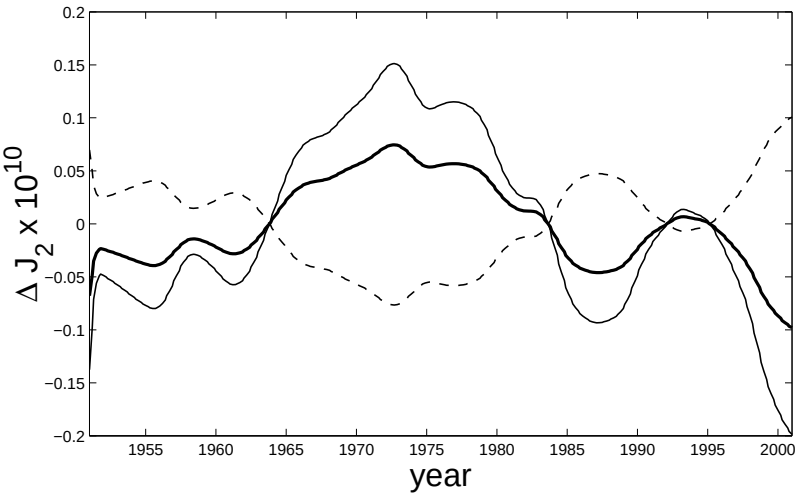

Figure 3.9: Variations in J_2 as a function of time predicted by our model (thick solid line), and its individual contribution from the k_2 term (thin solid line) and the k_m term (thin dashed line) of equation (3.59).

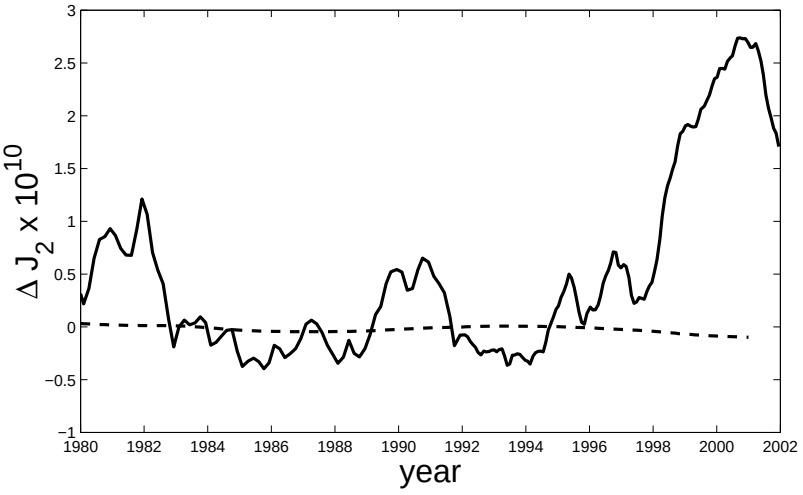

Figure 3.10: Comparison between the observed ΔJ_2 signal from which the secular linear trend has been removed (solid line) and variations in J_2 predicted by our model from equation (59) (dashed line).

ing slabs in the mantle (Alfonsi and Spada, 1998), and from the secular spin down and associated "rounding" of the Earth due to gravitational tidal breaking with the Moon (e.g. Stacey, 1992, p.96).

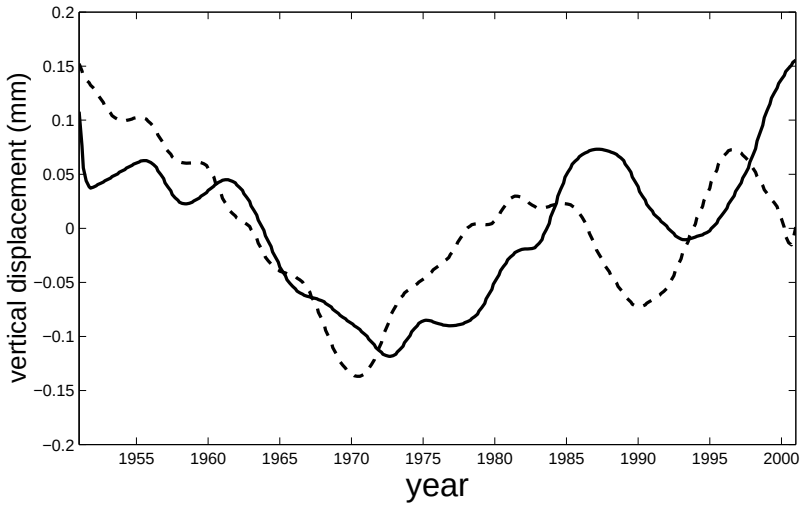

Figure 3.11: Variations in the zonal harmonic coefficients of degree 2 (solid line) and 4 (dashed line) of the vertical ground motion at the surface as a function of time.

We present in figure 3.11 the changes in the zonal harmonic coefficients of the radial displacement at the surface of the Earth, $\mathcal{D}_n(t)$, for degree $n = 2$ and $n = 4$. They are obtained from the Love numbers defined in (3.50):

$$\begin{aligned} \mathcal{D}_2(t) &= \frac{1}{\bar{g}}\left(h_2 \frac{\Psi_n^0(b,t)}{\bar{\rho}} - h_m Z_2^{(m)}(t) \right), \\ \mathcal{D}_n(t) &= h_n \frac{\Psi_n^0(b,t)}{\bar{\rho}\,\bar{g}}, \quad \text{for } n > 2, \end{aligned} \tag{3.60}$$

where we have again neglected the contribution from the change in inner core rotation rate. The changes in $\mathcal{D}_n(t)$ are on the order of 0.2 millimeter over the last few decades.

3.4 Discussion and Conclusion

The results of our study suggests that torsional oscillations in the core, in the simple way that they produce variable pressure at the CMB as we have described, cannot account for the observed changes in J_2 about the linear secular decreasing trend. The contribution to the linear secular trend itself that may be attributed to torsional oscillations is on the order of a few percent. The correlation between geomagnetic jerks and the maxima in the changes in

J_2 may then be merely a coincidence.

It is not impossible that the torsional oscillations remain the underlying cause of the changes in J_2 about the linear trend if there exists an amplification mechanism. For instance, circulation in the oceans may amplify a 5-year zonal degree 2 signal by a factor 10, just like the tidal sea-level amplitudes near coast lines are greatly amplified (e.g. Gill, 1982). However, because the prediction of our model and the observed signal are not well correlated, the amplification mechanism would have to be highly non-linear.

Even if the mechanism described in this study seem to not be responsible for the large sudden changes observed in J_2, the detection of the torsional oscillations in the gravity data may be possible in the near future. If the source of the changes in J_2 is identified and subtracted from the signal, it may be possible to isolate a background global change in the degree 2 zonal harmonic. The results presented in this chapter suggest that the changes in J_2 from the torsional oscillations are on the order of 10^{-11} per decade, which is at the level of the present noise level in the gravity data (Cox and Chao, 2002). However, the current GRACE satellite mission will provide data with a precision improvement of an order of magnitude (e.g. Kim and Tapley, 2002; Chao, 2003) and hence may allow the signal of the torsional oscillations to be observed in the changes in J_2. However, we stress that the recovery of the torsional oscillation signal may not be possible if the time varying parts of other effects which have similar amplitude cannot be eliminated from the data. Alternatively, one may use the results of our model to subtract the contribution from the torsional oscillations in the core in the time varying part of the gravity field in order to isolate the changes due to other effects.

It may also be possible in the future to observe the vertical ground motion associated with torsional oscillations using global GPS data (e.g. Herring, 1999). Our model predicts changes in vertical ground displacement at the surface on the order of 0.2 mm (figure 3.11). This is unfortunately below the current precision in measurements, which is a few millimeters. Perhaps with future improvements in the data, ground motion displacements may be used to observe torsional oscillations, although with the same caveats as for the gravity data. We note that the meridional displacements that our model predicts are an order of magnitude smaller than the vertical displacements and that there is little hope that they could be detected in the data.

The detection of torsional oscillations may be possible only in the lowest even harmonic

degrees of the gravity field. As our results suggest, the gravity signal of torsional oscillations will be far below the level of detection for harmonic degrees larger than 4. Even for degree 4, it is unclear that the torsional oscillations signal could be observed, even if one could remove the larger variations due to other effects. Hence, the components of the torsional oscillation flow that may be observed with the gravity and ground motion data are probably restricted to t_1^0 and t_3^0. But observing these two components alone could provide an invaluable check of consistency for the modelling of core angular momentum.

Because of the possibility that future gravity data might provide sufficient accuracy for identifying the low harmonic signal from torsional oscillations, we may want to include additional refinements in our model. One improvement is to add a surface ocean. The solid surface only adjusts partly to the imposed gravitational potential because of its elastic rigidity. The surface of the ocean on the other hand would deform exactly to the imposed potential. Hence, an additional radial mass displacement would occur and contribute to an additional change in potential. It is difficult to predict exactly the change in gravitational potential that would arise without doing the actual calculations. But we note that the density of water in the ocean is 3 times smaller than that of the crust and only represents a tiny fraction of the Earth's radius. Therefore, the oceans would probably not contribute to large changes in the gravitational potential. However, by incorporating a surface ocean in our model, we should be able to predict the time variations in the even harmonic degrees of the sea-level around the globe. These can be then be compared with altimetry data.

One possible additional refinement to our model is the incorporation of viscous dissipation in the mantle and inner core. We are currently defining the mantle and inner core to be perfectly elastic, but if we allow for anelastic effects, the amplitude of the perturbations may be altered and delayed. Using a realistic viscoelastic rheology for the mantle and inner core with a viscosity profile akin to that used in postglacial rebound studies (e.g. Peltier, 1974; Wu and Peltier, 1982) would probably not alter our results significantly. This is because the forcing of torsional oscillations acts at decadal periods, which is much shorter than the typical timescale of a thousand years on which the viscous relaxation is observed to occur. However, if there exists a layer with a smaller viscosity at the bottom of the mantle, then perhaps the anelastic effects on the gravity signal from the torsional oscillations may be important, if not in amplitude, then in delaying the observed signal. Such a low viscosity layer at the base of the mantle is hinted at by seismological observations of

ultra-low velocity zones (Wen and Helmberger, 1998; Garnero *et al.*, 1998). Therefore, the mechanism that we have presented in this study may in the future provide a useful tool for testing geodynamically the nature of these seismological observations.

Chapter 4

Inner core tilt and polar motion

4.1 Introduction

The Earth's rotation axis changes its orientation with respect to the mantle on timescales that range from days to millions of years (e.g. Lambeck, 1980). Tidal torques from the Moon and Sun acting on the equatorial bulge are responsible for polar motions in the diurnal frequency band, while readjustments of the moment of inertia of the mantle through post-glacial rebound and convection produce a slow drift of the pole (true polar wander). Between these two ends of the spectrum, there is an annual wobble associated with mass transport in the atmosphere, the 14-month Chandler wobble which represents the free Eulerian precession of the Earth, and a decade polar motion known as the Markowitz wobble. The latter is the focus of this chapter.

The Markowitz wobble is a somewhat irregular polar motion with a magnitude of roughly 20 to 50 milliarcseconds (mas) (Markowitz, 1960, 1968). Until recently, the existence of this oscillation was in doubt for several reasons, including changes in the star catalogues and modifications in data processing techniques (e.g. Lambeck, 1980; Dickman, 1981). The latest analyses seem to confirm the real nature of this signal (Wilson and Vicente, 1980; Dickman, 1981; Gross, 1990; McCarthy and Luzum, 1996). Various authors have attempted to characterize the Markowitz wobble; the general consensus is that the signal can be described as a highly eccentric motion of amplitude 20-30 mas oriented in

[3]The work presented in this chapter has been published previously in modified form and is reprinted from *Geophysical Journal International* (Dumberry and Bloxham, 2002), with permission from Blackwell Publishing

the general direction of 35°E longitude, with an ellipticity between 0.87 and 0.93, and with a period of 28 to 31 years (Poma, 2000). However, the mechanism responsible to generate such a polar motion is still not identified.

In the reference frame rotating with the Earth, there are no external torques with decade periodicity, which implies that the angular momentum of the whole Earth must be conserved at these timescales. The changes in the direction of rotation with respect to the mantle must then result either from exchanges of angular momentum between the mantle and its fluid envelope (the atmosphere and oceans), from exchanges of angular momentum between the mantle and the core, from changes in the moment of inertia of the Earth, or from a combination of these effects.

Coupling between the solid Earth and its external fluid envelope was first proposed by Dickman (1983), who argued that the decade polar motion could be explained in terms of a natural free wobble of the coupled ocean-solid Earth system. This hypothesis was disputed by Wahr (1984) on the basis that the coupling between the oceans and the solid Earth was too weak to produce such a low frequency motion (although see Dickman, 1985). More recently, Celaya *et al.* (1999) investigated the excitation of the decade polar motion that results from a numerical model of a coupled climate system which includes the effects of ground water storage, ocean currents, sea-floor pressure, atmospheric pressure and winds. Their study concluded that, while some of these effects may contribute to the observed signal, the amplitude of the Markowitz wobble cannot be explained completely by the surface forcing constituents currently included in their model.

Excitation of the Markowitz wobble by exchange of angular momentum between the core and the mantle through torques at the core mantle boundary (CMB) has also been investigated. Greff-Lefftz and Legros (1995) have shown that electromagnetic coupling is too weak by two or three orders of magnitude for reasonable profiles of conductivity in the lower mantle. Topographic coupling, where horizontal pressure gradients act on the ellipticity and other possible components of CMB topography has been proposed (Hinderer *et al.*, 1987, 1990) and investigated by a number of authors (Greff-Lefftz and Legros, 1995; Hide *et al.*, 1996; Hulot *et al.*, 1996). These studies all indicate that the direction of the resulting torque critically depends on the selected topography at the CMB, but that its amplitude is too small by about an order of magnitude for topography with amplitude of a few kilometers. Furthermore, concern has been raised regarding the method for calculating

the pressure coupling used in these studies (Kuang and Bloxham, 1997b), and the actual topographic torque may be even smaller. In any case, CMB coupling seems inadequate to produce the observed decade polar motion.

Another possible scenario to explain the Markowitz wobble, the one which is investigated in this chapter, involves the participation of the inner core. Busse (1970a) was the first to suggest that an inner core which is misaligned (or tilted) with respect to the mantle could influence the direction of the Earth's rotation on decade timescales, despite the fact that its moment of inertia is a very small fraction of that of the whole Earth (about 7×10^{-4}). His idea was that the Markowitz wobble could be associated with a free Eulerian precession of the inner core tilt and its rotation axis: the equivalent of the Chandler wobble but for the inner core. In the case of a rigid body, the precession frequency is determined by the body's dynamical ellipticity, and for the inner core this corresponds to a period of about 400 days. However, because the inner core is immersed in the fluid core, the frequency of this free precession is decreased by the density contrast at the inner core boundary (ICB). For a density contrast of 6%, this amounts to a prograde inner core wobble of about 24 years, a periodicity close to the observed polar motion.

In Busse's model, the precession of the inner core tilt was communicated to the mantle by surface pressure torques acting on the ICB and CMB. This torque develops as a consequence of the tilted figures of the inner core: in a tilted state, the outer surface of the inner core is no longer aligned with surfaces of constant centrifugal potential in the fluid core. This produces a pressure torque on the ICB, and a secondary flow in the fluid core, which then couples to the mantle by a similar pressure torque. Busse showed that because of the weak coupling between the inner core and the mantle that arises from such a torque, the natural frequencies of the system are not very different from the free wobble frequencies of the mantle and the inner core individually. The Markowitz wobble could then represent the signature of the inner core wobble. However, the weak pressure coupling between the inner core and the mantle results in a mantle response which is too small to be observed (Kakuta *et al.*, 1975).

In both of these studies, however, two important aspects of the Earth's internal dynamics were omitted. First, there was no dynamical equation governing the fluid core. Because the periodic motion of the inner core will create a flow in the outer core at the same period, it is questionable whether the role of the angular momentum of the fluid core can be neglected.

Second, and most importantly, the gravitational interaction between the tilted inner core and the rest of the Earth was not taken into account. A misalignment between the oblate figures of the inner core and the mantle will cause a gravitational torque in the equatorial direction that tries to reestablish the alignment of their figures. The fluid core also participates in the torque because its ellipsoidal surfaces of constant gravitational potential, which stay mostly aligned with the mantle, will also interact with a tilted inner core. When the combined effects of the fluid core dynamics and the gravitational and pressure torques acting on the mantle and the inner core are incorporated, the free precession associated with the tilted figure of the inner core is still prograde but reduced to a period of about 6.6 years (Mathews *et al.*, 1991a; Dehant *et al.*, 1993; Xu and Szeto, 1998). The period of the inner core wobble is now quite different from the observed periodicity of the Markowitz wobble and this weakens the case of the free precession considerably. In addition, as pointed out by Dickman (1981), the observation of a highly eccentric (and possibly retrograde) polar motion is difficult to reconcile with a free precession mode, which would produce a circular (and prograde) polar motion.

This suggests that if the inner core is indeed responsible for the decade polar motion, a free precession of its figure axis is not the explanation, although it does not discount the possibility that this free precession could explain part of the signal. Therefore, the only way that the inner core could play a role in the Markowitz wobble is if its tilt is controlled by equatorial torques at the ICB which vary on a decadal timescale. The resulting polar motion at the surface would then be the response of this forced oscillation. The investigation of this possible explanation for the Markowitz wobble is the focus of this chapter.

What is the torque required on the inner core in order to create a sufficiently large tilt of its figure to generate the observed polar motion? What will be the amplitude of that tilt? What are the mechanisms that can produce torques of the required amplitude at decade periods at the ICB? These are the questions that motivate our study.

A recent study by Greiner-Mai and Barthelmes (2001) has addressed some of these questions. They assumed a simple angular momentum balance between the polar motion of the Earth's rotation axis and the changes in the moment of inertia of the Earth caused by the tilted figure of the inner core. They then inverted for the tilt angle during the past century for the polar motion that corresponds to the Markowitz wobble. They obtained tilt variations of a few tenths of a degree. From this result, they estimated an applied torque

on the inner core of about 10^{22} N m, based on a calculation of the total gravitational torque exerted on a tilted inner core by Smylie *et al.* (1984). However, both of these calculations neglect the dynamical influence of the fluid core. An applied torque on the inner core implies an equal and opposite torque on the fluid core at the ICB. The angular momentum of the fluid core will then be altered and this will, in turn, change the gravitational and pressure coupling with the inner core. This suggests that consideration of the fluid core is important both for its influence on the dynamics of the inner core and for its role in the global angular momentum balance of the Earth. We therefore suspect that the values for the tilt of the inner core and the amplitude of the torque required to create such a tilt that were reported in the study of Greiner-Mai and Barthelmes (2001) may be incorrect. In addition, the presence of a resonance at the 6.6 year period of the free inner core wobble could amplify a decade timescale forced excitation of the inner core tilt and reduce the amplitude of the torque required to produce polar motions of observed amplitudes.

The possible role of the inner core in the decade polar motion is not well established because none of the previous studies that addressed the issue have considered the complete internal coupling dynamics of the Earth. In this chapter, we revisit the role of the tilted figure of the inner core by developing a model that incorporates both the effects of surface pressure torque and gravitational volume torque. This model is an adaptation of the one developed by Mathews *et al.* (1991a) for the study of the forced nutations of the Earth. We adapt the model to our study of decade polar motion by incorporating the effects of viscous relaxation of the inner core surface.

In our model, the tilt of the inner core and the perturbations in Earth's rotation are caused by a prescribed torque at the ICB. Our primary goal is to determine the torque required on the inner core in order to explain the observed decade polar motion. We demonstrate that a torque of about 10^{20} N m is sufficient. A torque of that amplitude produces a tilt of about 0.07 degrees of the figure of the inner core. Both of these results are obtained when the viscosity of the inner core is larger than 5×10^{17} Pa s. For smaller viscosities, the required torque is increased because the tilted figure of the inner core relaxes towards an alignment with the symmetry axis of the mantle.

Our second objective is to determine if the dynamics of the fluid core can generate the required torque at the ICB. We consider a scenario of electromagnetic coupling involving the action of torsional oscillations in the flow and we demonstrate that a torque of 10^{20}

N m at decade periods can be produced if the radial magnetic field at the ICB is on the order of 3-4 mT. This value is large but is not unreasonable considering that larger fields are expected at the ICB due to the concentrated shear in velocity. One interesting aspect of the electromagnetic torque produced according to this scenario is that the resulting polar motion is highly eccentric and polarized, two important characteristics of the Markowitz wobble.

The results of this chapter suggest therefore that, given our limited knowledge of the inner core viscosity and of the magnetic field near the ICB, forced variations of the inner core tilt cannot be discounted as a possible contribution to the excitation of the Markowitz wobble.

Finally, our results also show that a torque at the ICB of 10^{19} N m can also participate in the excitation of the Chandler wobble, if such a torque can be applied at the Chandler wobble period of 14 months. However, because mantle and ocean dissipation are not included in our model, the required torque that we calculate is probably underestimated.

This chapter is organized as follows. In the next section we present the observations of polar motion for the last century. In section 4.3 we discuss some of the basic physical arguments regarding rotating bodies, precession and internal coupling of the Earth. In section 4.4 and 4.5 we present some of the details of our model and show some of our important results. Finally, in section 4.6 we analyze the implications of these results in terms of Earth rotation, viscosity of the inner core, electromagnetic coupling at the ICB and the Chandler wobble excitation.

4.2 Data

In figure 4.1 we show the two equatorial components of the mean polar motion for the past century. The data used in this figure are from the International Earth Rotation Service (IERS) combined series EOP-C01, where the mean position of the pole was obtained by filtering the Chandler and the annual wobble from the original series. The mean position can be described by a linear drift and a decade oscillation with amplitudes that vary between 50 mas in the early part of the century to 20 mas for the more recent data. This is the Markowitz wobble.

An oscillation of a roughly 6-year period can also be seen in the data. This periodic-

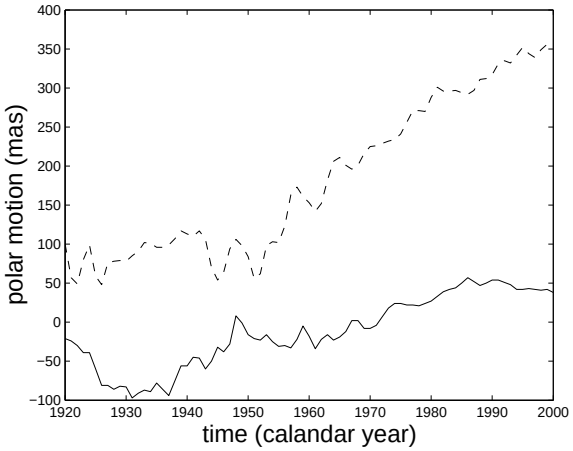

Figure 4.1: Components $m_1 = \omega_1/\Omega_o$ (solid line) and $m_2 = \omega_2/\Omega_o$ (dashed line) of the polar motion for the last century. The Chandler wobble and the annual wobble have been filtered from the original IERS data.

ity corresponds to the beat frequency between the Chandler wobble and annual wobble. Therefore, it is possible that this oscillation could be an artifact resulting from an incomplete elimination of the Chandler and annual wobble from the data (Dickman, 1981). However, in this chapter we argue that if the Markowitz wobble is explained by a torque at the ICB, then the free precession of the inner core tilt should also be excited. This mode has a periodicity of 6.6 years and hence, the periodic signal in figure 4.1 may represent this free mode.

4.3 Basic dynamics and internal coupling of the Earth

The equilibrium configuration of the Earth is one where the mantle, the fluid core and the solid inner core are all rotating at angular velocity Ω around an axis which coincides with the axis of geometric symmetry of the aligned oblate figures of the mantle ($\hat{\mathbf{e}}_3$) and inner core ($\hat{\mathbf{e}}'_3$) (figure 4.2a). Because the angular momentum of the whole Earth has to be conserved, a tilt of the inner core will also produce a small polar offset between the rotation axis and the mantle (figure 4.2b). In a recent study, Greiner-Mai and Barthelmes (2001) have used this simple balance to invert for the tilt of the inner core for the past century. They concluded that a tilt of a few tenths of a degree was required in order to explain the

decade polar motion.

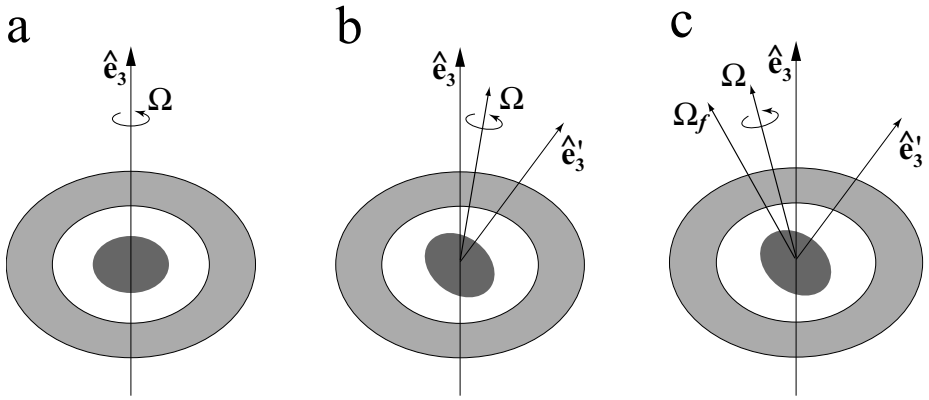

Figure 4.2: Equilibrium configurations of the Earth: (a) in its undisturbed state; (b) with a tilted inner core; (c) with a tilted inner core and proper considerations of the fluid core dynamics. $\hat{\mathbf{e}}_3$ is the symmetry axis of the mantle (light grey), $\hat{\mathbf{e}}_3'$ is the symmetry axis of the inner core (dark grey), Ω is the rotation axis of the Earth and Ω_f is the rotation axis of the fluid core. The steady applied torque is directed into the page. Not drawn to scale.

This equilibrium balance between the tilted figures of the inner core and mantle is correct on grounds of angular momentum conservation, but is incorrect when proper considerations of the Earth's internal dynamics are allowed. Any misalignment between the figures of the mantle and inner core will cause a gravitational torque in the equatorial direction that acts to reestablish the alignment of their figures. Similarly, pressure torques on the tilted figures of the inner core and mantle will arise from the angular velocity of the fluid core pushing on its misaligned envelope. Moreover, torques acting perpendicular to the axis of a rotating body will induce precessional motions and the tilted figure of the mantle and inner core will then precess around the rotation axis.

One could argue that a steady torque imposed at the ICB would balance the combined gravitational and pressure torques and maintain an equilibrium configuration if the free precessions are rapidly damped. If this is the case, the equilibrium configuration shown in figure 4.2(b) is still incorrect because it overlooks the changes in the angular momentum of the fluid core. The imposed torque on the solid inner core at the ICB implies an equal and opposite torque on the fluid core. Similarly, the gravitational and fluid pressure torques on the misaligned boundaries imply equal and opposite torques from the boundaries on the

fluid. These torques produce changes in the angular momentum of the fluid core which are characterized by variations in the direction of its rotation axis ($\mathbf{\Omega_f}$).

The correct equilibrium configuration that is established when a constant torque is applied at the ICB results not only from the tilt of the inner core and the polar offset, but also from the change in the angular momentum of the fluid core. This configuration is shown in figure 4.2(c). We defer the quantitative details of the angular momentum balance configurations of figures 4.2(b) and 4.2(c) to section 4.4, and for now simply state that the tilt angle in figure 4.2(c) is a factor 2.5 smaller than in figure 4.2(b), and with the reversed sign. The tilt angles derived by Greiner-Mai and Barthelmes (2001) are thus a factor 2.5 too large and with opposite direction.

Of course, we do not expect the complicated dynamics in the fluid core to apply a constant torque on the inner core. Time dependent equatorial torques at the inner core boundary will perturb the equilibrium and instigate free precessions. The polar motion at the surface will result from a superposition of the forcing due to the imposed torque at the ICB and the excitation of the free precession modes. If the periodicity of the imposed torque is close to one of the free precession periods, the amplitude of the forced wobble will be amplified.

4.4 Description of the Model

Models that describe the internal gravitational and pressure coupling between the mantle, the fluid core and the inner core have been developed for the study of the Earth's forced nutations (Sasao *et al.*, 1980; Wahr, 1981; Mathews *et al.*, 1991a; Dehant *et al.*, 1993). The nutations are the small changes of the direction of the Earth's rotation axis in space that are produced by the tidal torques from the Moon, the Sun and the other planets on the oblate figure of the Earth. Because the mantle, fluid core and inner core react differently under the same external torque, exchanges of angular momentum between them result from internal gravitational and pressure torques. Therefore, the amplitude of the observed nutations ultimately depends on the coupling between Earth's interior regions. Moreover, the structure of the Earth, its elastic properties and the coupling between its different regions, determines a set of eigenmodes of rotation. If a tidal torque has a frequency close to that of a normal mode, the associated nutation amplitude will be amplified by a resonant effect. The objec-

tive of the forced nutation studies is then to construct a model for the internal coupling in the Earth that successfully reproduces the observed nutations when subjected to the known spectrum of tidal forcing. Over the years, these models have grown in sophistication in response to the increased accuracy of the observations (Mathews and Shapiro, 1992; Sovers *et al.*, 1998).

The polar motion generated from an imposed torque at the ICB will result from the same internal coupling dynamics that are included in these models. Therefore we can take advantage of these existing models for the purpose of our study.

4.4.1 Adapted model from nutation theory

We use the model developed by Mathews *et al.* (1991a). We give here only a brief description of the model and refer the interested reader to the original paper. The model is that of an axisymmetric, oceanless, rotating Earth comprised of a mantle, fluid core and inner core. Surfaces of constant density are determined under the assumption of hydrostatic equilibrium between pressure and the combination of gravitational and centrifugal potential. Each region is allowed to deform elastically, but no dissipation effects are included. The basic objective of the model is to calculate the perturbations from an initial state of a uniform rotation $\Omega_\mathbf{o} = \Omega_o \hat{\mathbf{e}}_\mathbf{3}$ with respect to a reference frame fixed to the mantle. These perturbations are expressed in terms of departures in the orientation of the rotation axis of the whole Earth with respect to the mantle, ω, and departures of the rotation axis of the fluid core, $\omega_\mathbf{f}$, and of the inner core, $\omega_\mathbf{s}$, with respect to the rotation vector of the Earth $\Omega = \Omega_\mathbf{o} + \omega$. These are expressed in the conventional complex notation

$$\tilde{m} = m_1 + i m_2 = (\omega_1 + i\omega_2)/\Omega_o\,, \tag{4.1}$$

$$\tilde{m}_f = (m_f)_1 + i(m_f)_2 = ((\omega_f)_1 + i(\omega_f)_2)/\Omega_o\,, \tag{4.2}$$

$$\tilde{m}_s = (m_s)_1 + i(m_s)_2 = ((\omega_s)_1 + i(\omega_s)_2/\Omega_o\,, \tag{4.3}$$

where the directions 1 and 2 refer to the two equatorial directions in the mantle reference frame. The complex scalar $\tilde{m}$ thus represents the amplitude of the polar motion. A fourth

degree of freedom is added by allowing a tilted inner core with orientation $\hat{\mathbf{e}}_3'$ with respect to the orientation of the mantle $\hat{\mathbf{e}}_3$ (see figure 4.2). The difference $\hat{\mathbf{e}}_3' - \hat{\mathbf{e}}_3$ represents the tilt angle denoted by $\mathbf{n_s}$, and is expressed in the same standard notation by

$$\tilde{n}_s = (n_s)_1 + i(n_s)_2 \,. \tag{4.4}$$

The amplitudes of these perturbations are calculated by solving a system of four equations: one for the evolution of the angular momentum of the whole Earth ($\mathbf{H}$); one each for the evolution of the angular momentum of the fluid core ($\mathbf{H_f}$) and inner core ($\mathbf{H_s}$); and one kinematic equation governing the tilt of the inner core relative to the mantle. They are, respectively,

$$\frac{d}{dt}\mathbf{H} + \Omega \times \mathbf{H} = \mathbf{0} \,, \tag{4.5}$$

$$\frac{d}{dt}\mathbf{H_f} - \omega_\mathbf{f} \times \mathbf{H_f} = -\Gamma_\mathbf{app} \,, \tag{4.6}$$

$$\frac{d}{dt}\mathbf{H_s} + \Omega \times \mathbf{H_s} = \Gamma_\mathbf{s} + \Gamma_\mathbf{app} \,, \tag{4.7}$$

$$\frac{d}{dt}\mathbf{n_s} = \Omega_\mathbf{o}(\mathbf{m_s} \times \hat{\mathbf{e}}_3) \,. \tag{4.8}$$

The last of these equations, equation (4.8), will be altered in the next section in order to allow for viscous relaxation of the inner core surface. In the Mathews *et al.* (1991a) model, an external torque Γ representing the tidal forcing was applied on the whole Earth and appeared on the right hand side of (4.5). We are solely interested in the perturbations induced by an imposed torque at the ICB and neglect that tidal torque. This forces the angular momentum of the whole Earth to be conserved. Our prescribed equatorial forcing at the ICB is represented by the applied torque $\Gamma_\mathbf{app}$. The torque $\Gamma_\mathbf{s}$ represents the pressure and gravitational torques on the inner core. Following the standard notation, these torques are expressed as

$$\tilde{\Gamma}_s = (\Gamma_s)_1 + i(\Gamma_s)_2 \,, \tag{4.9}$$

$$\tilde{\Gamma}_{app} = (\Gamma_{app})_1 + i(\Gamma_{app})_2. \tag{4.10}$$

Buffett (1992) improved the original model by incorporating the effects of magnetic stress at the CMB and the ICB. This magnetic coupling arises as a consequence of the misalignment between the rotation axes of each region, which creates small differences in velocity at the boundaries which shear the radial magnetic field. In the context of the forced nutations, this additional coupling represents a fine tuning improvement of the data fit, and on this ground, it seems safe to neglect this small effect.

The magnetic stresses will turn out to be important in our model because of the timescale at which we are exciting the system. We are interested in the response of the Earth to torques that are applied at decade timescales, as opposed to the diurnal response of the nutation studies. At daily timescales, the radial magnetic field is essentially static, but at decade timescales, the variations in the outer core flow can create sufficiently large changes in the radial magnetic field by the process of advection. Therefore a significant torque at the ICB can be generated by the action of this outer core flow. Indeed, it will become clear in section 4.6.2 that the nature of the applied torque at the ICB that drives the system is most likely electromagnetic and that $\Gamma_{\mathbf{app}}$ is the prescribed form of this torque.

One can note that the prescribed torque at the ICB will evidently induce a misalignment between the rotation axis of the inner and outer core. This resulting differential velocity at the ICB will then produce an additional contribution to the magnetic stress. However, we have verified that this differential velocity is smaller by at least a factor 10 than the over-riding outer core velocity that is necessary to produced the applied torque in the first place. We therefore safely neglect this additional contribution in the electromagnetic torque.

The solutions of the above system are obtained as follows. The angular momentum vectors are expanded linearly in terms of the perturbations and include the effects of elastic deformation. The torque $\Gamma_{\mathbf{s}}$ is similarly expanded. Thus, this system of four equations is transformed into a set of algebraic conditions on $\tilde{m}, \tilde{m}_f, \tilde{m}_s$ and $\tilde{n}_s$. The forcing and the perturbations are assumed periodic and proportional to $e^{i\Omega_o \sigma t}$ where σ is the frequency of the forcing (in cycles per day). The entire problem can be written in a matrix form as

$$\mathsf{M} \cdot \mathbf{x} = \mathbf{b}, \tag{4.11}$$

with the matrix M, solution vector $\mathbf{x}$ and forcing vector $\mathbf{b}$ given by

$$\mathsf{M} = \begin{pmatrix} \sigma+(1+\sigma)\kappa-e & (1+\sigma)(\xi+A_f/A) & (1+\sigma)(\zeta+A_s/A) & (1+\sigma)\alpha_3 e_s A_s/A \\ \sigma+\sigma\gamma & 1+\sigma+\beta+e_f & \sigma\delta & -\sigma\alpha_1 e_s A_s/A_f \\ \sigma+\sigma\theta-\alpha_3 e_s & \sigma\chi+\alpha_1 e_s & 1+\sigma+\sigma\nu & (1+\sigma-\alpha_2)e_s \\ 0 & 0 & 1 & \sigma \end{pmatrix}, \tag{4.12}$$

$$\mathbf{x} = \begin{pmatrix} \tilde{m} \\ \tilde{m}_f \\ \tilde{m}_s \\ \tilde{n}_s \end{pmatrix}, \qquad \mathbf{b} = \begin{pmatrix} 0 \\ -\tilde{\Gamma}_{app}/iA_f{\Omega_o}^2 \\ \tilde{\Gamma}_{app}/iA_s{\Omega_o}^2 \\ 0 \end{pmatrix}. \tag{4.13}$$

The quantities that enter the matrix M are defined as follows. A, A_f and A_s are the equatorial moments of inertia and e, e_f and e_s are the dynamical ellipticities of the whole Earth, the fluid core (subscript f) and the inner core (subscript s). The parameter α_1 essentially represents the density contrast at the ICB and is slightly less than unity. The parameter α_3 is related to α_1 by $\alpha_1 = 1-\alpha_3$. The parameter α_2 represents the ability of the rest of the Earth to exert a torque on a tilted inner core and is defined as $\alpha_2 = \alpha_1 - \alpha_3\alpha_g$, where α_g represents the gravitational coupling alone. Finally, the parameters (κ, ξ, ζ), (γ, β, δ) and (θ, χ, ν) are three sets of compliances which characterize the effects of elastic deformations of the whole Earth, the fluid core and the inner core, respectively, which arise due to changes in centrifugal potential induced by the independent rotations of the three regions. These nine parameters are obtained by integrating the equations of elastic deformations for a specific Earth model. The values of all of the above parameters obtained from the basic Earth model PREM (Dziewonski and Anderson, 1981) are presented in Mathews *et al.* (1991b) and are reproduced here for convenience in Table 4.1.

The periods of the free precessions of the Earth are found with the condition $\det(\mathsf{M}) = 0$. Four natural modes emerge; the prograde and retrograde free core nutation which have periodicities close to 1 day; the Chandler wobble with a period of 400 days; and the inner core wobble which has a period of 6.6 years.

In the nutation problem, the amplitude of the perturbation $\mathbf{x}$ is calculated for a given tidal forcing at a selected frequency. We proceed similarly and prescribe an applied torque

Table 4.1: Parameters for Earth model PREM

Moments of Inertia, kg m^2		
$A = 8.0115 \times 10^{37}$	$A_f = 9.0583 \times 10^{36}$	$A_s = 5.8531 \times 10^{34}$
Ellipticities		
$e = 3.247 \times 10^{-3}$	$e_f = 2.548 \times 10^{-3}$	$e_s = 2.422 \times 10^{-3}$
Coupling constants		
$\alpha_g = 2.1752$	$\alpha_1 = 0.9463$	
$\alpha_2 = 0.8294$	$\alpha_3 = 0.0537$	
Compliances		
$\kappa = 1.039 \times 10^{-3}$	$\xi = 2.222 \times 10^{-4}$	$\zeta = 4.964 \times 10^{-9}$
$\gamma = 1.965 \times 10^{-3}$	$\beta = 6.160 \times 10^{-4}$	$\delta = -4.869 \times 10^{-7}$
$\theta = 6.794 \times 10^{-6}$	$\chi = -7.536 \times 10^{-5}$	$\nu = 7.984 \times 10^{-5}$

at the ICB with a given frequency.

4.4.2 Viscous relaxation of the inner core

The inner core is not perfectly elastic and has a finite viscosity. On long time scales, when its surface does not coincide with an equipotential, the geometric figure of the inner core will viscously deform towards the imposed equipotential surface. Thus, if the inner core was a perfect fluid, its axis of symmetry would be perfectly aligned with that of the mantle. This remains true even when an equatorial torque is applied at the ICB: the applied torque will induce an equatorial rotation of the inner core, but a secondary flow within the inner core will develop in order to keep its elliptical surface aligned with that of the mantle.

We allow viscous relaxation in our model by modifying the kinematic relation between the variations in the rotation of the inner core and the tilt of its geometric figure (equation 4.8). The extent of the relaxation depends on the frequency of the applied torque relative to the characteristic e-folding time of viscous relaxation, τ. We expect that for very high frequencies, the changes of the inner core tilt are essentially controlled by the variations in the rotation velocity of the inner core, as it is currently prescribed in (4.8). Conversely, for very low frequencies, the inner core tilt will remain essentially aligned with the mantle regardless of the variations in rotation of the inner core. These two situations can be satisfied

by multiplying the left hand side of (4.8) by a factor $(1+i/\sigma\tau)$. This is analogous to prescribing a time dependence which contains an oscillating and decaying part, $e^{i\Omega_o\sigma t(1+i/\sigma\tau)}$ to both $\tilde{n}_s$ and $\tilde{m}_s$ in equation (4.8). The last equation that appear in matrix M therefore becomes

$$\tilde{m}_s + \sigma(1+\frac{i}{\sigma\tau})\tilde{n}_s = 0\,. \tag{4.14}$$

Since we are not interested in the details of the secondary flow that develops to maintain the alignment between the inner core and mantle, this simple prescription for the adjustment of the inner core surface is sufficient for our present purpose.

The timescale of viscous relaxation is proportional to the viscosity of the inner core, η_s, and also depends on the assumed rheology of the inner core. Here, we are considering an incompressible, self-gravitating and homogeneous inner core with a uniform viscosity. In this case, τ and η_s are related by (Buffett, 1997)

$$\tau = \frac{C\eta_s}{a_s g \Delta\rho}\,, \tag{4.15}$$

where g and $\Delta\rho$ are the gravitational acceleration and the density jump at the ICB radius of a_s, and $C = 1.9$ is a numerical constant.

The viscosity of the inner core is a crucial parameter in our model because it influences directly the amplitude of the tilt of the inner core, and therefore the amplitude of the resulting polar motion at the surface. Unfortunately, it is not a well constrained quantity. Typical estimates from experiments at high-temperature on iron at ambient pressure give $\eta_s = 10^{13\pm3}$ (Frost and Ashby, 1982). However, the extrapolation of these values to pressure at core conditions may not be appropriate, and larger typical grain size in the inner core than those assumed in these experiments are likely to increase the value of the viscosity (Bergman, 1998). A geodynamic estimate of 3×10^{16} Pa s has been suggested by Buffett (1997) based on the seismic observations of the eastward super-rotation of the inner core. This corresponds to a time relaxation of the inner core figure of $\tau \approx 0.6$ year. The work of Greff-Lefftz *et al.* (2000) on the period of free retrograde core nutation suggests that the viscosity is larger than 10^{14} Pa s if the magnetic field at the ICB is on the order of a few milliTeslas, or alternatively, that the viscosity is smaller than 10^{14} Pa s if the magnetic field at the ICB is much larger.

Because of the uncertainty on the viscosity of the inner core at present, and because our model might serve as an additional constraint for the viscosity, we present calculations that use values of η_s ranging between 5×10^{15} Pa s and 5×10^{19} Pa s. For $\Delta\rho = 600$ kg m^{-3}, $g = 4.4$ m s^{-2} and $a_s = 1.2 \times 10^6$ m in equation (4.15), this corresponds to relaxation times between 0.1 years and 1000 years.

The dissipation of rotational energy associated with the free modes of precession is not included in our model. This includes the effects of mantle anelasticity, dissipation in the oceans (Smith and Dahlen, 1981) and electromagnetic dissipation (Buffett, 1992). Since we are solving the system in the frequency domain and are mostly interested in the amplitudes that result from the forced oscillations, these omissions do not invalidate our approach. However, as a consequence, the forced polar motion amplitude that we calculate at the resonance frequency of the free modes will be overestimated.

4.5 Results

4.5.1 Static case

It is instructive to calculate first the amplitude of the polar offset, the tilt of the inner core, and the changes in the rotation of the fluid core and inner core that results when a steady torque is imposed at the ICB and in the absence of free precessions. This amounts to solving equations (4.5) to (4.8) for $d/dt = 0$ and a fixed $\mathbf{\Gamma_{app}}$. (For this discussion, we do not consider the effects of viscous deformation of the inner core, i.e. we set $\tau \to \infty$).

It is immediately clear that equation (4.8) forces $\tilde{m}_s = 0$, which implies that the rotation axis of the inner core is aligned with that of the whole Earth. The equilibrium configuration is thus one where a polar offset $\tilde{m}$ is balanced by a tilted figure of the inner core and a misaligned rotation of the fluid core, as shown in figure 4.2(c). We note that since we are solving for $d/dt = 0$, we impose $\mathbf{\Omega} \times \mathbf{H} = \mathbf{0}$ in (4.5) and therefore $\mathbf{H}$ coincides with $\mathbf{\Omega}$ in figure 4.2. The relative balance between $\tilde{m}$, $\tilde{m}_f$ and $\tilde{n}_s$ results from solving (4.11) for $\tilde{m}_s = 0$ and without the last equation:

$$\begin{pmatrix} A(\kappa-e) & A\xi+A_f & \alpha_3 e_s A_s \\ 0 & 1+e_f & 0 \\ -\alpha_3 e_s & \alpha_1 e_s & (1-\alpha_2)e_s \end{pmatrix} \begin{pmatrix} \tilde{m} \\ \tilde{m}_f \\ \tilde{n}_s \end{pmatrix} = \begin{pmatrix} 0 \\ -\tilde{\Gamma}_{app}/iA_f\Omega_o^2 \\ \tilde{\Gamma}_{app}/iA_s\Omega_o^2 \end{pmatrix}. \tag{4.16}$$

Using the parameters listed in Table 4.1, we find that the amplitude of $\tilde{m}_f$ and $\tilde{n}_s$ relative to $\tilde{m}$ are

$$\tilde{m}_f \approx \frac{1}{35}\tilde{m}, \qquad \tilde{n}_s \approx -10^4\tilde{m}. \tag{4.17}$$

We note that if we neglect to consider the fluid core in the angular momentum balance of the whole Earth (first row of (4.16)), we retrieve the angular momentum balance between the polar offset and the tilted inner core pictured in figure 4.2(b), which is

$$\tilde{n}_s = \frac{(e-\kappa)A}{\alpha_3 e_s A_s}\tilde{m}. \tag{4.18}$$

This expression is similar to the one used by Greiner-Mai and Barthelmes (2001) to invert for the tilt of the inner core. This balance implies a ratio $\tilde{n}_s \approx 2.5 \times 10^4 \tilde{m}$. The amplitude of the tilt of the inner core required to explain the decade polar motion is thus reduced by a factor 2.5 when proper consideration of the fluid core dynamics is included. Moreover, the direction of $\tilde{n}_s$ relative to $\tilde{m}$ is reversed.

According to the ratios presented in (4.17), a polar displacement $\tilde{m}$ of 25 mas corresponds to an opposite tilt angle of the inner core of 2.5×10^5 mas, or 0.07 degrees. The applied torque on the inner core required to produce such polar offset is 1.7×10^{20} N m. This value is two orders of magnitude smaller than the estimate of the torque presented by Greiner-Mai and Barthelmes (2001), which was based on a calculation by Smylie *et al.* (1984) which did not include the dynamical effects of the fluid core. Again, this demonstrates clearly how the fluid core plays an important role in the dynamics of the inner core tilt.

The above analysis neglects two important factors. First, the presence of the free inner core wobble at a period of 6.6 years might enhance the response of the polar motion by resonant effects, which would decrease the required torque. Second, viscous relaxation of the inner core surface will tend to realign the oblate figures of the mantle and inner core,

and result in a smaller polar offset. An increased torque is therefore required to produce a polar motion of the same magnitude. These two effects are included in the full calculation presented in the next section.

4.5.2 Amplitude of polar motion generated by a periodic torque

In order to quantify the ability of our mechanism to excite sufficient polar motion, we now solve equation (4.11). We recall that the perturbations in rotation and the applied torque in (4.11) have an implied periodic time dependence $e^{i\Omega_o\sigma t}$. Therefore, the polar motion recovered from this system represents, for positive σ, a prograde circular trajectory at the surface. As was pointed out earlier, the observed decade polar motion is not circular but highly eccentric. However, our primary goal in this section is simply to establish the amplitude of the torque required to produce a polar motion amplitude of about 25 mas, not the precise details of the motion. Solving (4.11) is sufficient for that purpose. The case of a polarized polar motion will be addressed in section 4.6.2. All the calculations presented in this section use the parameters of the basic Earth model PREM (Dziewonski and Anderson, 1981) that are listed in Table 4.1.

In figure 4.3 we present the amplitude of the recovered circular polar motion, or "forced wobble" (i.e. $(m_1^2 + m_2^2)^{1/2}$), as a function of frequency. We show the results for three different characteristic timescales of the viscous relaxation of the inner core surface, $\tau =$ 100 years, $\tau = 10$ years and $\tau = 1$ year. In all cases, the amplitude of the imposed torque at the ICB was kept constant at 10^{20} N m.

The amplitude of the forced wobble is enhanced near the resonant frequencies of the Chandler wobble ($\approx 2.5 \times 10^{-3}$ cycles/day) and the inner core wobble ($\approx 4.1 \times 10^{-4}$ cycles/day). Not surprisingly, the largest wobble amplitude is achieved when the relaxation time of the inner core shape is the longest (i.e. largest inner core viscosity). At the period of the Markowitz wobble, (≈ 30 years, which corresponds to $\approx 9.1 \times 10^{-5}$ cycles/day), with an imposed torque of 10^{20} N m, the amplitude of the forced wobble is similar to that of the observed decade variations of 25 mas when $\tau \geq 10$ years, while it is clear that it is not the case when $\tau = 1$ year.

This can be seen more clearly in figure 4.4 where we have fixed the periodicity at 30 years, and varied both the relaxation time of the inner core and the amplitude of the

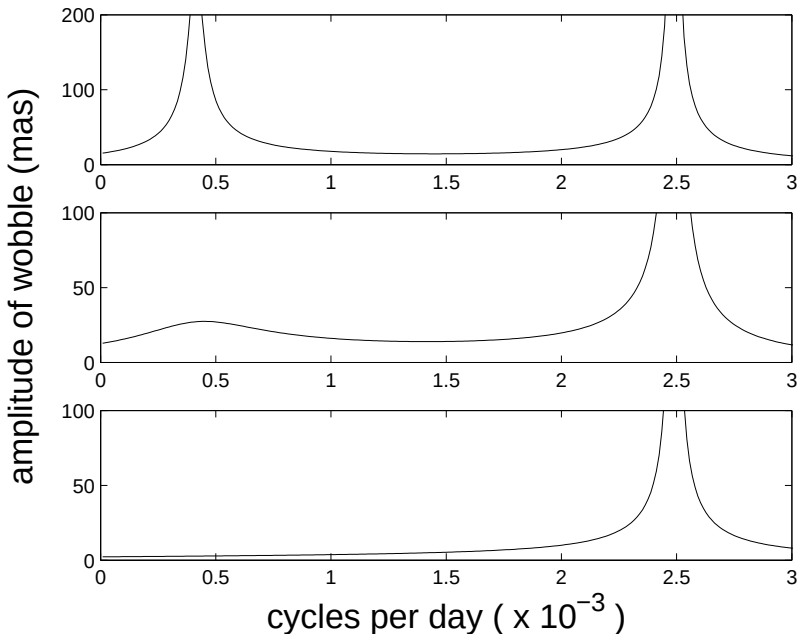

Figure 4.3: Amplitude of the forced wobble as a function of the frequency for an applied torque of 10^{20} N m and for a time relaxation of the inner core shape of 100 years (top), 10 years (middle) and 1 year (bottom).

torque. The amplitude of the forced wobble is now represented as contour lines. The dashed contour line corresponds to an amplitude of 25 mas. The equatorial torque on the inner core required to explain the Markowitz wobble is of order 10^{20} N m for τ larger than 10 years. Below $\tau = 10$ years, the torque required increases proportionally to the decrease in the relaxation time. Figure 4.4 also shows the inner core tilt (in degrees) from the same calculation. The inner core tilt scales proportionally to the forced wobble at the surface. The dashed contour corresponds to a tilt of 0.07 degrees. We note that for τ larger than 10 years, we retrieve the results of the static case presented in the previous section. This illustrates that, in the case of a large inner core viscosity, the resonant effect of the inner core wobble is not very large at periods of 30 years.

In contrast, the resonant effect is most important at the periodicity of the free inner core wobble (2409 days). In figure 4.5 we show the results obtained when the periodicity is fixed to that value. Compared with a periodicity of 30 years, the torque required to generate the same forced wobble is similar for τ less than 10 years, but decreased by a few orders of magnitude for larger τ.

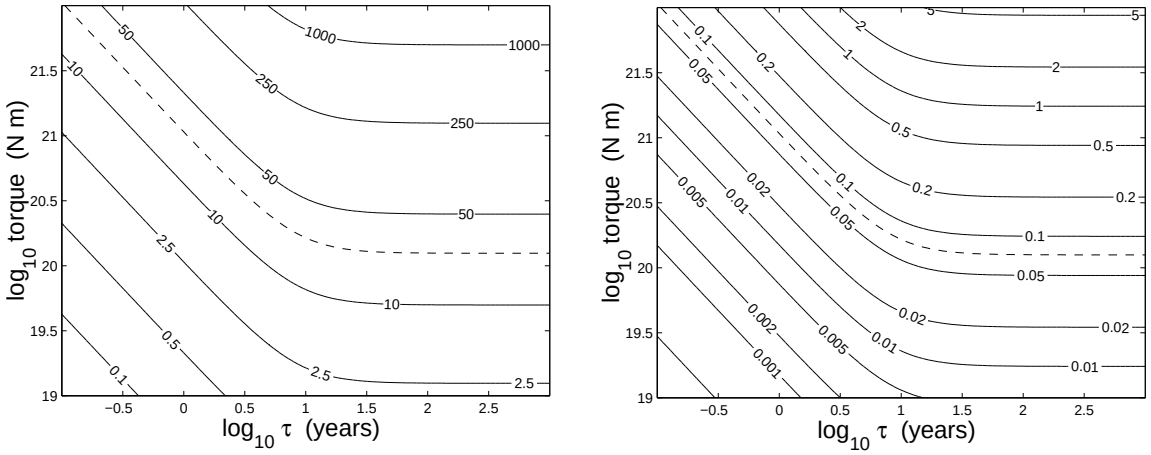

Figure 4.4: Contours of amplitude of the forced wobble (in mas) (left) and amplitude of inner core tilt (in degrees) (right) as a function of the applied torque and relaxation time of the inner core surface, at a fixed periodicity of 30 years. The dashed contour corresponds to a forced wobble of 25 mas.

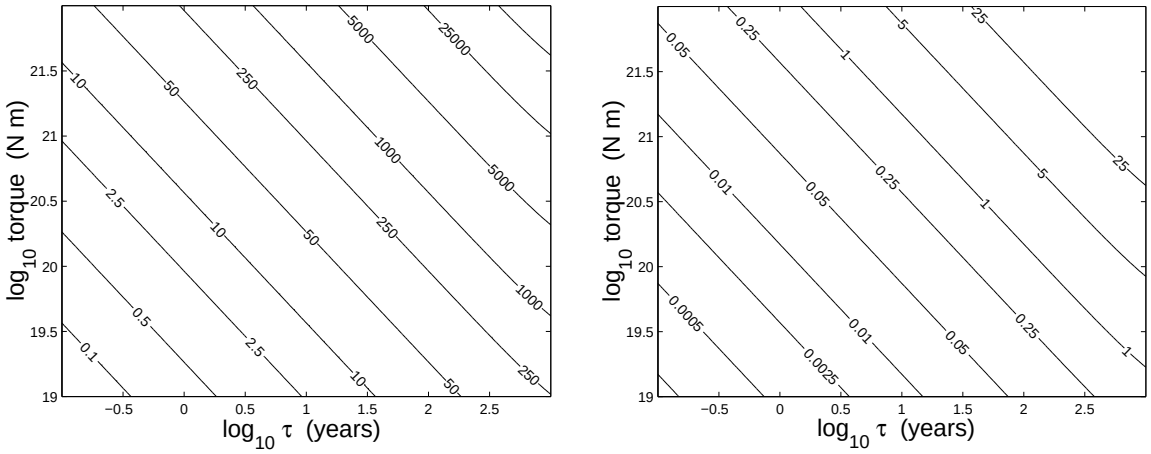

Figure 4.5: Contours of amplitude of the forced wobble (in mas) (left) and amplitude of inner core tilt (in degrees) (right) as a function of the applied torque and relaxation time of the inner core surface, at the fixed periodicity of the inner core free wobble (2409 days).

Interestingly, figure 4.3 suggests that an imposed torque at the ICB is quite effective at exciting the Chandler wobble. In figure 4.6 we have set the periodicity at 400 days, the Chandler wobble period of an oceanless Earth, and again computed the amplitude of the wobble and the tilt of the inner core as a function of both the imposed torque and the

relaxation time of the inner core. The observed amplitude of the Chandler wobble, roughly 150 to 200 mas (the dashed contour on the figure corresponds to 150 mas), is recovered with a torque which is about one order of magnitude smaller than that required to produce the decade polar motion.

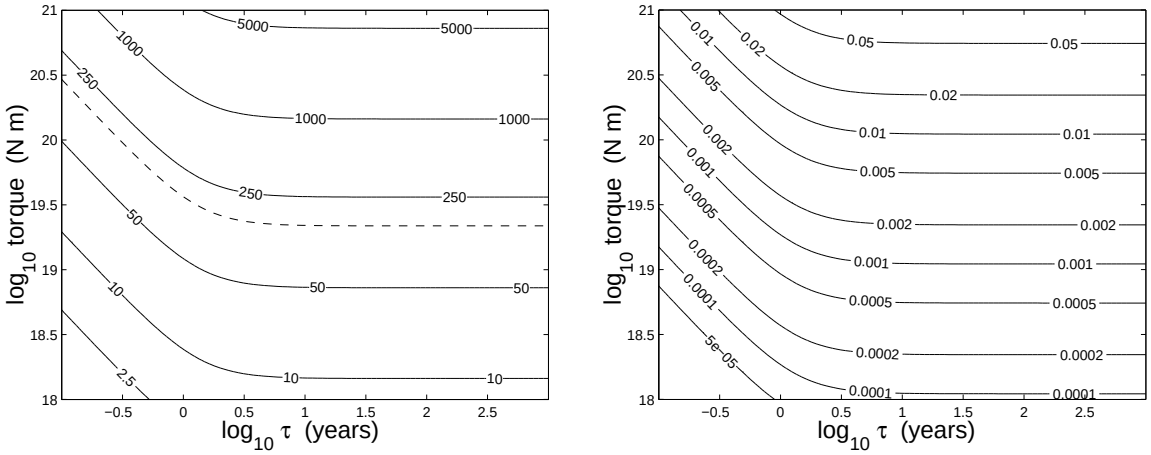

Figure 4.6: Contours of amplitude of the forced wobble (in mas) (left) and amplitude of inner core tilt (in degrees) (right) as a function of the applied torque and relaxation time of the inner core surface, at the fixed periodicity of the Chandler wobble (400 days). The dashed contour corresponds to a forced wobble of 150 mas.

4.6 Discussion

4.6.1 Amplitude of the torque

The results of our model suggest that the required amplitude for the decade polar motion, about 25 mas, can be achieved by a torque on the inner core on the order of 1-2 $\times 10^{20}$ N m if the time relaxation of the inner core shape is larger than a decade, which corresponds to an inner core viscosity greater than 5×10^{17} Pa s. The associated tilt of the inner core is ~ 0.07 degrees.

As we will see in the next section, a torque of 10^{20} N m is at the high end of the estimated equatorial torque that can be applied on the inner core. Hence, this implies that a viscosity of 5×10^{17} Pa s is the lower limit that permits a sufficient polar motion to be

generated by a forced tilting of the inner core. How does this value compare with current estimates of viscosity?

Experiments on iron at high temperature suggests $\eta_s \sim 10^{13\pm3}$ Pa s (Frost and Ashby, 1982), which is considerably smaller than our lower limit. However, these estimates are uncertain due to pressure extrapolation, and larger viscosities cannot be ruled out. In addition, in these experiments, a grain size smaller than 5 mm is necessary to achieve a viscosity of less than 10^{16} Pa s and typical grain size in the core are probably much larger (Bergman, 1998). For instance, a growth model of the inner core suggests a grain size of about 5 m and a viscosity upper bound of order 10^{21} Pa s (Yoshida *et al.*, 1996).

The geodynamic estimate of the viscosity by Buffett (1997) gives an upper bound of 3×10^{16} Pa s from reconciling axial gravitational coupling between the mantle and the inner core and the seismic observations of the eastward super-rotation of the inner core. However, the original seismic observations of a super-rotation rate of 1° per year (Song and Richards, 1996; Su *et al.*, 1996) have since been disputed, and the revised rate is smaller by at least a factor 10 (Laske and Masters, 1999; Souriau and Poupinet, 2000; Poupinet *et al.*, 2000). This elevates the upper bound for the viscosity by at least one order of magnitude, and it is now consistent with our requirement of 5×10^{17} Pa s.

Another attempt to constrain the viscosity of the inner core was proposed by Greff-Lefftz *et al.* (2000). They calculated the joint effect of the magnetic dissipation at the ICB and the viscous relaxation of a viscoelastic inner core on the free modes of nutations of the Earth. They concluded that the observed periodicity of the retrograde free core nutation reflects a viscosity larger than 10^{14} Pa s if the magnetic field at the ICB is on the order of a few milliTeslas, or alternatively, that the viscosity is smaller than 10^{14} Pa s if the magnetic field at the ICB is much larger. According to their first scenario, the viscosity of the inner core could be higher than the lower limit required by our model.

The work of Smylie and McMillan (2000) focused on the viscosity in a possible "slushy" layer in the outermost 300 to 400 km of the inner core, which would be the seat of compositional convection. They inferred a viscosity of $\eta_s \approx 10^{11}$ Pa s based on the observation of the periods of the two translational Slichter modes of the inner core (Courtier *et al.*, 2000). It is clear that the presence of such a "slushy" layer will have a profound effect on the rotational dynamics involving the inner core, as its low viscosity can readily accommodate any changes in the imposed potential. However, at present, the observation of the

Slichter modes remains controversial (Hinderer and Crossley, 2000). Moreover, a model of sedimentary compaction applied to the inner core growth suggest that the thickness of this "slushy" layer is on the order of 100 m when its viscosity is 10^{18} Pa s, and that its thickness vary in proportion to the square root of the viscosity, implying even larger viscosities for a thicker layer (Sumita *et al.*, 1996).

In short, the present knowledge of the viscosity of the inner core does not discount the possibility that the inner core tilt might play an observable role in the decade variations of the polar motion. Alternatively, if the inner core tilt participates in the decade polar motion, then the results of our model constrain the inner core viscosity to be larger than 5×10^{17} Pa s.

We have found that, at the free inner core wobble period of 2409 days and for a viscosity of 5×10^{17} Pa s, the torque required to generate a polar wobble of a few tens of mas is about a factor 2 smaller than that required at a 30 year period. For larger viscosities, this factor becomes very large. Hence, our results suggest that torques on the inner core at decade periods can readily excite the inner core wobble to observable levels, if the viscosity of the inner core is sufficiently large.

This fact was noted by Greff-Lefftz *et al.* (2000). In their study of the influence of inner core viscosity on the normal modes of rotation, they calculated that the damping of the inner core wobble would be rapid if the viscosity was lower than 10^{16} Pa s. For larger viscosities, the wobble can be sustained and if torques are acting at the ICB with a sufficient magnitude, we should observe a 6.6 year signal in the polar motion data and the gravimetric measurements. (We note that if the free inner core wobble is indeed present in the data, its excitation is most probably due to torques at the ICB since it is difficult to conceive of a different way to generate a large tilt of the inner core.)

Therefore, the detection of such a signal represents a good test for our hypothesis because if the Markowitz wobble is indeed a forced response from an imposed torque at the ICB, we expect that the inner core wobble will be excited to comparable amplitudes. The polar motion presented in figure 4.1 may indicate that a 6.6 year signal is indeed present in the data, however a thorough analysis would be required in order to confirm that this signal is real and not an artifact due to incomplete filtering of the annual and Chandler wobble. Obviously, the detection of this signal is a requirement, but not a formal proof for our hypothesis; it is possible that the torques on the inner core are too weak to create the

Markowitz wobble but large enough and at the correct periodicity to excite the free inner core wobble to an observable amplitude.

On the other hand, if it can be clearly demonstrated that the free inner core wobble is absent from the data, then it implies that the inner core viscosity is smaller than $\sim 10^{17}$ Pa s, or alternatively, that the torques at the ICB are weaker than $\sim 10^{20}$ N m. In either cases, the inner core tilt cannot be responsible for the Markowitz wobble.

4.6.2 Nature of the torque

So far our efforts have focused on determining the amplitude of the equatorial torque required at the ICB to produce the observed polar motion. We now turn our attention to the possible mechanisms that can generate such a torque. Mechanical coupling through viscous stresses at the ICB is probably very weak even when turbulent values of the viscosity are adopted (Aurnou and Olson, 2000). Inertial coupling from the pressure imposed by the fluid flow on the elliptical ICB requires knowledge of the flow and is difficult to evaluate. Another possibility is electromagnetic coupling, which we investigate here.

Electromagnetic torques between the fluid core and its envelope are a result of the Lorentz force which is created by the interaction of the magnetic field normal to the boundary and the electrical current flowing along the boundary (Rochester, 1960). In terms of the magnetic field **B**, the torque at the ICB can be expressed as

$$\Gamma = \frac{1}{\mu} \int_{ICB} (\mathbf{r} \times \mathbf{B})\, B_r \, dS, \tag{4.19}$$

where μ is the permeability of free space and the integral is taken on the assumed spherical inner core surface. The magnetic field in the core is maintained by complex dynamics involving the convective flow motion. One can therefore imagine a complicated morphology for the magnetic field at the ICB. At any given time, we expect that this magnetic field will produce a net equatorial torque on the inner core, unless a fortuitous cancellation occurs as a result of the surface integration. However, the real question is whether the amplitude and periodicity of this torque are within the range of values required to explain the Markowitz wobble.

In order to force a polar motion with decade periods, the torque on the inner core must have the same periodicity. This requires changes in the magnetic field on decade timescales.

Since the changes in the magnetic field result from the dynamics in the fluid core, it is necessary to first identify a dynamical process in the fluid core with typical timescales of decades, and second, establish whether this process is capable of imposing equatorial torques on the inner core with the required magnitude. One possible such process is torsional oscillations. These are the rigid azimuthal oscillations of cylindrical shells aligned with the rotation axis (Taylor, 1963; Braginsky, 1970). The action of this torsional oscillation flow on the radial magnetic field threading the ICB can indeed produce equatorial torques on the inner core, as demonstrated in the remainder of this section.

Tangential azimuthal flow at the ICB will deform the radial magnetic field and produce an azimuthal magnetic traction on the surface of the inner core. If one pictures an axisymmetric radial magnetic field, it is obvious that the resulting torque will be entirely in the axial direction. However, the radial magnetic field will have a non-axisymmetric part which will give rise to an equatorial component of the torque.

This can most easily be demonstrated with the help of simple cartoons. Suppose, as in figure 4.7(a), that the radial magnetic field at the ICB is concentrated in two small areas at mid-latitudes, one in the southern hemisphere where the field enters the inner core and the other one in the northern hemisphere where it leaves it. An azimuthal flow acting on the inner core will generate a local azimuthal magnetic traction at the location of the field patches. The direction of the resulting torque on the inner core is perpendicular to the plane defined by the position vector (from the center of the inner core to the field patch) and the surface force vector. This torque has an equatorial component, as shown in figure 4.7(b). A reversed flow would produce a torque in the opposite direction. Thus, an azimuthal flow oscillating at decade timescales, a torsional oscillation flow, produces variations in the direction of the torque at the same timescale.

An order of magnitude estimate of the amplitude of the equatorial torque can be made from an oscillating azimuthal flow acting on a tilted dipole field at the ICB. Although the field at ICB is more complicated than a tilted dipole, for the simple calculation that follows, the contribution of the multipole components of the field to the electromagnetic torque can be incorporated in terms of an "effective" dipole field. The details of this calculation are presented in appendix A.4. The torque that is obtained is

$$\Gamma \approx -\frac{\pi a_s^3 g_1^0 g_1^1 \Delta u_\phi}{\mu(\eta\sigma_d)^{1/2}}, \tag{4.20}$$

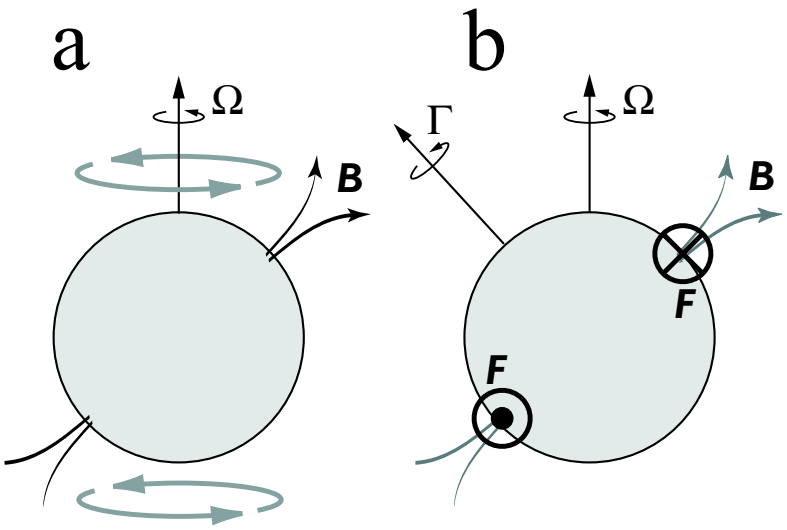

Figure 4.7: (a) Hypothetical configuration of the magnetic field (black arrows) and azimuthal flow (grey arrows) near the inner core. (b) The surface force **F** produced by the shear of the flow on the radial part of the magnetic field is directed into (out of) the page in the northern (southern) hemisphere. The resulting torque on the inner core is $\Gamma = \mathbf{r} \times \mathbf{F}$.

where a_s is the radius of the inner core, η is the magnetic diffusivity (which is related to the electrical conductivity σ_e by $\eta = 1/\mu\sigma_e$), σ_d is the frequency of oscillation of the azimuthal flow, Δu_ϕ is the difference in axial velocity between the inner core and the fluid cylindrical shells. g_1^0 and g_1^1 are the Gauss coefficients of the axial and equatorial "effective" dipole field, defined for the present context at the surface of the inner core. We emphasize that this "effective" dipole field is largely unrelated to the dipole field at the CMB that is observed at the surface.

The rigid azimuthal velocity of the fluid shells inside the tangent cylinder can be evaluated with the flow inversions at the CMB (Jault *et al.*, 1988; Jackson *et al.*, 1993; Zatman and Bloxham, 1997; Pais and Hulot, 2000; Hide *et al.*, 2000). The amplitude of the velocity in this region of the core is not well constrained because it represents a small fraction of the total area of the CMB. Recent studies have estimated a steady westward component of the flow of 0.5 - 1° per year (Olson and Aurnou, 1999; Pais and Hulot, 2000), but the oscillating part of this flow is unknown. Nevertheless, a reasonable estimate of the amplitude of this oscillating flow is 10^{-4} m s^{-1}, in agreement with typical torsional oscillations amplitude in the bulk of the core. With this estimate for the velocity, together with typical values of

electrical conductivity in the core of $\sigma_e = 5 \times 10^5$ S m^{-1} (e.g. Gubbins and Roberts, 1987), which gives $\eta = 1.6$ m^2 s^{-1}, and with $a_s = 1200$ km and $\sigma_d = 2\pi/30$ yrs^{-1}, equation (4.20) implies that in order to get a torque of 10^{20} N m, we need $g_1^0 g_1^1 \approx 20$ mT^2. For instance, if we partition this value into $g_1^0 = 6.3$ mT and $g_1^1 = 3$ mT, this gives an "effective" dipole tilt of about 25 degrees and a RMS radial magnetic field of roughly 4 mT. With the same dipole tilt and parameters as above but with a velocity of 2×10^{-4} m s^{-1}, the RMS field is reduced to ~ 3 mT. These estimates for the radial magnetic field are large but not unreasonable. Results of the Kuang-Bloxham numerical simulation of the geodynamo (Kuang and Bloxham, 1997a, 1999) suggest that the RMS amplitude of B_r may be as large as 3 mT at the ICB. Inferences from the forced nutations suggest a minimum RMS field of 4.6 mT (Buffett *et al.*, 2002). Therefore, on that order of magnitude basis, we conclude that electromagnetic torques produced by torsional oscillations could be capable of imposing an equatorial torque of 10^{20} N m on the inner core.

A detailed investigation of the equatorial torque according to this scenario is definitely not possible due to our limited knowledge of the radial field structure and the differential velocity at the ICB. Another avenue would be to investigate the equatorial torque that emerges in the numerical simulations of the geodynamo. Typical values of the electromagnetic equatorial torque in the Kuang-Bloxham model (Kuang and Bloxham, 1997a, 1999) are on the order of the required 10^{20} N m. It is thus tempting to confirm that the mechanism described above is indeed supported by the dynamics of the fluid core. However, such a claim would be misguided: care has to be taken when inferring results from the geodynamo models. The parameter regime in which the Earth's dynamo operates is not yet attainable in the numerical simulations (recent reviews include Dormy *et al.* (2000),Glatzmaier (2002) and Kono and Roberts (2002)) and it is unclear whether the former result can be appropriately scaled to the Earth's core. The ability of the Kuang-Bloxham model to reproduce the required torque on the inner core may be promising, but remains inconclusive.

As we can see in figure 4.7, the electromagnetic torque produced in the fashion described above has a specific orientation determined by the morphology of the radial magnetic field at the ICB. If the radial magnetic field is steady over several periods of oscillation of the flow, the resulting torque will then oscillate along a specific longitudinal plane. This represents an appealing aspect of our model because the observed Markowitz wobble is indeed highly eccentric and polarized along a specific longitude. In fact, a good test for any

mechanism that tries to explain the Markowitz wobble is its ability to produce a polarized polar motion at the surface.

In figure 4.8, we present the polar motion which is generated from an applied torque at the ICB that oscillates with a period of 30 years along a specific orientation (in this case, direction $\hat{\mathbf{e}}_1$). The resulting polar motion is polarized, with an orientation that is at 90° to the torque for large inner core viscosity. The ellipticity of the motion is roughly 0.92 and the sense of rotation is prograde. The fact that the resulting polar motion is not perfectly polarized is a consequence of an enhancement of the motion in the prograde direction which is due to the resonant effect of the inner core free wobble mode, a purely prograde mode. (The ratio of amplitudes of a polar motion produced by a prograde versus a retrograde torque is roughly 1.69 at a 30 year period.)

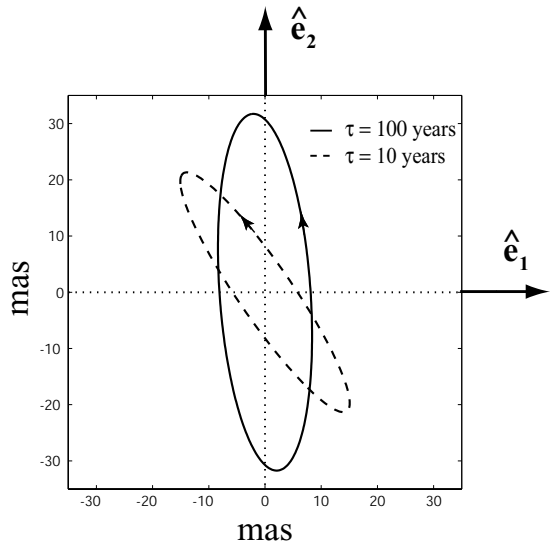

Figure 4.8: Polar motion at the surface which results from a periodical applied torque of 10^{20} N m oscillating along $\hat{\mathbf{e}}_1$. The solid trajectory corresponds to τ = 100 years and the dashed trajectory to τ = 10 years.

Dickman (1981) has suggested that the Markowitz wobble is predominantly a retrograde motion. If further analyses of the decade polar motion signal confirm this fact, then the scenario presented above cannot be reconciled with the observation. However, at the current level of uncertainties in the data, a prograde motion cannot be ruled out (Dickman, 1983).

Hence, electromagnetic coupling on the inner core tilt provides not only a torque which might be of sufficient magnitude, but also one that produces an eccentric polar motion with a preferred orientation. We therefore conclude that electromagnetic coupling on the inner core due to the action of torsional oscillations cannot be discounted as the driving mechanism for the observed Markowitz wobble.

4.6.3 Excitation of the Chandler wobble

The Chandler wobble has been observed in the Earth rotation data for more than a century, but the mechanism responsible for its excitation is still not fully resolved. Lately, sea-floor pressure at the bottom of the oceans (Gross, 2000) and barometric pressure and winds (Celaya *et al.,* 1999) have been shown to be the most promising candidates.

The results of figure 4.6 might suggest the possibility that the inner core participates in the excitation process. A required torque of amplitude 10^{19} N m on the inner core is not unreasonable from considerations of electromagnetic coupling, as we have demonstrated in the previous section. The problem, of course, is to generate a torque of such amplitude near the periodicity of the Chandler wobble (435 days). Typical timescales for the dynamics in the fluid core are much longer than a year. However, a recent study indicates that higher wave-number torsional oscillations with short period can explain the sudden variations in the geomagnetic field data (Bloxham *et al.*, 2002). The short period torsional oscillations could then generate an electromagnetic torque on the inner core by the mechanism described in the previous section and provide a forcing near the Chandler frequency. Other possible mechanism might involve non-linear interactions in the dynamics that could produce a rapid torque but this is of course highly speculative and the details of how this mechanism might operate are certainly not known.

An additional word of caution comes from the fact that dissipation of rotational energy in the mantle and the oceans is not considered in our model. Therefore, one expects that the value of the required torque that we have calculated is underestimated. Nevertheless, this finding is interesting and further consideration should be given to both the potential mechanism that can produce a rapid torque and the proper incorporation of mantle and ocean dissipation in our model.

4.7 Conclusions

In this chapter we have developed a model to investigate the possibility that a tilted inner core could participate in the irregularities in the direction of the Earth's rotation axis with respect to the mantle. We have shown that the required torque produced at the ICB in order to explain the Markowitz wobble of decade periods is on the order of 10^{20} N m if the homogeneous viscosity of the inner core exceeds 5×10^{17} Pa s. This torque produces inner core tilt amplitudes of 0.07 degrees. Torques of larger magnitude are required if the viscosity of the inner core is smaller.

A torque of such amplitude with decade periods could be produced by electromagnetic coupling between the inner core and the torsional oscillations in the fluid core. Such a torque has the appealing feature of producing an elliptical and polarized polar motion, two defining characteristics of the observed Markowitz wobble.

A good test to determine if such a mechanism is indeed responsible for the Markowitz wobble is the detection of a 6-year period in the polar motion data and gravimetric measurements. This period corresponds to the free inner core wobble mode and we have shown that this mode is easily excited by torques at the ICB. The absence of such a signal in the data would most likely indicate that decade torques at the ICB are probably too small to explain the amplitude of the Markowitz wobble.

If the Markowitz wobble results from a different mechanism, then the model presented in this chapter can be used to constrain the equatorial torque at the ICB and the inner core viscosity. For instance, if the viscosity can be shown by independent means to be larger than 5×10^{17} Pa s, it would imply that the equatorial torque at the ICB is less than $\sim 10^{20}$ N m. Alternatively, if one shows that the torque at the ICB is on the order of 10^{20} N m, then our model would constrain the viscosity of the inner core to be smaller than 10^{17} Pa s.

Chapter 5

Azimuthal flows in the Earth's core and changes in length of day at millennial timescales

5.1 Introduction

The Earth's magnetic field is believed to be generated by convective motion in the fluid core, a process known as the geodynamo. The details involved in this process are not fully understood, partly because we have few observations that can be used to constrain the dynamics. The magnetic field itself, the very product of the geodynamo, has been measured directly at fixed observatories distributed around the globe only since the 1840's (e.g. Stern, 2002). The addition of magnetic field data recorded in ship logs and other sources has pushed back the historical magnetic field observations to 1590 (Bloxham *et al.*, 1989; Jackson *et al.*, 2000). These observations have provided many advances in our current understanding of the geodynamo. However, they cover a timespan shorter than the typical 500-1000 year timescale on which the dynamics responsible for maintaining the magnetic field are believed to operate (e.g. Hollerbach, 2003).

Archaeomagnetic field models on the other hand offer a much more promising perspective for the study of core dynamics at the latter timescales. These are global magnetic field models covering the last few millennia, built from a compilation of paleomagnetic field data obtained from archaeomagnetic artifacts, lake sediments and lava flows (Daly and Le Goff,

1996; Hongre *et al.*, 1998; Constable *et al.*, 2000; Korte and Constable, 2003). Although these models only capture some of the crudest features of the Earth's magnetic field, they extend our continuous record back to 3000 years before present. In recent years, there has been a considerable improvement and extension of the database from which they are constructed. There is hope that some of the millennial magnetic field variations involved in the geodynamo are reliably captured in archaeomagnetic field models.

In this study, we attempt to relate a part of the archaeomagnetic secular variation (ASV) to dynamic processes involved in the geodynamo. We focus on one particular aspect of the ASV, the longitudinal drift of some of the magnetic field structures, where general patterns of westward and eastward motion seem to alternate with a periodicity on the order of a thousand years. We investigate the possibility that these variations are caused by advection from oscillating azimuthal flows in the core.

Additional information on core flows at millennial timescales can be obtained from a different geophysical dataset: the observed millennial variations in the Earth's rotation rate, recorded as changes in length of day (LOD) (Stephenson and Morrison, 1995; Morrison and Stephenson, 2001). Direct measurements of the variations in the amplitude of the Earth's rotation has been made possible by the advent of atomic clock in 1955 (e.g. Munk and MacDonald, 1960; Lambeck, 1980). Telescopic observations of the occultations of stars by the Moon and of the transits of Mercury across the Sun's face can be used to extend the continuous record back to 1620, albeit only for the largest decadal and century variations (e.g. Stephenson and Morrison, 1984). Observations of Solar and Lunar eclipses documented by the ancient and medieval civilizations of Babylon, China, Europe and Arabia provide a means to reconstruct the variations in LOD further in the past. By integrating the celestial motions of the Earth-Moon-Sun system backward in time and requiring that the eclipses occur at the location and time they were recorded, it is possible to retrace the last 2700 years of the Earth's rotation rate (Stephenson and Morrison, 1984, 1995; Morrison and Stephenson, 2001). The eclipse record successfully captures the lengthening of the day at the rate predicted by the measured tidal dissipation between the Earth and the Moon (and a smaller contribution from the Sun) (Christodoloudis *et al.*, 1988), minus the effects from the decrease of the Earth's oblateness (Yoder *et al.*, 1983; Rubincam, 1984; Cheng *et al.*, 1989) resulting from post-glacial rebound (O'Connell, 1971; Wu and Peltier, 1982; Mitrovica and Peltier, 1993). More importantly for our present purpose, the eclipse record

also suggests the presence of an oscillation in the LOD about this gradual increase, with a periodicity of about 1500 years.

The similarity of the periodicities involved in the millennial LOD variations and of the oscillating longitudinal drifts of the ASV is tantalizing in that it may indicate that both observations result from a common mechanism originating in the fluid core. Indeed, if the millennial LOD variations are due to angular momentum exchange between the mantle and core, the changes in core angular momentum are carried by time-dependent azimuthal flows, the very type of flow consistent with the observed periodic drifts of magnetic field structures.

The aim of this chapter is to investigate whether time-dependent azimuthal flows in the core may consistently explain both the millennial variations in LOD and the ASV. Our approach to the problem is from a geodynamo perspective and we critically assess whether the form of the required azimuthal flows is also consistent with our expectations of core dynamics at millennial timescales.

Considerable success has been achieved by applying similar ideas at decade timescales. Torsional oscillations, a component of the flow predicted by theory which consists of azimuthal oscillations of rigid coaxial cylindrical surfaces (Taylor, 1963; Braginsky, 1970), can be inferred from historical geomagnetic secular variations (Zatman and Bloxham, 1997, 1998; Pais and Hulot, 2000; Hide *et al.*, 2000). Because the azimuthal velocity involved in the torsional oscillations is invariant in the direction of the rotation axis, the knowledge of the core surface flow is sufficient to calculate the angular momentum changes in the core carried by this flow. When compared with the corresponding changes in angular momentum of the mantle, which are obtained from the variations in the length of day, the agreement between the two is good, at least from about 1900 onward (Jault *et al.*, 1988; Jackson *et al.*, 1993). The conclusions that can be drawn from this result are many-fold. First, it confirmed that the decade variations in the LOD are due to exchanges of angular momentum between the core and the mantle. Secondly, it confirmed that torsional oscillations occur in the core and are well recovered in core flows. And third, it added credence to the quality of the LOD data, the historical magnetic field models and the core flows derived from these models.

Here, we apply the same concept at millennial timescales. We demonstrate the existence of time-dependent azimuthal flows consistent with both the ASV and the millennial

variations in LOD. However, these flows are characterized by a shear in the axial direction, in contrast to the decade timescales variations. We interpret these as oscillations in the thermal and magnetic winds, which we expect on theoretical grounds to occur in the core at these timescales.

5.2 Variations in thermal and magnetic winds in the core at millennial timescales

Theoretical arguments suggest that, at decade timescales, the flow that carries the changes in angular momentum of the core is comprised of oscillating rigid cylindrical surfaces aligned with the rotation axis. This view is supported by observations. The same theoretical foundation can be used to demonstrate that at millennial timescales, we do not expect this type of flow to be dominant. Before we proceed with any attempts to observe aspects of core dynamics in the ASV and millennial LOD variations, it is useful to briefly present these theoretical arguments and the form of the flows that we expect at millennial timescales.

Fluid particles in the core must obey the momentum equation. When using the radius of the core r_c as a typical lengthscale, the decay time of magnetic field $\tau_\eta = r_c^2/\eta$ as a typical timescale, and $\mathcal{B} = \sqrt{2\Omega\rho\mu\eta}$ as a magnetic field scale (where ρ is density, Ω is the Earth's rotation frequency, μ is the permeability of free space, $\eta = 1/\mu\sigma$ is the magnetic diffusivity and σ is electrical conductivity), the non-dimensional momentum equation, in the Boussinesq-anelastic approximation, is (e.g. Gubbins and Roberts, 1987)

$$R_o(\frac{\partial \mathbf{v}}{\partial t} + \mathbf{v}\cdot\nabla\mathbf{v}) + \mathbf{e_z}\times\mathbf{v} = -\nabla P + (\nabla\times\mathbf{B})\times\mathbf{B} + R_a\Theta\mathbf{r} + E\nabla^2\mathbf{v}. \tag{5.1}$$

In the above equation, the vectors $\mathbf{v}$, $\mathbf{B}$, $\mathbf{r}$ and $\mathbf{e_z}$ are respectively the velocity field, the magnetic field, the radius vector and the unit vector in the direction of the Earth's rotation, t is time, P is pressure and Θ is the deviation in temperature from a background adiabatic state. The non-dimensional numbers R_o, E and R_a are respectively the Rossby, Ekman and Rayleigh numbers and are defined as

$$R_o = \frac{\eta}{2\Omega r_c^2}, \quad E = \frac{\nu}{2\Omega r_c^2}, \quad R_a = \frac{g\alpha\beta r_c^2}{2\Omega\eta}, \tag{5.2}$$

where ν is the kinematic viscosity, g is the gravitational acceleration at the core-mantle boundary (CMB) and α is the coefficient of volume expansion. β is a typical value of the temperature gradient and consequently, the typical scale of Θ is βr_c. Using typical values for Earth's core, we get (e.g. Gubbins and Roberts, 1987)

$$R_o \approx 10^{-9}, \quad E \approx 10^{-15}. \tag{5.3}$$

This suggests that, to a first order, one may neglect the influence of inertia and viscous forces in the force balance, which leads to the so-called magnetostrophic balance,

$$\mathbf{e_z} \times \mathbf{v} = -\nabla P + (\nabla \times \mathbf{B}) \times \mathbf{B} + R_a \Theta \mathbf{r}. \tag{5.4}$$

In this study we are interested in flows in the Earth's core that carry axial angular momentum: the axisymmetric part of the azimuthal component. Whether or not the axisymmetric azimuthal part of the flow behaves rigidly in the axial direction can be addressed by considerations of the above magnetostrophic balance. First, let's consider the dynamics responsible for generating flow gradients in z. Taking the axisymmetric part of $\mathbf{e}_\phi \cdot \nabla \times$ (5.4), we get

$$-\frac{\partial \overline{v_\phi}}{\partial z} = \left[\overline{\nabla \times \mathbf{F}} \right]_\phi, \tag{5.5}$$

where the overbar denotes an axisymmetric (ϕ-averaged) quantity and where $\mathbf{F}$ is the sum of the Lorentz and buoyancy forces,

$$\overline{\mathbf{F}} = \overline{(\nabla \times \mathbf{B}) \times \mathbf{B}} + R_a \overline{\Theta} \mathbf{r}. \tag{5.6}$$

When the right hand side of (5.5) vanishes, which occurs when $\mathbf{F} = \mathbf{0}$ or when $\mathbf{F}$ is entirely in the azimuthal direction, $\overline{v_\phi}$ cannot have gradients in z. In other words, $\overline{v_\phi}$ is constant on cylindrical surfaces aligned with the rotation axis. This result is the well-known Proudman-Taylor constraint (Proudman, 1916; Taylor, 1917), which restricts flows to be two-dimensional in rapidly rotating fluids. In the Earth's core, the added constraint of the spherical boundary geometry limits the two-dimensional flows to rigid rotations of cylindrical surfaces (Bullard and Gellman, 1954).

The buoyancy force is entirely in the radial direction, so the azimuthal velocity associ-

ated with that part of **F** cannot be rigid and necessarily has a gradient in z. This part of the flow is referred to as the thermal wind and is related to the temperature by

$$\frac{\partial \overline{v_\phi}}{\partial z} = R_a \left[\mathbf{r} \times \nabla \overline{\Theta} \right]_\phi , \tag{5.7}$$

$$= R_a \frac{\partial \overline{\Theta}}{\partial \theta} , \tag{5.8}$$

where θ is colatitude. Hence, provided $\overline{\Theta}$ varies with colatitude, azimuthal flows with gradients in z are expected. We are interested here in the time-dependency of this thermal wind flow and whether or not we expect significant changes to occur on a 1500-year timescale. Taking the time derivative of both sides of the thermal wind balance,

$$\frac{\partial}{\partial t} \frac{\partial \overline{v_\phi}}{\partial z} = R_a \frac{\partial}{\partial t} \frac{\partial \overline{\Theta}}{\partial \theta} , \tag{5.9}$$

the variations in time in the axial gradients of the azimuthal flows are related to time-dependent variations of latitudinal gradients in $\overline{\Theta}$. The latter reflect globally integrated changes in temperature that result from convective motions. Taking typical velocity of fluid particles in convective rolls to correspond to core surface flow velocities, about 10 km/yr, gives a turnover timescale of roughly 500 years. We may then expect that for timescales of 500 years and longer, changes in the temperature perturbation due to convective motions are significant enough to alter $\overline{\Theta}$, which leads to a time-dependent thermal wind. A similar argument can be constructed around the Lorentz force and its associated magnetic wind.

At a timescale of 1500 years, variations in thermal and magnetic wind are then likely to occur and we expect that the time-dependent azimuthal flows have gradients in z. However, the above arguments say nothing about the relative importance of rigid azimuthal flows. Hence, even though axial shear in azimuthal flow may be produced, their amplitude may be much weaker than the rigid component of the flow. To complete the dynamical picture, we also need to consider whether we expect large amplitude rigid motions.

The dynamics responsible for rigid azimuthal flows can also be deduced with the magnetostrophic balance as a starting point. Upon integration of the azimuthal component of (5.4) on cylindrical surfaces aligned with the rotation axis, the Coriolis, pressure and buoyancy terms all vanish identically. This then leads to a morphological constraint on the

magnetic field,

$$\int_{\Sigma} ((\nabla \times \mathbf{B}) \times \mathbf{B})\, d\Sigma = 0\,, \tag{5.10}$$

where $d\Sigma = s\, d\phi\, dz$ and (s, ϕ, z) are cylindrical coordinates. In other words, the axial Lorentz torque on cylinder surfaces must cancel. This result is known as Taylor's constraint (Taylor, 1963).

One expects that the complex dynamics involved in the geodynamo lead to a time-dependent magnetic field which produces non-vanishing Lorentz torques. These torques must then be balanced by one of the terms that were left out of the magnetostrophic balance. The relative importance of inertial acceleration vs viscous forces to provide this balance depends on the timescale of the magnetic field variations considered. For changes that occur on a timescale shorter than the spin-up time $\tau_\nu = R_o E^{-1/2}$ due to viscous stresses at solid-fluid boundaries, inertia is dominant. Using the values in (5.3), we get $\tau_\nu \sim 10^4$ years. For the timescales of the dynamics associated with rigid flows (see below), non-vanishing Lorentz torques are balanced by inertial accelerations and the integral constraint becomes

$$R_o \frac{\partial}{\partial t} \frac{\{\overline{v_\phi}(s)\}}{s} = \frac{1}{4\pi s^2 (1-s^2)^{\frac{1}{2}}} \int_{\Sigma} ((\nabla \times \mathbf{B}) \times \mathbf{B})\, d\Sigma\,, \tag{5.11}$$

where $\{\}$ denotes a z-averaged quantity.

The inertial acceleration thus induced has a feedback on the Lorentz torque: it produces changes in the azimuthal component of the magnetic field, and in so doing produces a secondary Lorentz torque that opposes the original torque. The above system allows oscillatory azimuthal motions of rigid cylinder surfaces about a position where Taylor's constraint is satisfied. These are known as torsional oscillations and their typical periodicity is $\tau_{to} = R_o^{1/2}/B_s$ (Braginsky, 1970). For a typical magnetic field strength of 5 Gauss, this leads to periods with a characteristic timescale of decades.

Mathematically, equation (5.11) does not require the azimuthal velocity to be rigid, but only that its integrated average over the cylinder balances the Lorentz torque. However, for torsional oscillations, the restoring force for the wave motion is entirely due to the azimuthal component of the Lorentz force (Braginsky, 1970). Hence, the right hand side of (5.5) vanishes and torsional oscillations are indeed oscillations of rigid cylindrical surfaces.

The presence of torsional oscillations does not prevent non-rigid time-dependent az-

imuthal flow to occur at decade timescales. Indeed, we expect that changes in the three-dimensional structure of the magnetic field and temperature perturbation lead to changes in the magnetic and thermal winds even at decade timescales. However, we expect these perturbations also to excite torsional oscillations efficiently, therefore leading to a time-dependent behavior which includes an important component of rigid rotations. Hence, that the time-dependent azimuthal flows in the core at decade timescales appear to be dominated by rigid azimuthal flows (Jault *et al.*, 1988; Jackson *et al.*, 1993; Zatman and Bloxham, 1997) is partly a consequence of the fact that the magnetic and thermal winds may not vary sufficiently on such short timescale. More importantly though, their dominance arises as a consequence of the presence of a natural mode of oscillation in the core at decade timescale - torsional oscillations - which involves rigid azimuthal flows.

Our primary interest in this study is azimuthal fluid motions with a 1500 year timescale, not decades. If rigid flows occur at millennial timescales, these are not torsional oscillations because the latter have characteristic periods with a timescale two orders of magnitude smaller. Therefore, rigid flows at these timescales can only represent a diffusive readjustment of the background differential rigid rotation between the cylinder surfaces. However, we expect diffusive readjustments to be consistent with the changes in thermal and magnetic winds and thus affect all three dimensions of the fields. In other words, we expect the diffusive readjustment velocity to include gradients in z.

Clearly, if the changes in millennial LOD result from an exchange of angular momentum with the core, then the latter must be carried by azimuthal flows. Hence, it must be that the z-averaged azimuthal flow is non-zero for at least some of the cylinders in the core. The question is whether the non-zero z-averaged flows represent an actual rigid flow, or a flow with a shear in z for which the average in z does not equal zero. According to the theoretical development above, the latter option seems to be more reasonable for two main reasons: (1) we expect the changes in convection to produce time-dependent variations in the thermal and magnetic winds; (2) the natural modes of oscillations involving rigid rotations have typical periods that are two orders of magnitude smaller.

Although none of the arguments above are definitely conclusive, they tend to support the view that time-dependent changes in azimuthal flows at millennial timescales are mostly comprised of variations in axial gradients. Therefore, we expect that the time-dependent flows that can explain both the millennial LOD and the ASV involve shear in the axial

direction, in contrast to the rigid flows at decade timescales.

5.3 Inversion for fluid flows at the surface of the core

We now proceed to build time-dependent flows at the surface of the core that are consistent with the observed ASV. Flow maps inverted from the historical secular variation of the magnetic field are based on the frozen flux hypothesis (Roberts and Scott, 1965; Backus, 1968), which assumes that the advection of the magnetic field by the flow dominates diffusion. The radial component of the induction equation in this diffusionless limit is

$$\frac{\partial B_r}{\partial t} = -\nabla_h \cdot (B_r \mathbf{u}_h) \,. \tag{5.12}$$

The knowledge of B_r and $\partial B_r/\partial t$ is then used to invert for the horizontal component of the flow $\mathbf{u}_h$. The flow obtained with the above equation is non-unique and additional dynamical assumptions must be specified in order to reduce the ambiguity. Assumptions that are frequently made are that the flow is steady (Gubbins, 1982), tangentially geostrophic (Hills, 1979; Le Mouël, 1984), or purely toroidal (Whaler, 1980). For a review of the subject, see Bloxham and Jackson (1991).

In the present study, we are only interested in flows that carry angular momentum: the part of the azimuthal component that is axisymmetric and also symmetric about the equator. In the context of historical geomagnetic secular variation, the time-dependent part of this component of the flow has been obtained by inverting for a flow comprised of a steady part and a time-dependent geostrophic part (Zatman and Bloxham, 1997, 1998; Pais and Hulot, 2000; Hide *et al.*, 2000). The azimuthal part of the latter contains an axisymmetric component. Alternatively, one can invert for a flow for which the time-dependent part is specified entirely in terms of axisymmetric azimuthal flows symmetric about the equator (Bloxham *et al.*, 2002). Even though this last method involves a very parsimonious representation of the time varying flow, it successfully explains the part of the secular variation due to torsional oscillations, which is shown to include geomagnetic jerks.

Here, we proceed along the lines of the latter method. We seek flows which can best explain the ASV, but for which the time-dependent part is restricted to contain only the ax-

isymmetric, equatorially symmetric azimuthal component. Using vector spherical harmonics, the time-dependent part of the flow $\mathbf{u}_T(\theta,t)$, where θ is colatitude, can be represented entirely in terms of toroidal flow decomposition as

$$\mathbf{u}_T(\theta,t) = \nabla \times (\mathcal{T}(\theta,t)\mathbf{e_r}), \tag{5.13}$$

with

$$\mathcal{T}(\theta,t) = \sum_{n\,odd} t_n^0(t) P_n^0(\cos\theta), \tag{5.14}$$

where $\mathbf{e_r}$ is a unit vector in the radial direction, $\mathcal{T}$ is a so-called toroidal scalar and $P_n^0(\cos\theta)$ are Legendre polynomials. The flow is then entirely specified in terms of the coefficients $t_n^0(t)$. We restrict the flow model to contain only *odd* values of *n*, which forces flow symmetry across the equator.

Several concerns can be raised about the application of the above method for extracting core flow variations at millennial timescales. First and foremost, for timescales longer than a few centuries, diffusion of the magnetic field is expected to play a role in the dynamics. This compromises seriously the assumption of frozen flux. Indeed, part of the ASV consists of growth or decay in intensity of specific magnetic features (Constable *et al.*, 2000; Korte and Constable, 2003). The dynamics governing these changes certainly involve diffusion. However, the restricted time-dependent flow that we invert should not be sensitive to these aspects of the dynamics. Our inverted flow is in principle only sensitive to the part of the secular variation which consists of longitudinal displacements of magnetic field structures. It is difficult to imagine how diffusion would destroy completely the effect of advection by a time-dependent axisymmetric zonal flow. Hence, for our choice of time-dependent flows, we expect the frozen flux assumption to remain valid.

A second worry, also related to diffusion, concerns the steady part of the flow. For kinematic dynamos in a nearly steady state, the secular variation at the surface results from a near balance between the right hand side of (5.12) and diffusion (Gubbins and Kelly, 1996; Love, 1999). In this case, the inverted steady part of the flow that is obtained when using (5.12) leads to an erroneous result. In addition, using a self-consistent numerical model of the geodynamo, Rau *et al.* (2000) found that the limited resolution of the secular variation from the core could result in artifacts in the core flows. Although these concerns may

not apply to the geodynamo, they should be kept in mind. We recall however that we are only interested in the time-dependent part of the flow. The steady flow that we invert may be erroneous, but we believe that it does not invalidate our results on the time-dependent flows. Of course, one may point out that for the millennial timescales dynamics that we try to extract, our inverted time-dependent flows may suffer from the same limitation that applies to the steady part.

We note in addition that an inherent assumption in our procedure is that the longitudinal drift of magnetic field features is due to advection by fluid motion. An alternative view is that these may represent the azimuthal propagation of a wave in which case the underlying mean azimuthal flow may be unrelated to the direction of the observed drift. Indeed, the historical secular variation most probably contains a part which is due to waves rather than fluid motion (Hide, 1966; Jackson, 2003). This is certainly a possibility and the results that we infer in this study are subject to this caveat.

All these concerns can be addressed *a posteriori*, once we have verified whether there exists a connection between our inverted flows and the millennial variations in LOD. As a case in point, some of the above concerns can also be raised about the validity of the inverted decade timescale variations in the zonal flows. Yet, the agreement of the observed variations in the LOD with those predicted from core flows suggests that the time-dependent part of the zonal flows is well retrieved and indeed represents fluid motion as opposed to waves. The confidence in the time-dependent zonal flows that we invert at millennial timescale is similarly subject to an independent test with the variations in the LOD. Absence of correlation may not unambiguously resolve the issue, as it may indicate that our inverted flows are flawed but could also imply that millennial variations in the LOD are not due to core-mantle angular momentum exchange. A positive correlation on the other hand, despite the chance that it may be fortuitous, will tend to support the validity of the inverted flow.

5.4 Inversion results and changes in length of day

We use the archaeomagnetic field model CALS3K.2, which is an upgraded version of CALS3K.1 (Korte and Constable, 2003), obtained with the same modeling method. The main improvements stem from the inclusion of intensity data, which makes the model no

longer dependent on intensity assumptions related to the axial dipole part of the field, and an iterative improvement by rejection of data that could not be fit within twice the average error estimate of the model (Monika Korte, personal communication). The model covers the period 1000 B.C. to 1950 A.D.. The magnetic field is expanded spatially in real spherical harmonics truncated at degree 10 and is expanded in time on a cubic B-splines basis on a sequence of 53 equally spaced knots. The flow model that we invert is similarly truncated at degree 10 and expanded in cubic B-splines on the same knots sequence. We seek flows that have millennial timescale variations. This is for two reasons. First, to minimize the possibility of modeling parts of the ASV which are due to over-fitting of the data in the archaeomagnetic model itself. Secondly, our aim is to verify a possible correlation between the inverted azimuthal flows and changes in rotation rate of the mantle. The eclipse record, from which the variations in the LOD are reconstructed, is not precise enough to constrain variations that occur on timescales shorter than about a 1000 years. Therefore, only the part of the azimuthal flow which varies on millennial timescale can be compared with the changes in rotation rate of the mantle.

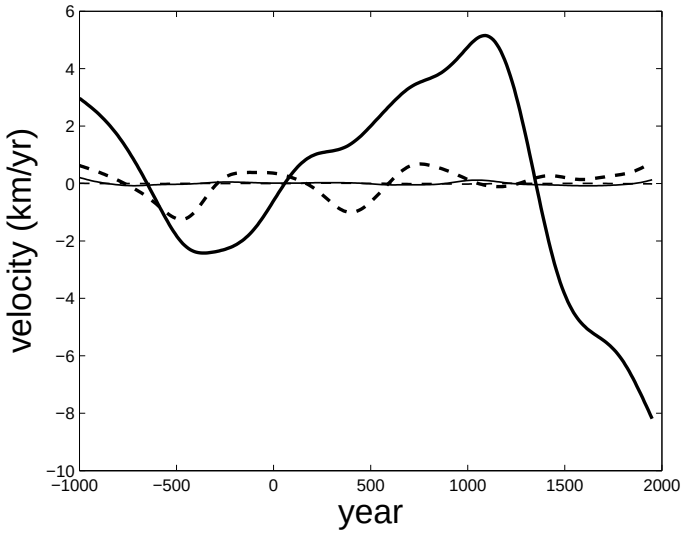

Figure 5.1: Time-dependent part of the coefficients t_1^0 (thick solid line), t_3^0 (thick dashed line), t_5^0 (thin solid line) and t_7^0 (thin dashed line) of the inverted flow model.

The time-dependent part of the coefficients t_1^0, t_3^0, t_5^0 and t_7^0 of our flow model inversion is shown in figure 5.1. On figure 5.2, we show the evolution of a few of the Gauss coefficients

of the archaeomagnetic field model (thick solid line) and the fit obtained from the addition of a steady flow and the flow model of figure 5.1 (dashed line). We do not show the zonal Gauss coefficients ($m = 0$) because they are not influenced by purely zonal azimuthal flows, and consequently our time-dependent flow model is not expected to reproduce any of the time-dependent features of these coefficients. We note that the magnetic field predicted from the flow model can only be determined up to an arbitrary initial condition value. We chose this value to correspond to the field model at 1000 B.C. and a different choice can improve the fit slightly. It is clear that only some features of the long term average trend of the ASV are captured by our parsimonious flow model. Our model also does progressively worse as we consider higher harmonic Gauss coefficients.

That we only fit a small portion of the secular variation with our restricted flow model is not a surprise: the axisymmetric longitudinal drifts of magnetic features, the part of the ASV that our flow can capture, represent only a small fraction of the total ASV. Most of the ASV is due to more complicated time-dependent behavior, including non-axisymmetric and/or meridional drifts, and growth or decay of local flux patches. To illustrate this point, we produced an inversion for which the constraint on the form of the time-dependent flow is slightly relaxed, allowing other components of the flow than just the t^0_{odd} to be time-dependent. The fit of the ASV for this flow model is shown in figure 5.2 (thin line). Clearly, a much larger part of the ASV is explained. In fact, relaxing the constraint even more, we found solutions that can virtually explain all of the ASV. Hence, the fact our parsimonious flow model only fits a small part of the ASV does not invalidate our inversion but only reflects that it plays small role in the total ASV. Indeed, when the constraint on the geometry of the time-dependent flow is relaxed, the general character of the $t^0_{odd}(t)$ part of the flow is not altered. We show in figure 5.3 the $t^0_{odd}(t)$ part of the flow for the inversion that corresponds to the thin line in figure 5.2. The amplitude of the coefficients is different than in figure 5.1, but their features remain identical. Therefore, we believe that our inverted parsimonious time-dependent flow model in figure 5.1 accurately captures the part of the ASV due to axially symmetric zonal drifts.

It is important to stress that, for the inversion with a relaxed flow geometry constraint, we do not believe that the components of the time-dependent flow model other than the zonal odd toroidal part have any real physical significance. These components of the flow model certainly suffer from the caveats of frozen flux as we explained in the previous

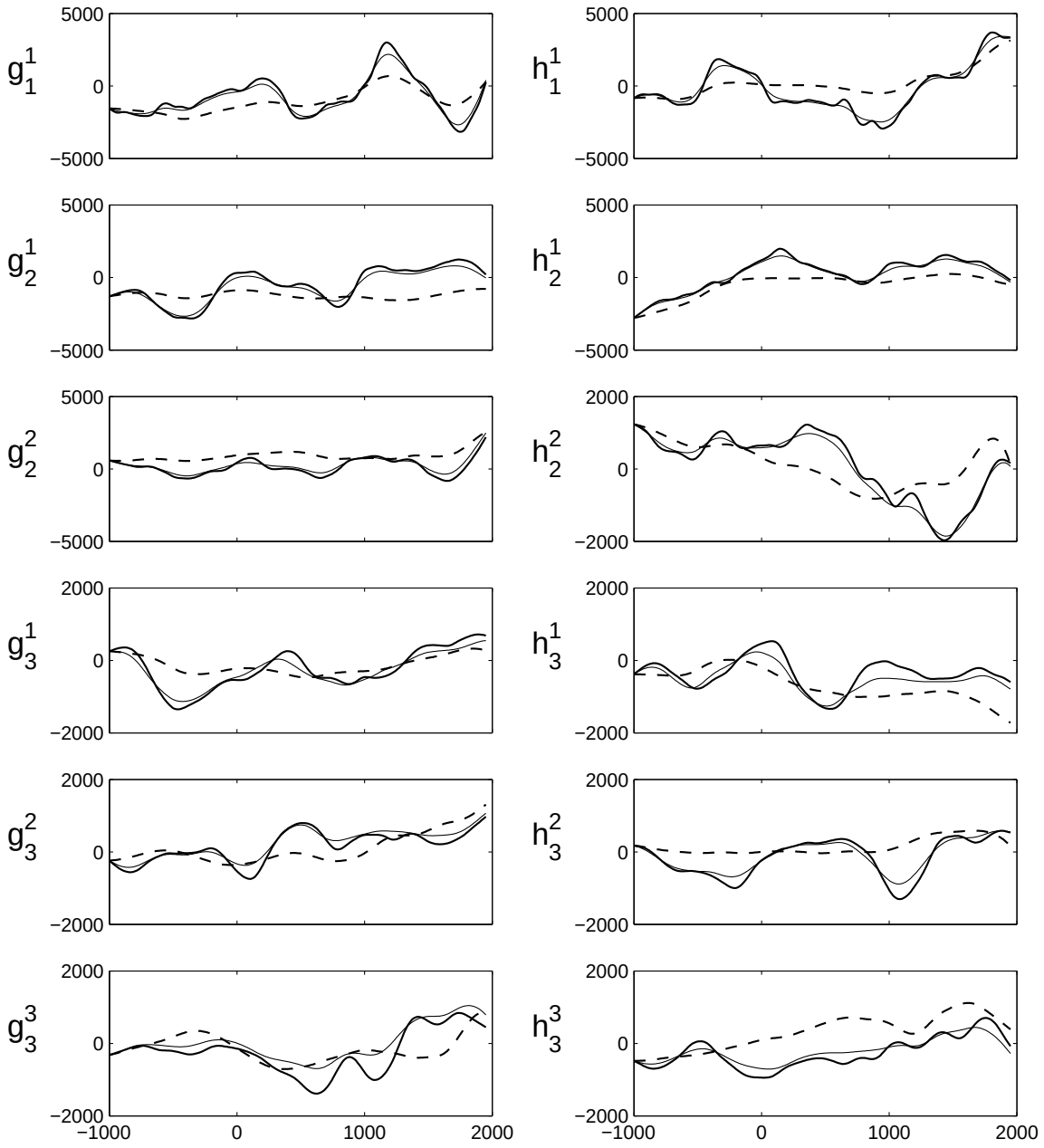

Figure 5.2: Evolution of some of the Gauss coefficients g_l^m and h_l^m of the archaeomagnetic field model CALS3K.2 (thick solid lines), the fit generated from our inverted flow model when the time-dependent part is restricted to toroidal odd zonal harmonics (dashed lines), and the fit when this restriction is relaxed (thin solid line). Units of the vertical axes are in nT and units of the horizontal axes are in years.

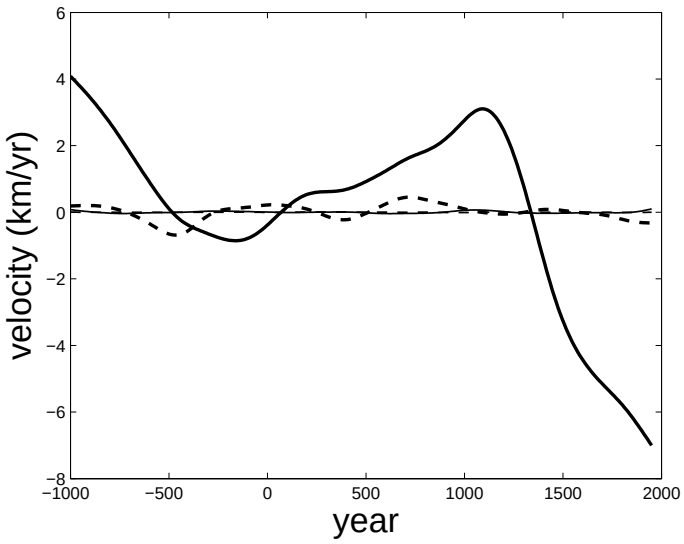

Figure 5.3: Time-dependent part of the coefficients t_1^0 (thick solid line), t_3^0 (thick dashed line), t_5^0 (thin solid line) and t_7^0 (thin dashed line) of the flow model for the inversion for which the restriction on the time-dependent flow is relaxed.

section. The point of this exercise was simply to demonstrate that most of the ASV is due to dynamics other than that due to axisymmetric zonal flows. We make no claim that the part of the ASV not explained by our parsimonious flow model is due to flows which respect frozen flux. In fact, we believe it is most likely not the case. In addition, the components other than the zonal odd toroidal part cannot be constrained with the LOD data and are not useful for our present purpose. Hence, we limit our investigation to the inversion presented in figure 5.1 and the dashed line of figure 5.2 for which the time-dependent part is restricted to the toroidal odd zonal coefficients.

The largest part of the time-dependency in figure 5.1 is carried by t_1^0 alone. This is partly a consequence of our choice of damping in the inversion. This may also be partly due to the smoothness in the archaeomagnetic field model: the lowest degree harmonics contain the most changes and smaller scale structures are discriminated against. Consequently, the zonal flows that can explain these features may also be biased toward smallest harmonics. By 1500 A.D., t_1^0 is negative, implying westward motion, in agreement with the currently observed generally westward drift in the core flow models inverted from historical secular variations. However, the amplitude of the oscillating zonal flows is on the order of 4 km/yr,

a fraction of the largest presently observed westward drift velocities of about 20 km/yr. Hence, the oscillating flow that we recover only represents a part of the total flow at the surface.

We now verify whether our inverted flow model is also consistent with the observed changes in angular momentum of the mantle recorded as variations in LOD. At decade timescales, angular momentum in the core is carried by torsional oscillations and for this specific case, the inverted time-dependent flow at the top of the core allows a straightforward calculation of the angular momentum, which, in a mantle-fixed reference frame, is given by (Jault and Le Mouël, 1991; Jackson *et al.*, 1993)

$$L_c(t) = \frac{I_c}{r_c}\left(t_1^0(t) + \frac{12}{7}t_3^0(t)\right), \tag{5.15}$$

where r_c is the radius of the core and I_c its axial moment of inertia. The good agreement between the observed variations in LOD and the prediction determined from (5.15) (Jault *et al.*, 1988; Jackson *et al.*, 1993) underpins our understanding of core dynamics at decade timescales. As discussed in section 5.2, we do not expect the angular momentum in the core at millennial timescales to be carried by rigid flows and hence we do not expect that (5.15) applies. However, the assumption of rigid flows allows a straightforward calculation of the angular momentum of the core and is a convenient and instructive first test. On figure 5.4, we compare the observed variations in the millennial LOD to the prediction based upon the assumption that the time-dependent flow in figure 5.1 represents rigid cylindrical flows in the core. This prediction is calculated from (Jackson *et al.*, 1993)

$$\Delta LOD(t) = \frac{2\pi}{\Omega^2}\frac{L_c(t)}{(I_m + I_c)} \tag{5.16}$$

where Ω is the Earth's frequency of rotation, I_m is the axial moment of inertia of the mantle and $L_c(t)$ is given by (5.15). The two curves have similar amplitudes, and their phase appear to be related, although anti-correlated.

The similarity in amplitudes and phase between the observed and predicted variations in the millennial LOD is indicative of a connection between azimuthal core flows and the observed exchanges of angular momentum of the mantle. Hence, it suggests that, as for decade timescales, the variations in rotation rate of the mantle are due to exchanges of angular momentum with the core. However, the fact that the phases of the curves are not

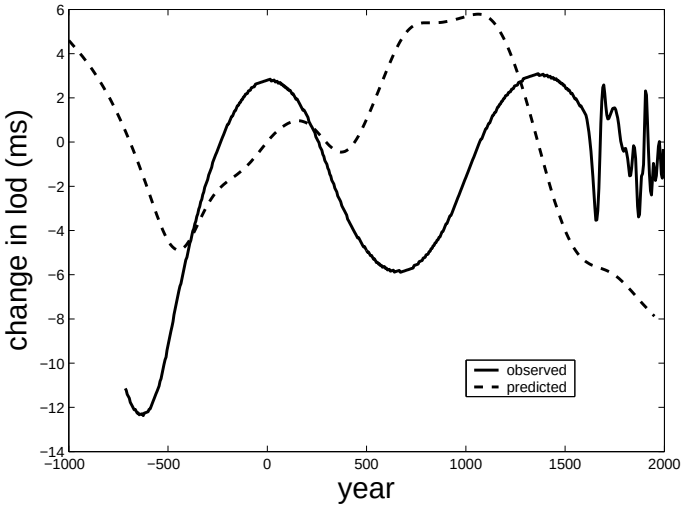

Figure 5.4: Comparison between the observed variations in the length of day obtained from historical eclipses (solid line) and the prediction from our inverted flow model (dashed line) based upon the assumption of rigid cylindrical flows in the core and conservation of angular momentum with the mantle. The observed changes in LOD from 1620 onward are those obtained from telescopic observations and modern techniques.

correlated suggests that, contrary to the case at decade timescales, the angular momentum of the core at millennial timescale does not appear to be carried by flows that are rigid in the direction of the rotation axis. This is consistent with our theoretical expectation that on millennial timescales, the time-dependent azimuthal flows are no longer rigid but contain a shear in the z-direction. Moreover though, the anti-correlation observed in figure 5.4 suggests that the time-dependent average zonal velocity on each cylinder is roughly *equal and opposite* to the azimuthal flow near the CMB. For it to be the case, the structure of the time-dependent azimuthal flow profile in z on a cylinder must be such that the direction of the flow near the extremities is opposite of that near the center and that the integrated average velocity of the cylinder must be about equal and opposite to the velocity at the ends of the cylinder. Hence, the two curves on figure 5.4 can be made to be better correlated if we have a time-dependent azimuthal velocity profile such as that shown in figure 5.5. The comparison of the observed changes in LOD and the prediction based on a velocity profile such as that of figure 5.5 is shown in figure 5.6. Obviously, the correlation remains far from perfect, especially before 500 B.C. and after 1500 A.D.. This is indicative that the

time-dependent flow profile is certainly more complicated than the simple cartoon of figure 5.5. At the same time, because we are able to reconcile a good portion of the predicted and observed LOD variation with such a simple velocity profile, it suggests that this type of flow profile may contain a large part of the thousand year timescales variation in the core.

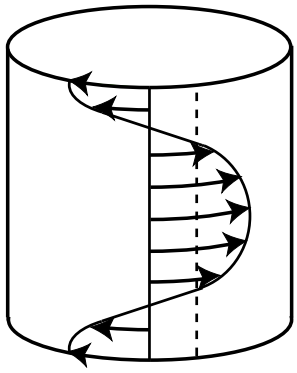

Figure 5.5: Schematic of the snapshot in time of the time-dependent azimuthal velocity profile (black curved line) on a cylinder surface for changes on millennial timescales. The black arrows represent the direction of the flow, and the dotted vertical line the average azimuthal velocity on the cylinder, which is opposite to the direction of the flow near the end of the cylinder. Half of a period later, the flow profile and the average azimuthal velocity are reversed.

In addition, we note that the velocity profile figure 5.5 is also consistent with considerations of the torque between the mantle and the core. Consider a change in axial angular momentum of the core in one direction produced by a change in zonal flows. To conserve angular momentum, an equal change in mantle angular momentum in the opposite direction must take place. This implies that the change in rotation rate of the mantle must be necessarily in the opposite direction to the flows that carry the bulk changes of angular momentum in the core. Yet, the very same flows must also have the ability to apply the torque which accelerates the mantle in the reverse direction. Regardless of the nature of the torque, in order to drag the mantle in one direction, the part of the flow that accomplishes the torque must be in that same direction, i.e. opposite to the flows that carry the bulk angular momentum in the core. Time-dependent azimuthal flows with a shear in z such as that shown in figure 5.5 have this attribute and can consistently explain both the change in

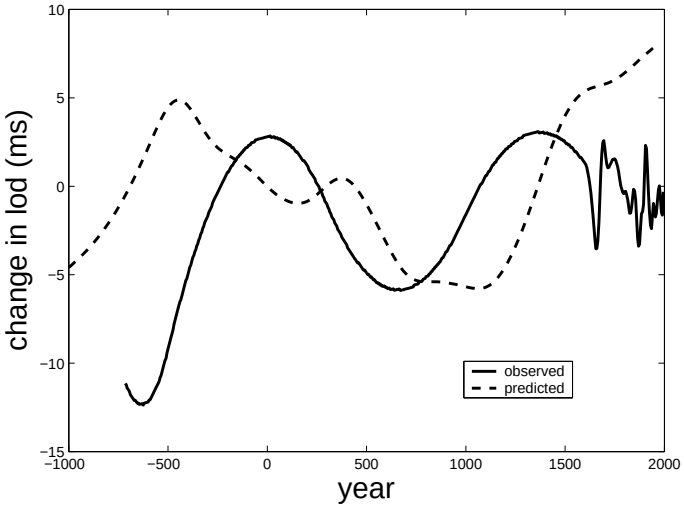

Figure 5.6: Comparison between the observed variations in the length of day obtained from historical eclipses (solid line) and the prediction from our inverted flow model (dashed line) based upon the assumption that the azimuthal flow at the ends of cylinders is equal and opposite to the average velocity over the cylinder.

angular momentum of the core and the torque on the mantle.

One may then ask, how is it possible then that the rigid cylindrical flow structure at decade timescales is capable of applying both the torque on the mantle and a change in core angular momentum in the reverse direction? The answer is by a shear in the s-direction (the direction away from the rotation axis). The cylinders that are the most efficient at transmitting the torque (those with $s \leq r_{ic}$ if the torque is from gravitational coupling between the inner core and the mantle (Buffett, 1996a), or those with $s \approx r_c$ if the torque is due to electromagnetic coupling at the CMB (Rochester, 1960) and provided the rms B_r is everywhere equal on the CMB) are different from the cylinders that carry the most angular momentum (middle of the core). Hence, with a shear in s, the cylindrical flows organize themselves in a way to be consistent with both the angular momentum balance and the torque. In fact, the requirement of satisfying both of these constraints determines the resulting normal modes of torsional oscillations (Buffett, 1998; Mound and Buffett, 2003). The inverted historical time-dependent rigid zonal flows are indeed suggestive that this is the case. The change in core angular momentum as given by (5.15) is the result of an almost perfect cancellation between the larger individual contribution from $t_1^0(t)$ and $t_3^0(t)$ (Jackson *et al.*, 1993; Jault

et al., 1996). The fact that other flow coefficients ($t_5^0(t)$, $t_7^0(t)$, etc.) are also of similar magnitude than $t_1^0(t)$ and $t_3^0(t)$ is indicative that the cylindrical flow structure is accomplishing the difficult task of simultaneously satisfying the angular momentum balance while providing the torque on the mantle.

At millennial timescales, our flow inversion suggests that the situation is quite different. Most of the time-dependent variations in the core surface flows are carried by $t_1^0(t)$ alone. Hence, if the torque on the mantle is due to coupling at the CMB, most of it is done by this $t_1^0(t)$ component. Conservation of angular momentum then implies that the bulk of the azimuthal flow in the core must be in the reverse direction, supporting a velocity profile such as that of figure 5.5.

The arguments presented here suggest that the angular momentum balance in the core at millennial timescale is quite different from decade timescales. At decade timescales, the core mostly conserves its angular momentum by an exchange of angular momentum between rigid cylindrical surfaces at different radii, as provided by the dynamics of torsional oscillations. At millennial timescales, the core mostly conserves its angular momentum by an exchange of angular momentum in the direction along the rotation axis by the establishment of time-dependent flows with a shear in z.

At this point one may reasonably wonder whether our inference of flow geometry within the core is stretching too far the results of our flow inversion. Indeed, the global archaeomagnetic field models certainly contain errors because significantly fewer data are available for the southern hemisphere than for the northern hemisphere. Likewise, the millennial LOD variations could also be affected by a few erroneous eclipse record. Additional pitfalls mentioned in the previous section can invalidate our inverted flows and the dominance of the t_1^0 term may result from an artifact of the degree of smoothing on the model. However, the angular momentum balance at millennial timescales that we have provisionally recovered from the data is consistent with our theoretical expectations of core dynamics at these timescales. Azimuthal velocity gradients in z arise as a result of a combination of magnetic and thermal winds. Since we expect the morphology of both the magnetic field and the temperature perturbation to change significantly over a thousand year timescale, we expect millennial timescale variations in azimuthal flows with a shear in z. Of course, we have not demonstrated that the geometry of these flows is also such that the velocity at the ends of the cylinder are about equal and opposite to the bulk velocity of the entire cylinder surface.

This depends on the internal structure of the magnetic field and temperature perturbation and requires a more substantial analysis.

5.5 Discussion and conclusions

The model of time-dependent azimuthal flows at the surface of the core that we obtained from inversion suggests that there is a correlation between the angular momentum carried by these flows and the millennial variations in the LOD determined from the historical eclipse record. This correlation hinges upon a flow geometry on cylindrical surfaces characterized by a shear in the axial direction as opposed to a rigid rotation. This type of flow is expected on theoretical grounds from variations in the three dimensional structure of the magnetic field and temperature within the core, which produce changes in the magnetic wind and thermal wind, respectively. Hence, despite all the possible pitfalls concerning our inversion, we have recovered core surface flow variations on millennial timescales that are consistent with our theoretical expectations and also compatible with an independent geophysical observation.

There remains the possibility that the inverted time-dependent flow is invalid for any of the reasons discussed in this paper, or simply that the archaeomagnetic field model may not be reliable enough to extract surface flow motion in the core. If this is the case, the correlation with the changes in LOD may be fortuitous. It is also possible that our theoretical view of the millennial timescales dynamics in the core is incorrect. Our argument about the correlation between the core flows and the changes in LOD would then be much weaker. However, if the changes in the rotation rate of the mantle at millennial timescales are not due to exchanges of angular momentum with the core, they must be from exchanges of angular momentum with the fluid envelope at the surface. Therefore, an indirect way of assessing the validity of our result is by investigating whether surface processes participate in the axial angular momentum balance.

Angular momentum changes in the fluid envelope can be produced by two different processes: a change in the mean zonal surface velocities, or latitudinal mass displacement. An estimate of these effects can be obtained. Let's consider first the possibility that zonal accelerations are responsible for the millennial variations in LOD. Observations of the changes in atmospheric zonal wind velocities during the interval 1949-1997 as a result of

the global warming trend indicate that the total atmosphere angular momentum has been increasing (Abarca del Rio, 1999). The corresponding rate of change in LOD is on the order of 0.56 milliseconds/century (ms/cy). The global rate of increase in temperature during that interval is ~ 0.79 °C/cy. Adopting for simplicity a linear correspondence between the two implies an increase of 0.7 ms in LOD for each degree C change in temperature. Therefore, in order to explain the observed millennial LOD variations (peak-to-peak $\sim$ 10 ms), a change in global temperature of ~ 13 °C is required, an unlikely scenario. An alternative estimate of the change in LOD due to the effect of global warming has been obtained using a suite of coupled ocean-atmosphere general circulation models (de Viron *et al.*, 2002). The dominant effect is produced by changes in zonal wind velocities and a mean rate of increase in LOD of 0.11 ms/cy is obtained from a doubling of CO_2 in the atmosphere, although it is as large as 0.44 ms/cy for one of the model. Even for this most extreme case, the concentration of CO_2 would need to change by a factor 5-6 in order to produce the observed millennial variations in the LOD, an equally unlikely scenario.

The second possible surface mechanism is through latitudinal mass displacements, which produce changes in the axial moment of inertia of the whole Earth. A corresponding change in the rotation rate must take place to conserve angular momentum. At millennial timescales, the largest contribution to fluctuations of surface mass distribution is most probably from exchanges between oceans and high latitude glacier ice mass that are produced by climate variations. Changes in ocean mass produce variations in global sea-level and the associated change in LOD is 2.75×10^{-3} ms for each cm of uniform sea-level increase (Chao and O'Connor, 1988). To that we must add the effect of the change in ice mass, which, for simplicity, we can take to be about equivalent. This means that in order to produce the observed peak-to-peak millennial changes in LOD of 10 ms, we need peak-to-peak variations in global sea-level of about 20 meters. The existing record of sea-level changes during the last millennia suggests variations with a magnitude that is at least 10 times smaller (e.g. Tanner, 1992; Kearney, 1996; Nunn, 1998). However, because the record can only reveal local changes and because our estimate of the required sea-level change may be overestimated, let us proceed further with this hypothesis. The magnitude of the sea-level change resulting from a change in global temperature is a complicated problem, but for the sake of the argument, let's suppose that a change on the order of a couple of °C is sufficient to produce the required sea-level change and mass redistribution

to explain the millennial LOD variations. The observed changes in temperature for the past few millennia (for example from Greenland ice sheet boreholes (Dahl-Jensen *et al.*, 1998)) may then be compatible with this scenario. However, the warmest period is observed to be between 500 A.D. and 1000 A.D., which should correspond to an increase in sea-level and a maximum in the change in LOD. Yet, the observed variation in LOD is at a minimum during that time interval (see figure 5.4), indicating that this mechanism is probably not the main cause of the observed changes. If this effect participates, it must be compensated by a larger inverse effect.

Although the above estimates remain crude, they indicate that it is unlikely that the observed millennial changes in LOD can be accounted by surface processes. This is one additional indication that the mechanism responsible for these changes most likely originates in the Earth's core.

If our inverted flow and theoretical arguments are correct, the conclusions are many fold. First, it suggests that angular momentum exchange between the core and the mantle is responsible for the millennial variations in LOD. Secondly, because we have been able to explain consistently two independent geophysical observations with a mechanism expected on theoretical grounds, this provides additional confidence for both of these datasets. Hence, that despite the uncertainties in the reconstruction of both the millennial changes in LOD from historical eclipses and the millennial changes in the magnetic field obtained from various sources, some of the features that they contain are reliable.

A third conclusion concerns the angular momentum dynamics in the core at millennial timescales, which is dominated by azimuthal flows with a shear in the z-direction. This is a completely different situation than at decade timescales, where the angular momentum dynamics is characterized by rigid cylindrical flows with a shear in the s direction. The rigid flows at decade timescale owe their existence to a normal mode of oscillation - torsional oscillations - whereas we expect that flows with an axial shear result from the evolution of the magnetostrophic balance.

An interesting question emerges: what is the timescale at which the changes in the magnetostrophic balance, and hence changes in the axial shear, become important? This may be observable in the historical geomagnetic field models. The good agreement between the observed decadal variations in the LOD and that predicted with (5.15) and (5.16) is the foundation of our belief that the decade timescale dynamics in the core involve torsional

oscillations. Yet, there is a striking misalignment prior to 1900 (see figure 1.2). Perhaps the misalignment is a consequence of some amount of time-dependent shear in z. Indeed, the typical timescale associated with the flow variation before 1930 - mostly comprised of a single sinusoidal like variation with a period of 60 years - is longer than any of the variations that occur after 1940, where the misalignment between the observed and predicted LOD is less pronounced. This may suggest that the timescale at which the dynamical effects of the shear in z becomes important is around 60 years. Obviously, the discrepancy between the two curves may also be simply a consequence of the decreasing quality of the data as we go further in the past.

The changes in the magnetostrophic balance can also be inferred by looking at the relative contribution of the zonal toroidal coefficient with *even* harmonic degrees with respect to the total flow. These correspond to flows that are anti-symmetric about the equator and therefore necessarily involve a shear in z. Their contribution are the largest at 1950 and 1890 (see figure 8b of Jackson, 1997) and at these two epochs, the amplitude of the observed and predicted LOD do not match well. This may be another indication that changes in the magnetostrophic balance are already important at decade timescales. Moreover, it is immediately following these two events that the largest LOD changes are observed, ones that are well explained by purely rigid flows. This may further indicate that flows with an axial shear participate in the excitation of torsional oscillations. However, one may also note that the contribution of the non-rigid components has been much smaller in the recent past where data quality is better, indicating that their earlier larger values may be due to flow model errors.

A more extensive analysis of the historical record of the magnetic field is required in order to confirm these assertions. This may be possible by using the historical field model GUFM which extends back to 1590 (Jackson *et al.*, 2000), in combination with the change in LOD observed from the start of the telescopic era in the 1620's (Stephenson and Morrison, 1984; McCarthy and Babcock, 1986).

Our analysis at millennial timescales has so far been focused on the angular momentum budget and we have said very little about the coupling mechanism that accomplishes the torque. Our inversion suggests that flows at the surface of the core are in the same direction as the changes in mantle rotation rate. This indicates that the changes in mantle rotation rate probably result from the dragging action by these flows, and that the coupling takes

place at the CMB. One likely possibility is electromagnetic coupling (Bullard *et al.*, 1950; Rochester, 1960), which is efficient if there is a layer of highly conducting material at the base of the mantle. This coupling mechanism may play a role at decade timescales (Holme, 1998a). If it is the case, we expect it to be important at millennial timescales as well. Another possibility is that the entrainment at the CMB is the result of viscous stresses. The latter are important when the viscous spin-up timescale is similar to the timescale considered. A spin-up time of 1500 years requires an effective Ekman number of $\sim 10^{-14}$, corresponding to an effective kinematic viscosity of $\sim 2 \times 10^{-5}$ m^2 s^{-1}, a value only one order of magnitude larger than the molecular estimate (Poirier, 1988; Alfé *et al.*, 2000; Dobson, 2002).

Axial gravitational coupling between density heterogeneities in the mantle and an inner core with longitudinal variations in topography (Buffett, 1996a) is incompatible with our inversion result. For if the mantle rotation rate is, say, increased by an eastward super rotation of the inner core, flows near the ICB that drags the inner core must be eastward. Assuming that azimuthal flows at the CMB are in the reverse direction, the flows at the CMB should be westward, i.e. opposite to the change in mantle rotation rate. This is contrary to the result of our inversion. Hence, if our dynamical assumption that the changes in axial gradients are more important than rigid rotations is correct, then gravitational coupling between the inner core and mantle must be either inefficient, or compensated by greater torques at the CMB.

The latter torque is probably the most efficient one at decade timescales (Buffett, 1998; Mound and Buffett, 2003). That it is no longer important at millennial timescale can be explained by viscous relaxation of the topography at the ICB. This may provide an upper bound for the viscosity of the inner core. Following the mapping of Buffett (1997) that we used in chapter 4, a characteristic relaxation time of 1000 years would correspond to an inner core viscosity of 5×10^{19} Pa s.

One important question remains: Why do the variations in core flows and in the LOD appear to occur with a periodicity 1500 years? First and foremost, we must keep in mind that the length and periodic nature of the millennial changes in the LOD is not firmly established from the eclipse data (Leslie V. Morrison, personal communication). At best, we can only be confident about the gross timescale and phase of the changes. The same can be said about our inverted flow model. Hence, the correlation we observe only supports that

1500 years represents the characteristic timescale of the recent variations in the geodynamo.

Whether this timescale underlies a dynamic component of the geodynamo with a periodic nature is unknown. It may simply represents an indication of the recent changes in the thermal and magnetic winds in the core as a result of the vagaries of the geodynamo. The time-variations of the fields in the core are controlled by two competing processes: diffusion which tends to decrease the spatial variations in the fields, and buoyancy driven instabilities in the form of MAC waves (Braginsky, 1967) which tend to increase them. Indeed, the geodynamo can be thought of as a resistive finite amplitude MAC wave instability (e.g. Roberts and Soward, 1992). The chaotic evolution of this balance is expected to scan many timescales and may have forced the recent changes in the axial gradients of azimuthal flows to include a broad variation of 1500 years. However, another possibility is that this is the timescale at which a resonant excitation of a natural mode of vibration occurs. Hence, that similar to decade timescales, where oscillations of rigid rotations result from the excitation of a normal mode, it may be that there is a natural mode of oscillation at millennial timescales involving primarily axisymmetric azimuthal flows that have a shear in z. Hence, we would expect that the chaotic evolution of the convective flows produce changes in the axial gradients at many different timescales, but that a resonant excitation of a normal mode occurs near 1500 years. This normal mode would most likely consist of MAC waves, albeit a special axisymmetric case.

Whether such natural modes of vibration exist will be the subject of a future study. Since the natural modes of oscillations depend on both the magnetic field and the temperature perturbation, important information about these fields inside the core and about the geodynamo could be extracted. This investigation is also necessary in order to test our assertion that the geometry of the millennial time-dependent flows is such that the velocity at the ends of the cylinders is about equal and opposite to the average velocity over the cylinder. Finally, this will also permit a proper assessment of the nature of the torque.

Work in progress and future investigations

We conclude this thesis with a brief description of some work in progress and future investigations that spawned from some of the results presented in this thesis

Excitation of torsional oscillations

Because the full numerical simulations of the geodynamo do not operate in the same parameter regime as the Earth's core, care has to be taken when extrapolating the results of the model. One may then criticize the mechanism for the excitation of torsional oscillations described in chapter 2 simply on the basis that it relies on a dynamical regime which is different than that of the Earth's core. Efforts in obtaining numerical solutions that are closer to the Earth's parameter regime will be pursued.

Another approach is to develop a much simpler numerical model that contains only the elements of the dynamics that are relevant to the excitation hypothesis. Hence, to integrate in time the changes in rigid flow that are produced by a given differential rotation acting on an initial magnetic field morphology. This could be tracked by a numerical integration of a coupled system that only involves the torque balance and the changes in the magnetic field governed by the induction equation. Effects of the various types of coupling at the solid surfaces can easily be introduced in this model. The advantage of such a simpler model is that the parameters can all assume Earth-like values without heavy penalties on the computation time. This then allows a proper analysis of the dependence of each of the model parameters on the solutions. The hypothesis can therefore be thoroughly tested and the range of parameters which produce Earth-like torsional oscillations can be established. This model is currently at the development stage.

Torques on the inner core and the Markowitz wobble

While we demonstrate in chapter 4 that electromagnetic torques at the ICB may be sufficient to explain the Markowitz wobble, this result is obtained under the assumption that the inner core does not undergo axial acceleration as a result of the dragging action of torsional oscillations. Because of the strong electromagnetic coupling at the ICB (e.g Gubbins, 1981), the inner core is likely entrained by the flow. The differential axial velocity at the ICB is then greatly diminished. As a result, the equatorial electromagnetic torque on the inner core, which scales linearly with the differential velocity (see equation 4.20), is also much weaker. It is then doubtful that this mechanism can reproduce the amplitude of the observed Markowitz wobble.

However, the electromagnetic entrainment of the inner core by torsional oscillations lead to a different type of coupling mechanism, one which may produce sufficiently large equatorial torques: gravitational coupling between the inner core and the mantle. Density heterogeneities in the mantle cause global perturbations in the surfaces of constant gravitational potential. To a good approximation, the fluid-solid interface at the ICB corresponds to one such equipotential surface, and its topography reflects the density structure of the mantle. As the inner core is axially rotated, the ICB topography is no longer aligned with the density heterogeneities in the mantle. This results in a gravitational torque in the axial direction (Buffett, 1996a,b). Although it is not as easily visualized, the axial misalignment between the ICB topography and the density heterogeneities in the mantle may also produce a torque in the equatorial direction.

An order of magnitude analysis, using typical amplitudes of seismically inferred density structure in the lower mantle (e.g. Ishii and Trump, 2001) (which also determines the height of the ICB topography) and typical amplitude of axial rotation of the inner core, suggests that a torque on the order of 10^{20} N m can be produced by this mechanism. It may then be sufficient to explain the Markowitz wobble. Producing a more quantitative model of this torque is the next step in our work on the inner core tilt and the Markowitz wobble. If this mechanism proves to be correct, the observation of the Markowitz wobble may then be used as a way to constrain the history of the axial rotation of the inner core. This may provide a way to further test the hypothesis that the axial component of this torque explains the exchange of angular momentum between the core and the mantle at decade timescales

(Zatman, 2003), and to shed new light on the seismically detected inner core super-rotation (Song and Richards, 1996; Su *et al.*, 1996; Laske and Masters, 1999; Souriau and Poupinet, 2000). If the history of the inner core rotation can be determined, this would also provide good constraints on flows in the core close to the ICB and valuable information about the geodynamo. In addition, because this mechanism depends on the density distribution deep inside the Earth, it may also provide a geodynamic test for the internal density models of Earth inferred by seismic tomography or other means (see Becker and Boschi, 2002, and references therein).

Core-mantle torques at decade timescales

In chapter 5, we described how flows in the core must have the ability to produce the torque on the mantle while conserving angular momentum of the core-mantle system. Following a suggestion by Jeremy Bloxham, we can use this very concept as a way to discriminate between the various proposed core-mantle coupling mechanism at decade timescales.

The axial angular momentum balance between the core and the mantle at timescales of decades involves torsional oscillations. Most likely, the latter must also be responsible for imposing the torque on the mantle. Electromagnetic coupling at the CMB can be tested by trying to invert for a torsional oscillations model which fits the secular variation, satisfies the LOD variations, and also required to produce the required torque on the mantle. This is very similar to the approach taken by Holme (1998a,b), who showed that it was indeed possible to find general time-dependent flows that are consistent with all three. We propose to test the same concept but to restrict the time-dependent part of the flow model to rigid zonal flows, and hence directly test if a there exists a torsional oscillations model that has the geometry to also explain the torque. Although the axial rotation of the inner core is less constrained and therefore the gravitational coupling between the mantle and the inner core is more difficult to evaluate (although see above), this mechanism can be investigated along the same lines.

This will complement the work of Buffett (1998) and Mound and Buffett (2003), who investigated, using a normal mode formalism, the efficiency of various core-mantle coupling compatible with torsional oscillations. They use a foreword model approach and require only that the amplitude of torsional oscillations and the predicted LOD are similar

to the observations. By an inverse modeling approach, we can impose that the torsional oscillations flow model matches the observations more closely, and further test the core-mantle coupling.

Bibliography

Abarca del Rio, R. (1999). The influence of global warming in Earth rotation speed. *Ann. Geophysicae, 17*, 806–811.

Alfé, D., G. Kresse, and M. Gillan (2000). Structure and dynamics of liquid iron under core conditions. *Phys. Rev., B61*, 132–142.

Alfonsi, L. and G. Spada (1998). Effect of subductions and trends in seismically induced Earth rotational variations. *J. Geophys. Res., 103*, 7351–7362.

Alfvén, H. (1942). On the existence of electromagnetic-hydromagnetic waves. *Nature, 150*, 405–406.

Alterman, Z., H. Jarosch, and C. L. Pekeris (1959). Oscillations of the Earth. *Proc. Roy. Soc. London, Ser. A, 252*, 80–95.

Aurnou, J. and P. Olson (2000). Control of inner core rotation by electromagnetic, gravitational and mechanical torques. *Phys. Earth Planet. Inter., 117*, 111–121.

Backus, G. E. (1968). Kinematics of geomagnetic secular variation in a perfectly conducting core. *Philos. Trans. Roy. Soc. London, Ser. A, A263*, 239–266.

Becker, T. and L. Boschi (2002). A comparison of tomographic and geodynamic mantle models. *Geochem. Geophys. Geosyst., 3*. Doi:10.1029/2001GC000168.

Bergman, M. (1998). Estimates of the Earth's inner core grain size. *Geophys. Res. Lett., 25*, 1593–1596.

Bloxham, J. (1992). The steady part of the secular variation of the Earth's magnetic field. *J. Geophys. Res., 97*, 19,565–19,579.

Bloxham, J. (1998). Dynamics of angular momentum in the Earth's core. *Ann. Rev. Earth Planet. Sci., 26*, 501–517.

Bloxham, J. and D. Gubbins (1985). The secular variation of the Earth's magnetic field. *Nature, 317*, 777–781.

Bloxham, J., D. Gubbins, and A. Jackson (1989). Geomagnetic secular variation. *Philos. Trans. Roy. Soc. London, Ser. A, 329*, 415–502.

Bloxham, J. and A. Jackson (1991). Fluid flow near the surface of Earth's outer core. *Rev. of Geophys., 29*, 97–120.

Bloxham, J., S. Zatman, and M. Dumberry (2002). The origin of geomagnetic jerks. *Na-*

ture, *420*, 65–68.

Braginsky, S. (1963). Structure of the F layer and reasons for convection in the Earth's core. *Dokl. Acad. Nauk. SSSR*, *149*, 1311–1314. (Engl. transl. *Sov. Phys. Dokl.* pp. 8-10).

Braginsky, S. (1964). Magnetohydrodynamics of the Earth's core. *Geomag. Aeron.*, *4*, 698–712.

Braginsky, S. (1967). Magnetic waves in the earth's core. *Geomag. Aeron.*, *7*, 851–859.

Braginsky, S. I. (1970). Torsional magnetohydrodynamic vibrations in the Earth's core and variations in day length. *Geomag. Aeron.*, *10*, 1–10.

Braginsky, S. I. (1975). Nearly axisymmetric model of the hydromagnetic dynamo of the Earth. *Geomag. Aeron.*, *15*, 122–128.

Braginsky, S. I. (1978). Nearly axisymmetric model of the hydromagnetic dynamo of the Earth II. *Geomag. Aeron.*, *18*, 225–231.

Braginsky, S. I. (1984). Short-period geomagnetic secular variation. *Geophys. Astrophys. Fluid Dyn.*, *30*, 1–78.

Braginsky, S. I. (1988). The Z Model of the geodynamo with magnetic friction. *Geomag. Aeron.*, *28*, 407–412.

Braginsky, S. I. (1993). MAC-oscillations of the hidden ocean of the core. *J. Geomag. Geoelectr.*, *45*, 1517–1538.

Braginsky, S. I. (1994). The nonlinear dynamo and Model-Z. In: *Lectures on Solar and Planetary Dynamos*, eds. M. R. E. Proctor and A. D. Gilbert, pp. 219–244. Cambridge University Press.

Braginsky, S. I. (1999). Dynamics of the stably stratified ocean at the top of the core. *Phys. Earth Planet. Inter.*, *111*, 21–34.

Buffett, B. A. (1992). Constraints on magnetic energy and mantle conductivity from the forced nutations of the Earth. *J. Geophys. Res.*, *97*, 19,581–19,597.

Buffett, B. A. (1996a). Gravitational oscillations in the length of the day. *Geophys. Res. Lett.*, *23*, 2279–2282.

Buffett, B. A. (1996b). A mechanism for fluctuations in the length of day. *Geophys. Res. Lett.*, *23*, 3803–3806.

Buffett, B. A. (1997). Geodynamic estimates of the viscosity of the Earth's inner core. *Nature*, *388*, 571–573.

Buffett, B. A. (1998). Free oscillations in the length of day: inferences on physical properties near the core-mantle boundary. In: *The core-mantle boundary region*, eds. M. Gurnis, M. E. Wysession, E. Knittle, and B. A. Buffett, vol. 28 of *Geodynamics series*, pp. 153–165. AGU Geophysical Monograph, Washington, DC.

Buffett, B. A., P. M. Mathews, and T. A. Herring (2002). Modeling of nutation-precession: effects of electromagnetic coupling. *J. Geophys. Res.*. In press.

Bullard, E. (1949a). The magnetic field within the Earth. *Proc. Roy. Soc. London, Ser. A, 197*, 433–453.

Bullard, E. (1949b). Electromagnetic induction in a rotating sphere. *Proc. Roy. Soc. London, Ser. A, 199*, 413–443.

Bullard, E. (1956). Edmond Halley (1656-1741). *Endeavour*, *15*, 189–199.

Bullard, E., C. Freedman, H. Gellman, and J. Nixon (1950). The westward drift of the Earth's magnetic field. *Philos. Trans. Roy. Soc. London, Ser. A, 243*, 67–92.

Bullard, E. and H. Gellman (1954). Homogeneous dynamos and terrestrial magnetism. *Philos. Trans. Roy. Soc. London, Ser. A, 247*, 213–278.

Busse, F. H. (1970a). The dynamical coupling between inner core and mantle of the Earth and the 24-year libration of the pole. In: *Earthquake Displacement Fields and the Rotation of the Earth*, eds. D. Mansinha, D. E. Smylie, and A. E. Beck, vol. 20 of *Astrophysics and Space Science Library*, pp. 88–98. D. Reidel Publishing company, Dordrecht, Holland.

Busse, F. H. (1970b). Thermal instabilities in rapidly rotating systems. *J. Fluid Mech.*, *44*, 441–460.

Busse, F. H. and L. L. Hood (1982). Differential rotation driven by convection in a rapidly rotating annulus. *Geophys. Astrophys. Fluid Dyn.*, *21*, 59–74.

Cardin, P. and P. Olson (1994). Chaotic thermal convection in a rapidly rotating spherical shell: consequences for flow in the outer core. *Phys. Earth Planet. Inter.*, *82*, 235–259.

Celaya, M. A., J. M. Wahr, and F. O. Bryan (1999). Climate-driven polar motion. *J. Geophys. Res.*, *104*, 12,813–12,829.

Chao, B., A. Y. Au, J.-P. Boy, and C. M. Cox (2003). Time-variable gravity signal of an anomalous redistribution of water mass in the extratropic Pacific during 1998-2002. *Geochem. Geophys. Geosyst.*, *4*, 1096. Doi:10.1029/2003GC000589.

Chao, B. F. (1995). Anthropogenic impact on global geodynamics due to reservoir water impoundment. *Geophys. Res. Lett.*, *22*, 3529–3532.

Chao, B. F. (2003). Geodesy is not just for static measurements any more. *EOS*, *84*, 145.

Chao, B. F., R. S. Gross, and D. Dong (1995). Changes in the global gravitational energy induced by earthquakes. *Geophys. J. Int.*, *122*, 784–789.

Chao, B. F. and W. P. O'Connor (1988). Effect of a uniform sea-level change on the Earth's rotation and gravitational field. *Geophys. J.*, *93*, 191–193.

Cheng, M., R. Eanes, C. Shum, B. Schutz, and B. Tapley (1989). Temporal variations in low degree zonal harmonics from Starlette orbit analysis. *Geophys. Res. Lett.*, *16*, 393–396.

Chinnery, M. A. (1975). The static deformation of an Earth with a fluid core: a physical approach. *Geophys. J. R. Astr. Soc.*, *42*, 461–475.

Christensen, U. R. (2002). Zonal flow driven by strongly supercritical convection in rotating spherical shells. *J. Fluid Mech., 470*, 115–133.

Christodoloudis, D., D. Smith, R. Williamson, and S. Klosko (1988). Observed tidal breaking in the Earth/Moon/Sun system. *J. Geophys. Res., 93*, 6216–6236.

Constable, C., C. Johnson, and S. Lund (2000). Global geomagnetic field models for the past 3000 years: transient or permanent flux lobes? *Philos. Trans. Roy. Soc. London, Ser. A, 358*, 991–1008.

Courtier, N., B. Ducarme, J. Goodkind, J. Hinderer, Y. Imanishi, N. Seama, H. Sun, J. Merriam, B. Bengert, and D. E. Smylie (2000). Global superconducting gravimeter observations and the search for the translational modes of the inner core. *Phys. Earth Planet. Inter., 117*, 3–20.

Courtillot, V. and J. L. Le Mouël (1984). Geomagnetic secular variation impulses. *Nature, 311*, 709–716.

Cox, C. M. and B. F. Chao (2002). Detection of large-scale mass redistribution in the terrestrial system since 1998. *Science, 297*, 831–833.

Crossley, D. J. (1975). The free oscillation equations at the center of the Earth. *Geophys. J. R. Astr. Soc., 41*, 153–163.

Crossley, D. J. and D. Gubbins (1975). Static deformation of the Earth's liquid core. *Geophys. Res. Lett., 2*, 1–4.

Dahl-Jensen, D., K. Mosegaard, N. Gundestrup, D. Clow, S. Johnson, A. Hansen, and N. Balling (1998). Past temperatures directly from the Greenland ice sheet. *Science, 282*, 268–271.

Dahlen, F. A. (1972). Elastic dislocation theory for a self-gravitating elastic configuration with an initial static stress field. *Geophys. J. R. Astr. Soc., 28*, 357–383.

Dahlen, F. A. (1974). On the static deformation of an Earth model with a fluid core. *Geophys. J. R. Astr. Soc., 36*, 461–485.

Dahlen, F. A. and S. B. Fels (1978). A physical explanation for the static core paradox. *Geophys. J. R. Astr. Soc., 55*, 317–332.

Dahlen, F. A. and J. Trump (1998). *Theoretical global seismology*. Princeton university press, Princeton, New Jersey.

Daly, L. and M. Le Goff (1996). An updated and homogeneous world secular variation database. part 1. smoothing of the archeomagnetic results. *Phys. Earth Planet. Inter., 93*, 159–190.

de Viron, O., V. Dehant, H. Goosse, and M. Crucifix (2002). Effect of global warming on the length-of-day. *Geophys. Res. Lett., 29*. Doi:10.1029/2001GL013672.

Dehant, V., J. Hinderer, H. Legros, and M. Lefftz (1993). Analytical approach to the computation of the Earth, the outer core and inner core rotational motions. *Phys. Earth Planet. Inter., 76*, 259–282.

Denis, C., M. Almavict, Y. Rogister, and S. Tomecka-Suchon (1998). Methods for computing internal flattening, with applications to the Earth's structure and geodynamics. *Geophys. J. Int.*, *132*, 603–642.

Dickey, J. O., S. L. Marcus, O. de Viron, and I. Fukumori (2002). Recent Earth oblateness variations: unraveling climate and postglacial rebound effects. *Science*, *298*, 1975–1977.

Dickman, S. R. (1981). Investigation of controversial polar motion features using homogeneous international latitude service data. *J. Geophys. Res.*, *86*, 4904–4912.

Dickman, S. R. (1983). The rotation of the ocean-solid Earth system. *J. Geophys. Res.*, *88*, 6373–6394.

Dickman, S. R. (1985). Comments on "Normal modes of the coupled Earth system" by John M. Wahr. *J. Geophys. Res.*, *90*, 11,553–11,556.

Dobson, D. (2002). Self-diffusion in liquid Fe at high pressure. *Phys. Earth Planet. Inter.*, *130*, 271–284.

Dormy, E., J.-P. Valet, and V. Courtillot (2000). Numerical models of the geodynamo and observational constraints. *Geochem. Geophys. Geosyst.*, *1*. Paper number 2000GC000062.

Dumberry, M. and J. Bloxham (2002). Inner core tilt and polar motion. *Geophys. J. Int.*, *151*, 377–392.

Dumberry, M. and J. Bloxham (2003). Torque balance, Taylor's constraint and torsional oscillations in a numerical model of the geodynamo. *Phys. Earth Planet. Inter.*, *140*, 29–51.

Dziewonski, A. M. and D. L. Anderson (1981). Preliminary reference Earth model. *Phys. Earth Planet. Inter.*, *25*, 297–356.

Elsasser, W. (1956). Hydromagnetic dynamo theory. *Rev. Mod. Phys.*, *28*, 135–163.

Elsasser, W. M. (1946a). Induction effects in terrestrial magnetism. I. theory. *Phys. Rev.*, *69*, 106–116.

Elsasser, W. M. (1946b). Induction effects in terrestrial magnetism. II. the secular variations. *Phys. Rev.*, *70*, 202–212.

Elsasser, W. M. (1947). Induction effects in terrestrial magnetism. III. electric modes. *Phys. Rev.*, *72*, 821–833.

Fang, M. (1998). Static deformation of the outer core. In: *Dynamics of the ice age Earth: a modern perspective*, ed. P. Wu, vol. 3-4 of *GeoResearch Forum*, pp. 155–190. Trans Tech publications, Zürich, Switzerland.

Fang, M., B. H. Hager, and T. A. Herring (1996). Surface deformation caused by pressure changes in the fluid core. *Geophys. Res. Lett.*, *23*, 1493–1496.

Fearn, D. R. (1994). Nonlinear planetary dynamos. In: *Lectures on Solar and Planetary Dynamos*, eds. M. R. E. Proctor and A. D. Gilbert, pp. 219–244. Cambridge University Press.

Fearn, D. R. (1998). Hydromagnetic flow in planetary cores. *Rep. Prog. Phys.*, *61*, 175–235.

Fearn, D. R. and M. R. E. Proctor (1987a). Dynamically consistent magnetic fields produced by differential rotation. *J. Fluid Mech.*, *178*, 521–534.

Fearn, D. R. and M. R. E. Proctor (1987b). On the computation of steady, self-consistent spherical dynamos. *Geophys. Astrophys. Fluid Dyn.*, *38*, 293–325.

Frost, H. J. and M. E. Ashby (1982). *Deformation Mechanism Maps*. Pergamon Press, Oxford.

Garnero, E. J., J. Ravenaugh, Q. Williams, T. Lay, and L. H. Kellogg (1998). Ultralow velocity zone at the core-mantle boundary. In: *The core-mantle boundary region*, eds. M. Gurnis, M. E. Wysession, E. Knittle, and B. A. Buffett, vol. 28 of *Geodynamics series*, pp. 319–334. AGU Geophysical Monograph.

Gavoret, J., D. Gilbert, M. Menvielle, and J. Le Mouël (1986). Long-term variations of the external and internal components of the Earth's magnetic field. *J. Geophys. Res.*, *91*, 4787–4796.

Gilbert, W. (1600). *De Magnete*. Peter Short, London. (Translated in 1900 from Latin by Silvanus Thompson and reproduced by Basic Books, N.Y., 1956).

Gill, A. E. (1982). *Atmosphere-Ocean dynamics*, vol. 30 of *International geophysics series*. Academic Press, London.

Glatzmaier, G. A. (2002). Geodynamo simulations - how realistic are they? *Ann. Rev. Earth Planet. Sci.*, *30*, 237–257.

Glatzmaier, G. A. and P. H. Roberts (1995). A three-dimensional convective dynamo solution with rotating and finitely conducting inner core and mantle. *Phys. Earth Planet. Inter.*, *91*, 63–75.

Greenspan, H. P. (1968). *The theory of rotating fluids*. Cambridge University Press.

Greff-Lefftz, M. and H. Legros (1995). Core mantle coupling and polar motion. *Phys. Earth Planet. Inter.*, *91*, 273–283.

Greff-Lefftz, M., H. Legros, and V. Dehant (2000). Influence of the inner core viscosity on the rotational eigenmodes of the Earth. *Phys. Earth Planet. Inter.*, *122*, 187–204.

Greiner-Mai, H. and F. Barthelmes (2001). Relative wobble of the Earth's inner core derived from polar motion and associated gravity variations. *Geophys. J. Int.*, *144*, 27–36.

Gross, R. S. (1990). The secular drift of the rotation pole. In: *Earth rotation and coordinate reference frames*, eds. C. Boucher and G. A. Wilkins, pp. 146–153. Springer-Verlag, New York, NY.

Gross, R. S. (2000). The excitation of the Chandler wobble. *Geophys. Res. Lett.*, *27*, 2329–2332.

Grote, E. and F. H. Busse (2001). Dynamics of convection and dynamos in rotating spherical fluid shells. *Fluid Dyn. Res.*, *28*, 349–368.

Gubbins, D. (1981). Rotation of the inner core. *J. Geophys. Res.*, *86*, 11,695–11,699.

Gubbins, D. (1982). Finding core motions from magnetic observations. *Philos. Trans. Roy. Soc. London, Ser. A*, *306*, 247–254.

Gubbins, D. and P. Kelly (1996). A difficulty with using the frozen flux hypothesis to find steady core motions. *Geophys. Res. Lett.*, *23*, 1825–1828.

Gubbins, D. and P. H. Roberts (1987). Magnetohydrodynamics of the Earth's core. In: *Geomagnetism*, ed. J. A. Jacobs, vol. 2, pp. 1–184. Academic Press, London.

Gubbins, D. and L. Tomlinson (1986). Secular variations from monthly means from Apia and Amberley magnetic observatories. *Geophys. J. R. Astr. Soc.*, *86*, 603–616.

Harrison, C. G. A. (1987). The crustal field. In: *Geomagnetism*, ed. J. A. Jacobs, vol. 1, pp. 513–610. Academic Press, London.

Herring, T. A. (1999). Geodetic applications of GPS. *Proc. of the IEEE*, *87*, 92–110.

Hide, R. (1966). Free hydromagnetic oscillations of the Earth's core and the theory of geomagnetic secular variation. *Philos. Trans. Roy. Soc. London, Ser. A*, *259*, 615–646.

Hide, R., D. H. Boggs, and J. O. Dickey (2000). Angular momentum fluctuations within the Earth's liquid core and torsional oscillations of the core-mantle system. *Geophys. J. Int.*, *143*, 777–786.

Hide, R., D. H. Boggs, J. O. Dickey, D. Dong, R. S. Gross, and A. Jackson (1996). Topographic core-mantle coupling and polar motion on decadal time-scales. *Geophys. J. Int.*, *125*, 599–607.

Hills, R. G. (1979). *Convection in the Earth's mantle due to viscous shear at the core-mantle interface and due to large-scale buoyancy*. Ph.D. thesis, N.M. State Univ., Las Cruces.

Hinderer, J. and D. Crossley (2000). Time variations in gravity and inferences on the Earth's structure and dynamics. *Surv. Geophys.*, *21*, 1–45.

Hinderer, J., C. Gire, H. Legros, and J.-L. Le Mouël (1987). Geomagnetic secular variation, core motions and implications for the Earth's wobble. *Phys. Earth Planet. Inter.*, *49*, 121–132.

Hinderer, J., H. Legros, D. Jault, and J.-L. Le Mouël (1990). Core-mantle topographic torque: a spherical harmonic approach and implications for the excitation of the Earth's rotation by core motions. *Phys. Earth Planet. Inter.*, *59*, 329–341.

Hollerbach, R. (1996). On the theory of the geodynamo. *Phys. Earth Planet. Inter.*, *98*, 163–185.

Hollerbach, R. (2003). The range of timescales on which the geodynamo operates. In: *Earth's core: dynamics, structure, rotation*, eds. V. Dehant, K. C. Creager, S.-I. Karato, and S. Zatman, vol. 31 of *Geodynamics series*, pp. 181–192. AGU Geophysical Monograph.

Hollerbach, R., C. F. Barenghi, and J. C. A. (1992). Taylor's constraint in a spherical

αω-dynamo. *Geophys. Astrophys. Fluid Dyn.*, *67*, 3–25.

Holme, R. (1998a). Electromagnetic core-mantle coupling - I. Explaining decadal changes in the length of day. *Geophys. J. Int.*, *132*, 167–180.

Holme, R. (1998b). Electromagnetic core-mantle coupling II: Probing deep mantle conductance. In: *The core-mantle boundary region*, eds. M. Gurnis, M. E. Wysession, E. Knittle, and B. A. Buffett, vol. 28 of *Geodynamics series*, pp. 139–152. AGU Geophysical Monograph, Washington, DC.

Hongre, L., G. Hulot, and A. Khokhlov (1998). An analysis of the geomagnetic field over the past 2000 years. *Phys. Earth Planet. Inter.*, *106*, 311–335.

Hulot, G., M. Le Huy, and J.-L. Le Mouël (1996). Influence of core flows on the decade variations of the polar motion. *Geophys. Astrophys. Fluid Dyn.*, *82*, 35–67.

Ishii, M. and J. Trump (2001). Even-degree lateral variations in the Earth's mantle constrained by free oscillations and the free-air gravity anomaly. *Geophys. J. Int.*, *145*, 77–96.

Israel, M., A. Ben-Manahem, and S. J. Singh (1973). Residual deformation of real Earth models with application to the Chandler wobble. *Geophys. J. R. Astr. Soc.*, *32*, 219–247.

Jackson, A. (1997). Time-depedency of tangentially geostrophic core surface motions. *Phys. Earth Planet. Inter.*, *103*, 293–311.

Jackson, A. (2003). Intense equatorial flux spots on the surface of the Earth's core. *Nature*, *424*, 760–763.

Jackson, A., J. Bloxham, and D. Gubbins (1993). Time-dependent flow at the core surface and conservation of angular momentum in the coupled core-mantle system. In: *Dynamics of the Earth's deep interior and Earth rotation*, eds. J.-L. Le Mouël, D. E. Smylie, and T. Herring, vol. 72, pp. 97–107. AGU Geophysical Monograph, Washington, DC.

Jackson, A., A. Jonkers, and M. R. Walker (2000). Four centuries of geomagnetic secular variation from historical records. *Philos. Trans. Roy. Soc. London, Ser. A*, *358*, 957–990.

Jault, D. (1995). Model Z by computation and Taylor's condition. *Geophys. Astrophys. Fluid Dyn.*, *79*, 99–124.

Jault, D. (2003). Electromagnetic and topographic coupling, and lod variations. In: *Earth's core and lower mantle*, eds. C. A. Jones, A. Soward, and K. Zhang, The fluid mechanics of astrophysics and geophysics. Taylor & Francis, London.

Jault, D., C. Gire, and J.-L. Le Mouël (1988). Westward drift, core motions and exchanges of angular momentum between core and mantle. *Nature*, *333*, 353–356.

Jault, D., G. Hulot, and J.-L. Le Mouël (1996). Mechanical core-mantle coupling and dynamo modelling. *Phys. Earth Planet. Inter.*, *98*, 187–191.

Jault, D. and J.-L. Le Mouël (1991). Exchange of angular momentum between the core and the mantle. *J. Geomag. Geoelectr.*, *43*, 111–129.

Jeffreys, H. (1970). *The Earth*. Cambridge University Press, London, UK, 5th edn.

Jeffreys, H. and R. O. Vicente (1966). Comparisons of forms of the elastic equations for the Earth. *Mem. Acad. R. Belgique, 37*, 5–31.

Jones, C. A. (1991). Dynamo models and Taylor's constraint. In: *Advances in Solar system magnetohydrodynamics*, eds. E. R. Priest and A. W. Hood, pp. 25–50. Cambridge University Press, Cambdridge.

Kakuta, C., I. Okamoto, and T. Sasao (1975). Is the nutation of the solid inner core responsible for the 24-year libration of the pole? *Publ. astr. Soc. Jpn., 27*, 357–365.

Kearney, M. (1996). Sea-level change during the last thousand years in Chesapeake Bay. *J. Coastal Res., 12*, 977–983.

Kim, J. and B. D. Tapley (2002). Error analysis of a low-low satellite-to-satellite tracking mission. *J. Guid. control dynam., 25*, 1100–1106.

Kono, M. and P. H. Roberts (2002). Recent geodynamo simulations and observations of the geomagnetic field. *Rev. of Geophys., 40(4)*, 1013. Doi:10.1029/2000RG000102.

Korte, M. and C. Constable (2003). Continuous global geomagnetic field models for the past 3000 years. *Phys. Earth Planet. Inter., 140*, 73–89.

Kuang, W. (1999). Force balances and convective state in the Earth's core. *Phys. Earth Planet. Inter., 116*, 65–79.

Kuang, W. and J. Bloxham (1997a). An Earth-like numerical dynamo model. *Nature, 389*, 371–374.

Kuang, W. and J. Bloxham (1997b). On the dynamics of topographical core-mantle coupling. *Phys. Earth Planet. Inter., 99*, 289–294.

Kuang, W. and J. Bloxham (1999). Numerical modeling of magnetohydrodynamic monvection in a mapidly rotating spherical shell: weak and strong field dynamo action. *J. Comp. Phys., 153*, 51–81.

Lambeck, K. (1980). *The Earth's variable rotation: geophysical causes and consequences*. Cambridge University Press, Cambridge.

Langel, R. A. (1987). The main field. In: *Geomagnetism*, ed. J. A. Jacobs, vol. 1, pp. 249–512. Academic Press, London.

Larmor, J. (1919a). Possible rotational origin of magnetic fields of Sun and Earth. *Elect. Rev., 85*, 512.

Larmor, J. (1919b). Possible rotational origin of magnetic fields of Sun and Earth. *Engineering, 108*, 461.

Laske, G. and G. Masters (1999). Limits on differential rotation of the inner core from an analysis of the Earth's free oscillations. *Nature, 402*, 66–69.

Le Mouël, J.-L. (1984). Outer core geostrophic flow and secular variation of Earth's magnetic field. *Nature, 311*, 734–735.

Lefftz, M. and H. Legros (1992). Influence of viscoelastic coupling on the axial rotation of

the earth and its fluid core. *Geophys. J. Int.*, *108*, 725–739.

Longman, I. M. (1963). A green's function for determining the deformation of the Earth under surface mass loads: 2. computations and numerical results. *J. Geophys. Res.*, *68*, 485–496.

Love, A. E. H. (1909). The yielding of the Earth to disturbing forces. *Proc. Roy. Soc. London, Ser. A*, *82*, 73–88.

Love, J. (1999). A critique of frezen-flux inverse modelling of a nearly steady geodynamo. *Geophys. J. Int.*, *138*, 353–365.

Macmillan, S. (1996). A geomagnetic jerk for the early 1990's. *Earth Planet. Sci. Lett.*, *137*, 189–192.

Malin, S. (1987). Historical introduction to geomagnetism. In: *Geomagnetism*, ed. J. A. Jacobs, vol. 1, pp. 1–50. Academic Press, London.

Malin, S. R. C. and E. Bullard (1981). The direction of the Earth's magnetic field at London, 1570-1975. *Philos. Trans. Roy. Soc. London, Ser. A*, *299*, 357–423.

Mandea, M., E. Bellanger, and J. L. Le Mouël (2000). A geomagnetic jerk for the end of the 20th century? *Earth Planet. Sci. Lett.*, *183*, 369–373.

Markowitz, W. (1960). Latitude and longitude and the secular motion of the pole. In: *Methods and Techniques in Geophysics*, ed. S. K. Runcorn, pp. 325–361. Interscience Publishers, London.

Markowitz, W. (1968). Concurrent astronomical observations for studying continental drift, polar motion, and the rotation of the Earth. In: *Continental drift, Secular motion of the pole and rotation of the earth*, eds. W. Markowitz and B. Guinot, pp. 25–32. Springer-Verlag, Dordrecht.

Mathews, P. M., B. A. Buffett, T. A. Herring, and I. I. Shapiro (1991a). Forced nutations of the Earth: Influence of inner core dynamics. 1. theory. *J. Geophys. Res.*, *96*, 8219–8242.

Mathews, P. M., B. A. Buffett, T. A. Herring, and I. I. Shapiro (1991b). Forced nutations of the Earth: Influence of inner core dynamics. 2. numerical results. *J. Geophys. Res.*, *96*, 8243–8257.

Mathews, P. M. and I. I. Shapiro (1992). Nutations of the Earth. *Ann. Rev. Earth Planet. Sci.*, *20*, 469–500.

McCarthy, D. D. and A. K. Babcock (1986). The length of day since 1956. *Phys. Earth Planet. Inter.*, *44*, 281–292.

McCarthy, D. D. and B. J. Luzum (1996). Path of the mean rotational pole from 1899 to 1994. *Geophys. J. Int.*, *125*, 623–629.

Merrill, R. T., M. W. McElhinny, and M. P. L. (1996). *The magnetic field of the Earth*, vol. 63 of *International Geophysics Series*. Academic Press, 2nd edn.

Mitrovica, J. X. and W. R. Peltier (1993). Present-day variations in the zonal harmonics of the Earth's geopotential. *J. Geophys. Res.*, *98*, 4509–4526.

Morrison, L. V. and F. R. Stephenson (2001). Historical eclipses and the variability of the earth's rotation. *J. of Geodynamics, 32*, 247–265.

Mound, J. E. and B. A. Buffett (2003). Interannual oscillations in the length of day: implications for the structure of mantle and core. *J. Geophys. Res., 108(B7)*, 2334. Doi:10.1029/2002JB002054.

Munk, W. H. and G. J. F. MacDonald (1960). *The rotation of the Earth*. Cambridge University Press, Cambridge.

Needham, J. (1962). *Science and civilisation in China, Vol. 4, Physics and Physical technology, part 1. Physics*. Cambridge University Press, Cambridge.

Nunn, P. (1998). Sea-level changes over the past 1,000 years in the Pacific. *J. Coastal Res., 14*, 23–30.

O'Connell, R. (1971). Pleistocene glaciation and the viscosity of the lower mantle. *Geophys. J. R. Astr. Soc., 23*, 299–327.

Olson, P. and J. Aurnou (1999). A polar vortex in the Earth's core. *Nature, 402*, 170–173.

Olson, P., U. Christensen, and G. A. Glatzmaier (1999). Numerical modeling of the geodynamo: mechanisms of field generation and equilibration. *J. Geophys. Res., 104*, 10,383–10,404.

Pais, A. and G. Hulot (2000). Length of day decade variations, torsional oscillations and inner core superrotation: evidence from recovered core surface zonal flows. *Phys. Earth Planet. Inter., 118*, 291–316.

Pedlosky, J. (1987). *Geophysical fluid dynamics*. Springer-Verlag, New York, 2nd edn.

Pekeris, C. L. and Y. Accad (1972). Dynamics of the liquid core of the Earth. *Philos. Trans. Roy. Soc. London, Ser. A, 273*, 237–260.

Peltier, W. R. (1974). The impulse response of a Maxwell Earth. *Rev. of Geophys., 12* (649–669).

Poirier, J.-P. (1988). Transport properties of liquid metals and viscosity of the Earth's core. *Geophys. J., 92*, 99–105.

Poma, A. (2000). The Markowitz wobble. In: *Polar motion: historical and scientific problems. IAU colloquium 178*, eds. S. Dick, D. McCarthy, and B. Luzum, vol. 208 of *ASP conference series*, pp. 352–354. Astronomical Society of the Pacific, San Francisco, USA.

Poma, A. and E. Proverbio (1980). Astronomical evidence of relationships between polar motion, Earth rotation and continental drift. In: *Mechanisms of continental drift and plate tectonics*, eds. P. A. Davies and S. K. Runcorn, pp. 345–357. Academic Press, London.

Poupinet, G., A. Souriau, and O. Coutant (2000). The existence of an inner core superrotation questioned by teleseismic doublets. *Phys. Earth Planet. Inter., 118*, 77–88.

Proudman, J. (1916). On the motions of solids in a liquid possessing vorticity. *Proc. Roy.*

Soc. London, Ser. A, 92, 408–424.

Rau, S., U. Christensen, A. Jackson, and J. Wicht (2000). Core flow inversion tested with numerical dynamo models. *Geophys. J. Int., 141*, 485–497.

Roberts, P. and S. Scott (1965). On the analysis of secular variation. *J. Geomag. Geoelectr., 17*, 137–151.

Roberts, P. H. and A. M. Soward (1992). Dynamo theory. *Ann. Rev. Fluid Mech., 24*, 459–512.

Rochester, M. G. (1960). Geomagnetic westward drift and irregularities in the Earth's rotation. *Philos. Trans. Roy. Soc. London, Ser. A, 252*, 531–555.

Rubincam, D. P. (1984). Postglacial rebound observed by LAGEOS and the effective viscosity of the lower mantle. *J. Geophys. Res., 89*, 1077–1087.

Sasao, T., T. Okubo, and M. Saito (1980). A simple theory on the dynamical effects of a stratified fluid core upon nutational motion of the Earth. In: *Proceedings of IAU Symposium*, eds. E. P. Federov, M. L. Smith, and P. L. Bender, vol. 78, pp. 165–183. D. Reidel, Hingham, Mass.

Schuh, H., S. Nagel, and T. Seitz (2001). Linear drift and periodic variations observed in long time series of polar motion. *J. Geodesy, 74*, 701–710.

Smith, M. L. and F. A. Dahlen (1981). The period and Q of the Chandler wobble. *Geophys. J. R. Astr. Soc., 64*, 223–281.

Smylie, D. E. and L. Mansinha (1971). The elastic theory of dislocation in real Earth models and changes in the rotation of the Earth. *Geophys. J. R. Astr. Soc., 23*, 329–354.

Smylie, D. E. and D. G. McMillan (2000). The inner core as a dynamic viscometer. *Phys. Earth Planet. Inter., 117*, 71–79.

Smylie, D. E., A. M. K. Szeto, and M. G. Rochester (1984). The dynamics of the Earth's inner and outer cores. *Rep. Prog. Phys., 47*, 855–906.

Song, X. D. and P. G. Richards (1996). Seismological evidence for differential rotation of the Earth's inner core. *Nature, 382*, 221–224.

Souriau, A. and G. Poupinet (2000). Inner core rotation: a test at the worldwide scale. *Phys. Earth Planet. Inter., 118*, 13–27.

Sovers, O. J., J. L. Fanselow, and C. S. Jacobs (1998). Astrometry and geodesy with radio interferometry: experiments, models, results. *Rev. Mod. Phys., 70*, 1393–1454.

Stacey, F. D. (1992). *Physics of the Earth*. Brookfield Press, Kenmore, Australia, 3rd edn.

Stephenson, F. R. and L. V. Morrison (1984). Long-term changes in the rotation of the Earth: 700 BC to AD 1980. *Philos. Trans. Roy. Soc. London, Ser. A, 313*, 47–70.

Stephenson, F. R. and L. V. Morrison (1995). Long-term fluctuations in the Earth's rotation: 700 BC to AD 1990. *Philos. Trans. Roy. Soc. London, Ser. A, 351*, 165–202.

Stern, D. (2002). A millennium of geomagnetism. *Rev. of Geophys., 40(3)*, 1007.

Doi:10.1029/2000RG000097.

Su, W. J., A. M. Dziewonski, and R. Jeanloz (1996). Planet within a planet: Rotation of the inner core of the Earth. *Science, 274*, 1883–1887.

Sumita, I., S. Yoshida, M. Kumazawa, and Y. Hamano (1996). A model for sedimentary compaction of a viscous medium and its application to inner-core growth. *Geophys. J. Int., 124*, 502–524.

Sun, Z.-P., G. Schubert, and G. A. Glatzmaier (1993). Transition to chaotic thermal convection in a rapidly rotating spherical fluid shell. *Geophys. Astrophys. Fluid Dyn., 69*, 95–131.

Takehiro, S. and J. R. Lister (2001). Penetration of columnar convection into an outer stably stratified layer in rapidly rotating spherical fluid shells. *Phys. Earth Planet. Inter., 187*, 357–366.

Takeushi, H. and M. Saito (1972). Seismic surface waves. In: *Methods of computational physics*, ed. B. A. Bolt, vol. 11, pp. 217–295. Academic Press, San Diego.

Tanner, W. (1992). 3000 years of sea-level change. *B. Am. Meteorol. Soc., 73*, 297–303.

Taylor, G. I. (1917). Motions of solids in fluid when the flow is not irrotational. *Proc. Roy. Soc. London, Ser. A, 93*, 99–113.

Taylor, J. B. (1963). The magneto-hydrodynamics of a rotating fluid and the Earth's dynamo problem. *Proc. Roy. Soc. London, Ser. A, 274*, 274–283.

Wahr, J. M. (1981). The forced nutations of an ellitical, rotating, elastic and oceanless Earth. *Geophys. J. R. Astr. Soc., 87*, 633–668.

Wahr, J. M. (1984). Normal modes of the coupled Earth and ocean system. *J. Geophys. Res., 89*, 7621–7630.

Wen, L. X. and D. V. Helmberger (1998). Ultra-low velocity zones near the core-mantle boundary from broadband PKP precursors. *Science, 279*, 1701–1703.

Whaler, K. (1980). Does the whole of the Earth's core convect. *Nature, 287*, 528–530.

Wilson, C. R. and R. O. Vicente (1980). An analysis of homogeneous ILS polar motion series. *Geophys. J. R. Astr. Soc., 62*, 605–616.

Wu, P. and D. R. Peltier (1982). Viscous gravitational relaxation. *Geophys. J. R. Astr. Soc., 70*, 435–485.

Xu, S. and A. M. K. Szeto (1998). The coupled rotation of the inner core. *Geophys. J. Int., 133*, 279–297.

Yoder, C. F., J. G. Williams, J. O. Dickey, B. E. Schutz, R. J. Eanes, and B. D. Tapley (1983). Secular variation of the Earth's gravitational harmonic j_2 coefficient from LAGEOS and nontidal acceleration of Earth rotation. *Nature, 303*, 757–762.

Yoshida, S., I. Sumita, and M. Kumazawa (1996). Growth model of the inner core coupled with the outer core dynamics and the resulting elastic anisotropy. *J. Geophys. Res., 101*,

28,085–28,103.

Zatman, S. (2003). Decadal oscillations of the Earth's core, angular momentum exchange, and inner core rotation. In: *Earth's core: dynamics, structure, rotation*, eds. V. Dehant, K. C. Creager, S.-I. Karato, and S. Zatman, vol. 31 of *Geodynamics series*, pp. 233–240. AGU Geophysical Monograph.

Zatman, S. and J. Bloxham (1997). Torsional oscillations and the magnetic field within the Earth's core. *Nature*, *388*, 760–763.

Zatman, S. and J. Bloxham (1998). A one-dimensional map of B_s from torsional oscillations of the Earth's core. In: *The core-mantle boundary region*, eds. M. Gurnis, M. E. Wysession, E. Knittle, and B. A. Buffett, vol. 28 of *Geodynamics series*, pp. 183–196. AGU Geophysical Monograph, Washington, DC.

Zatman, S. and J. Bloxham (1999). On the dynamical implications of models of B_s in the Earth's core. *Geophys. J. Int.*, *138*, 679–686.

Zhang, K. (1992). Spiralling columnar convection in rapidly rotating spherical fluid shells. *J. Fluid Mech.*, *236*, 535–556.

Zhang, K. (1995). Spherical shell rotating convection in the presence of toroidal magnetic field. *Proc. Roy. Soc. London, Ser. A*, *448*, 245–268.

Appendix

A.1 Elastic-gravitational equations in the solid Earth

The static elastic-gravitational equations in the mantle in terms of the 6 variables defined in (3.15) have to obey the differential equations

$$\begin{aligned}
\frac{\partial y_1}{\partial r} &= \frac{1}{\lambda_o+2\mu_o}\left(y_2-\frac{\lambda_o}{r}(2y_1-n(n+1)y_3)\right)\\
\frac{\partial y_2}{\partial r} &= \frac{2}{r}\left(\lambda_o\frac{\partial y_1}{\partial r}-y_2\right)+\left(\frac{2(\lambda_o+\mu_o)}{r}-\rho_o g_o\right)\left(2y_1-\frac{n(n+1)}{r}y_3\right)+\frac{n(n+1)}{r}y_4\\
&\quad +\rho_o\left(y_6-\frac{n+1}{r}y_5-2\frac{g_o}{r}y_1\right)\\
\frac{\partial y_3}{\partial r} &= \frac{1}{\mu_o}y_4+\frac{1}{r}(y_3-y_1)\\
\frac{\partial y_4}{\partial r} &= -\frac{\lambda_o}{r}\frac{\partial y_1}{\partial r}-\left(\frac{\lambda_o+2\mu_o}{r^2}(2y_1-n(n+1)y_3)-\frac{2\mu_o}{r^2}(y_1-y_3)\right)\\
&\quad -\frac{3}{r}y_4+\frac{\rho_o}{r}(y_5+g_o y_1)\\
\frac{\partial y_5}{\partial r} &= y_6-4\pi G\rho_o y_1-\frac{n+1}{r}y_5\\
\frac{\partial y_6}{\partial r} &= \frac{n-1}{r}y_6-4\pi G\rho_o\frac{n+1}{r}y_1+4\pi G\rho_o\frac{n(n+1)}{r}y_3
\end{aligned} \tag{A.1}$$

We note that the equations above are identical as those in Takeushi and Saito (1972) for zero frequency, except that y_5 and y_6 have opposite signs as a consequence of a different sign convention adopted in the present study. The equations in the inner core are identical.

A.2 Calculation of geostrophic pressure from core surface fbws

In this appendix, we present the details of the calculation relating the even degree zonal harmonics of the pressure at the CMB to torsional oscillations. We demonstrate that, for a general flow at the CMB, torsional oscillations are in fact the only component of the flow that participate in the axisymmetric pressure that is symmetric about the equator.

Near the CMB, the horizontal component of the flow is related to pressure through the geostrophic balance (Hills, 1979; Le Mouël, 1984),

$$2\rho_o \Omega \times \mathbf{v_h} = -\nabla p_g \,. \tag{A.2}$$

Taking $\mathbf{e_r}\times$ (A.2) and using $\mathbf{e_r} \times \mathbf{e_z} \times \mathbf{v_h} = -\cos\theta \mathbf{v_h}$, we get

$$2\Omega_o b \rho_o \cos\theta \mathbf{v_h} = \mathbf{e_r} \times \nabla_1 p_g \,, \tag{A.3}$$

where b is the radius of the core and ∇_1 is defined in (3.11). The geostrophic pressure is expanded in spherical harmonics according to (3.37), and we want to relate the coefficients of the latter in terms of core surface flows. It is convenient to expand $\mathbf{v_h}$ in a poloidal-toroidal decomposition,

$$\mathbf{v_h} = \nabla_1 \mathcal{S} + \nabla_1 \times (\mathcal{T}\mathbf{e_r}) = \nabla_1 \mathcal{S} - \mathbf{e_r} \times \nabla_1 \mathcal{T} \,, \tag{A.4}$$

where $\mathcal{S}$ and $\mathcal{T}$ are respectively the poloidal and toroidal scalars. The latter are expanded in spherical harmonics as,

$$\mathcal{S} = \sum_{n=0}^{\infty} \sum_{m=-n}^{n} s_n^m Y_n^m \,, \tag{A.5}$$

$$\mathcal{T} = \sum_{n=0}^{\infty} \sum_{m=-n}^{n} t_n^m Y_n^m \,. \tag{A.6}$$

We note that the custom in geomagnetism is to use a decomposition in terms of real sperical harmonics. However, it is convenient here to expand the flow coefficients as above so to be consistent with our expansion of pressure.

In order to relate the flow coefficients s_n^m and t_n^m to the coefficients of pressure $\Psi_n^m(b)$, we use the vector spherical harmonics $\mathbf{B}_n^m = \mathbf{B}_n^m(\theta,\varphi)$ and $\mathbf{C}_n^m = \mathbf{C}_n^m(\theta,\varphi)$, which are related to the spherical harmonic scalar $Y_n^m = Y_n^m(\theta,\varphi)$ by

$$\mathbf{B}_n^m = \nabla_1 Y_n^m = e_\theta \frac{\partial}{\partial\theta} Y_n^m + e_\varphi \frac{1}{\sin\theta}\frac{\partial}{\partial\varphi} Y_n^m, \tag{A.7}$$

$$\mathbf{C}_n^m = \mathbf{e_r} \times \nabla_1 Y_n^m = e_\varphi \frac{\partial}{\partial\theta} Y_n^m - e_\theta \frac{1}{\sin\theta}\frac{\partial}{\partial\varphi} Y_n^m. \tag{A.8}$$

Using these definitions, we can write (A.3) as

$$2\Omega_o b \rho_o \cos\theta \sum_{n'=0}^{\infty} \sum_{m'=-n'}^{n'} \left(s_{n'}^{m'} \mathbf{B}_{n'}^{m'} - t_{n'}^{m'} \mathbf{C}_{n'}^{m'} \right) = \sum_{n=0}^{\infty} \sum_{m=-n}^{n} \Psi_n^m(b)\, \mathbf{C}_n^m. \tag{A.9}$$

The coefficients $\Psi_n^m(b)$ are obtained by projecting the above equation on the basis $\mathbf{C}_n^{m*}$ and integrating over the surface of the unit sphere. Using the orthogonality rules on the spherical harmonics and the normalization defined in (3.13), we obtain, for each n and m,

$$\Psi_n^m(b) = \frac{2\Omega_o b \rho_o}{4\pi} \frac{2n+1}{n(n+1)} \times \sum_{n'=0}^{\infty} \sum_{m'=-n'}^{n'} \left(s_{n'}^{m'} \int_\Omega \mathbf{C}_n^{m*} \cdot \mathbf{B}_{n'}^{m'} \cos\theta \, d\Omega - t_{n'}^{m'} \int_\Omega \mathbf{C}_n^{m*} \cdot \mathbf{C}_{n'}^{m'} \cos\theta \, d\Omega \right). \tag{A.10}$$

The role of each flow coefficients in the pressure depends on an integral of spherical harmonics over a sphere. To solve these intgerals, one possibility is to use the fact that $\cos\theta = P_1^0(\cos\theta) = Y_1^0$. We then have integrals of triple products of spherical harmonics, which are non-zero for a set of conditions on the indices (see for instance Bullard and Gellman (1954) or Dahlen and Trump (1998)). For the even degree zonal coefficients of the geostrophic pressure, $\Psi_n^0(b)$ with $n = even$, the selction rules are such that the poloidal integral (the $s_{n'}^{m'}$ term) vanishes for all indices. The toroidal integral (the $t_{n'}^{m'}$ term) is non-zero only for $m' = 0$ and the only components of the flow that contribute are the $t_{n'}^0$ with $n' = odd$.

However, a perhaps more transparent way to demonstrate this, and also to solve these integrals, is instead simply to expand the above integrals using the definitions in (A.7-A.8).

The poloidal integral is

$$\begin{aligned}\int_\Omega \mathbf{C}_n^{m*}\cdot\mathbf{B}_{n'}^{m'}\cos\theta\,d\Omega &= \int_\Omega\left(\frac{\partial Y_n^{m*}}{\partial\theta}\frac{\partial Y_{n'}^{m'}}{\partial\varphi}-\frac{\partial Y_n^{m*}}{\partial\varphi}\frac{\partial Y_{n'}^{m'}}{\partial\theta}\right)\frac{\cos\theta}{\sin\theta}\,d\Omega\ ,\\ &= -\int_\Omega\frac{\cos\theta}{\sin\theta}\frac{\partial}{\partial\theta}\left(Y_{n'}^{m'}\frac{\partial Y_n^{m*}}{\partial\varphi}\right)d\Omega\ . \qquad (A.11)\end{aligned}$$

Further algebraic efforts are needed in order to solve the integral for a general set of indices. However, for the zonal coefficients of pressure ($m=0$), $\partial Y_n^0/\partial\varphi=0$ and the integral vanishes for all values of n, n' and m'. Hence, the poloidal flow components do not contribute to the axisymmetric pressure at the CMB. This simply illustrates the well known fact the axisymmetric part of tangential geostrophy can only be explained in terms of toroidal flows.

The toroidal integral, for $m=0$, is

$$\begin{aligned}\int_\Omega \mathbf{C}_n^{0*}\cdot\mathbf{C}_{n'}^{m'}\cos\theta\,d\Omega &= \int_\Omega\left(\frac{\partial Y_n^0}{\partial\theta}\frac{\partial Y_{n'}^{m'}}{\partial\theta}\right)\cos\theta\,d\Omega\ ,\\ &= \int_\Omega\left(\frac{\partial P_n^0}{\partial\theta}\frac{\partial Y_{n'}^{m'}}{\partial\theta}\right)\cos\theta\,d\Omega\ . \qquad (A.12)\end{aligned}$$

The right-hand side can be further decomposed as

$$\int_\Omega \mathbf{C}_n^{0*}\cdot\mathbf{C}_{n'}^{m'}\cos\theta\,d\Omega = \int_\Omega Y_{n'}^{m'}\sin\theta\frac{\partial P_n^0}{\partial\theta}\,d\Omega - \int_\Omega Y_{n'}^{m'}\frac{\cos\theta}{\sin\theta}\frac{\partial}{\partial\theta}\sin\theta\frac{\partial P_n^0}{\partial\theta}\,d\Omega\ . \qquad (A.13)$$

Using,

$$-\frac{1}{\sin\theta}\frac{\partial}{\partial\theta}\sin\theta\frac{\partial P_n^0}{\partial\theta} = L^2P_n^0 = n(n+1)P_n^0\,, \qquad (A.14)$$

we can write (A.13) as

$$\int_\Omega \mathbf{C}_n^{0*}\cdot\mathbf{C}_{n'}^{m'}\cos\theta\,d\Omega = \int_\Omega Y_{n'}^{m'}\sin\theta\frac{\partial P_n^0}{\partial\theta}\,d\Omega + n(n+1)\int_\Omega Y_{n'}^{m'}\cos\theta P_n^0\,d\Omega\ . \qquad (A.15)$$

The above integrals can be transformed into simple orthogonality integrals of spherical harmonics with the use of the following recurrence relations for the associated Legendre polynomials,

$$\sin\theta\frac{\partial P_n^0}{\partial\theta} = -\frac{n(n+1)}{2n+1}P_{n-1}^0 + \frac{n(n+1)}{2n+1}P_{n+1}^0\,, \tag{A.16}$$

$$\cos\theta P_n^0 = \frac{n}{2n+1}P_{n-1}^0 + \frac{n+1}{2n+1}P_{n+1}^0\,. \tag{A.17}$$

Equation (A.15) then becomes

$$\begin{aligned}\int_\Omega \mathbf{C}_n^{0^*}\cdot\mathbf{C}_{n'}^{m'}\cos\theta\,d\Omega &= \frac{n(n+1)}{2n+1}\left((n-1)\int_\Omega Y_{n'}^{m'}P_{n-1}^0\,d\Omega + (n+2)\int_\Omega Y_{n'}^{m'}P_{n+1}^0\,d\Omega\right)\\ &= 4\pi\frac{n(n+1)}{2n+1}\left(\frac{n-1}{2n-1}\delta_{n'(n-1)}\delta_{m'0} + \frac{n+2}{2n+3}\delta_{n'(n+1)}\delta_{m'0}\right)\end{aligned} \tag{A.18}$$

For a given harmonic degree n, the only non-zero integrals are therefore those with $m' = 0$, and n' equals to either $(n-1)$ or $(n+1)$. Hence, only the axisymmetric components of the toroidal flow participate in the zonal geostrophic pressure, and for each zonal harmonic degree of the latter, only two of the zonal toroidal flow coefficients contribute. Moreover, for a geostrophic pressure symmetric about the equator ($n = even$), only the flow coefficients with *odd* harmonic degree participate. In other words, the only flow components that participate in the even degree zonal harmonics of the pressure are torsional oscillations. The final expression for the zonal harmonic degree n of the geostrophic pressure at the CMB is obtained by substituting (A.18) into (A.10),

$$\Psi_n^0(b) = -\Omega_o b\rho_o\left(\frac{2(n-1)}{(2n-1)}t_{n-1}^0 + \frac{2(n+2)}{(2n+3)}t_{n+1}^0\right)\,. \tag{A.19}$$

A.3 Analytical solution of the elastic-gravitational equations near the origin

The solution in the inner core near the center of the Earth is detailed in Crossley (1975). At a small radius $r = \varepsilon$, the solution can be written in terms of three independent solutions. A

convenient way to write the complete solution, is in terms of three vectors $\mathbf{y^{\varepsilon 1}}$, $\mathbf{y^{\varepsilon 2}}$ and $\mathbf{y^{\varepsilon 3}}$, as

$$\mathbf{y^s}(\varepsilon) = C_1\mathbf{y^{\varepsilon 1}} + C_2\mathbf{y^{\varepsilon 2}} + C_3\mathbf{y^{\varepsilon 3}}, \tag{A.20}$$

where

$$\begin{aligned}
\mathbf{y^{\varepsilon 1}} &= \left[\varepsilon^{n-1}, 2(n-1)\mu_o\varepsilon^{n-2}, \frac{\varepsilon^{n-1}}{n}, \frac{2(n-1)}{n}\mu_o\varepsilon^{n-2}, -\frac{3\gamma}{2n+1}\varepsilon^n, 0\right]^T, \\
\mathbf{y^{\varepsilon 2}} &= \left[0,0,0,0,\frac{\varepsilon^n}{(2n+1)}, \varepsilon^{n-1}\right]^T, \\
\mathbf{y^{\varepsilon 3}} &= \left[\alpha_1\varepsilon^{n+1}, \alpha_2\varepsilon^n, \alpha_3\varepsilon^{n+1}, \varepsilon^n, \alpha_5\varepsilon^{n+2}, \alpha_6\varepsilon^{n+1}\right]^T,
\end{aligned} \tag{A.21}$$

with

$$\begin{aligned}
\alpha_3 &= \frac{p_2}{p_1} - \frac{\rho_o}{C_3 p_1}\left(C_1\gamma n(1-\frac{3}{2n+1}) + C_2\frac{n}{2n+1}\right), \\
\alpha_1 &= -n\alpha_3 + \frac{1}{\mu_o}, \\
\alpha_2 &= -q_1\alpha_3 + q_2, \\
\alpha_5 &= \frac{3\gamma}{2(2n+3)}\left(-(n+3)\alpha_1 + n(n+1)\alpha_3\right), \\
\alpha_6 &= 3\gamma\alpha_1 + (2n+3)\alpha_5,
\end{aligned} \tag{A.22}$$

and

$$\begin{aligned}
\gamma &= \frac{4\pi}{3}G\rho_o \\
p_1 &= 2n^2(n+2)\lambda_o + 2n(n^2+2n-1)\mu_o, \\
p_2 &= n(n+5) + 2n(n+3)\frac{\lambda_o}{\mu_o}, \\
q_1 &= 2n(n+2)\lambda_o + 2n(n+1)\mu_o, \\
q_2 &= 2(n+1) + (n+3)\frac{\lambda_o}{\mu_o}.
\end{aligned} \tag{A.23}$$

In the above equations, ρ_o, λ_o and μ_o correspond to the reference state values evaluated at

$r = \varepsilon$. We note that the small differences between the analytical solution presented above and that of Crossley (1975) are a result of the different definitions of y_5^s and y_6^s used in the present study.

A.4 Electromagnetic torque from torsional oscillations acting on a tilted dipole field

The electromagnetic torque on the inner core that results from an oscillating azimuthal flow is given by

$$\Gamma = \frac{1}{\mu}\int_{ICB} (\mathbf{r}\times\mathbf{b})\,\mathbf{B}\cdot\mathbf{dS}\,, \tag{A.24}$$

where $\mathbf{B}$ is the magnetic field, $\mathbf{b}$ is the magnetic field perturbation created by the shear in the flow at the ICB, μ is the permeability of free space, $\mathbf{r}$ is the position vector directed away from the center and $\mathbf{dS} = a_s^2 \sin\theta\, d\phi\, d\theta\, \mathbf{e_r}$ is a surface element at the approximately spherical ICB. The torque can be expanded in spherical coordinates as

$$\Gamma = \frac{a_s^3}{\mu}\int_0^{\pi}\int_0^{2\pi} \left(B_r\, b_\theta\, \mathbf{e}_\phi - B_r\, b_\phi\, \mathbf{e}_\theta\right) \sin\theta\, d\phi\, d\theta\,. \tag{A.25}$$

In terms of the Cartesian unit vectors $\mathbf{e_1}$, $\mathbf{e_2}$ and $\mathbf{e_3}$, where $\mathbf{e_1}$ and $\mathbf{e_2}$ are the equatorial directions, the unit vectors $\mathbf{e}_\phi$ and $\mathbf{e}_\theta$ are given by

$$\mathbf{e}_\phi = -\sin\phi\,\mathbf{e_1} + \cos\phi\,\mathbf{e_2}\,, \tag{A.26}$$

$$\mathbf{e}_\theta = \cos\theta\cos\phi\,\mathbf{e_1} + \cos\theta\sin\phi\,\mathbf{e_2} - \sin\theta\,\mathbf{e_3}\,, \tag{A.27}$$

and using these definitions in (A.25), the equatorial component in, say, direction $\mathbf{e_1}$ is

$$\Gamma_1 = \frac{a_s^3}{\mu}\int_o^{\pi}\left(\int_0^{2\pi} -B_r\, b_\theta \sin\phi\, d\phi\right)\sin\theta\, d\theta + \left(\int_0^{2\pi} -B_r\, b_\phi \cos\phi\, d\phi\right)\cos\theta\sin\theta\, d\theta\,. \tag{A.28}$$

In the scenario that a torque is produced by an oscillating azimuthal flow shearing the radial magnetic field at the ICB, the induced magnetic field will be in the azimuthal direction. We therefore neglect the b_θ term. The solution for b_ϕ at the ICB that results from

periodic tangential motion across the boundary was calculated by Buffett (1998) and its amplitude is given by

$$b_\phi = \frac{B_r \Delta u_\phi \sin\theta}{2\sqrt{\eta \sigma_d}}, \tag{A.29}$$

where η is the magnetic diffusivity, σ_d is the frequency of oscillation of the azimuthal flow, and Δu_ϕ is the azimuthal velocity difference between the inner core and the flow. This solution takes into account the effects of magnetic diffusion. The equatorial torque in direction $\mathbf{e_1}$ becomes

$$\Gamma_1 = -\frac{a_s^3}{\mu} \frac{\Delta u_\phi}{2\sqrt{\eta \sigma_d}} \int_o^\pi \left(\int_0^{2\pi} B_r^2 \cos\phi \, d\phi \right) \cos\theta \sin^2\theta \, d\theta. \tag{A.30}$$

The precise amplitude of the torque depends on the morphology of the radial magnetic field. As an example, we can calculate the torque that results when the radial magnetic field is a superposition of an axial dipole and an equatorial dipole field oriented in $\mathbf{e_1}$. At the ICB, in terms of Gauss coefficients defined at the surface of the inner core, this field is described by

$$B_r = -2 g_1^0 \cos\theta - 2 g_1^1 \cos\phi \sin\theta. \tag{A.31}$$

Taking the square of (A.31) and inserting it in (A.30), the integrals of the $(g_1^0)^2$ term and $(g_1^1)^2$ term are both zero and only the cross term, $8 g_1^0 g_1^1 \cos\phi \cos\theta \sin\theta$, contributes. The integration of

$$\Gamma_1 = -\frac{a_s^3}{\mu} \frac{\Delta u_\phi}{2\sqrt{\eta \sigma_d}} \int_o^\pi \left(\int_0^{2\pi} 8 g_1^0 g_1^1 \cos^2\phi \, d\phi \right) \cos^2\theta \sin^3\theta \, d\theta, \tag{A.32}$$

gives

$$\Gamma_1 = -\frac{16\pi a_s^3 g_1^0 g_1^1 \Delta u_\phi}{15\mu(\eta\sigma_d)^{1/2}}. \tag{A.33}$$